Comparative Shrinkage Properties of Pavement Materials Including Recycled Concrete Aggregates With and Without Cement Stabilisation

By
Gustave Semugaza

Thesis presented in fulfilment of the requirements for the degree of
*Master of Engineering in the Faculty of Engineering at
Stellenbosch University*

Supervisor: Ms Chantal Rudman
Lecturer at Stellenbosch University

Co-supervisor: Professor Kim J. Jenkins
Senior Lecturer at Stellenbosch University
SANRAL Chair in Pavement Engineering

March 2016

DECLARATION

By submitting this thesis electronically, I declare that the entirety of the work contained therein is my own, original work, that I am the sole author thereof (save to the extent explicitly otherwise stated), that reproduction and publication thereof by Stellenbosch University will not infringe any third party rights and that I have not previously in its entirety or in part submitted it for obtaining any qualification.

Signature: ………………………………………..

Date: …………………………………………..

i

ABSTRACT

The construction of pavement base/subbase layers necessitates quality materials such as natural aggregates. The use of locally available materials offers numerous advantages, including the reduction in the need for quarrying and transporting, which reduces the cost of construction. Unfortunately, these local materials don't always perform adequately for structural purposes, and require stabilisation. Cement is considered as a binder that can treat various types of materials and provide good results. Although cement stabilisation increases the material strength properties, cement-stabilised materials are prone to shrinkage, which is recognised as the major source of different forms of cracking, identified as the most severe distress for pavements with Cement stabilised layers (CSL). Owing to friction from the layer below, high tensile stresses are induced in CSL, and cracking results when these stresses exceed the tensile strength of the material.

The use of low cement content has been considered as basic measures to mitigate shrinkage, but it is not necessarily the case for all materials. In addition, the use of polymer cement additives has been considered for reducing the shrinkage in pavement layers. The Super-Absorbent Polymers (SAP) can reduce the shrinkage due to their high capacity of retaining large quantity of water. Both these factors were investigated, with the addition of SAP to Hornfels.

The shortage of natural materials and strict laws on opening new borrow pits and landfills have made the recycling of wastes one of the highest requirements in many countries. A number of countries adopted the use of recycled Construction and Demolition Waste (CDW) as unbound base/subbase materials for pavements construction. Recycled CDW include Recycled Concrete and Masonry (RCM) and Recycled Concrete Aggregates (RCA). However, most of previous research has only considered cement stabilisation for natural materials. The consideration of cement stabilisation for these materials, which present self-cementing properties due to their nature, is essential.

To evaluate the effect of self-cementing properties on the material shrinkage potential, this research compared the shrinkage properties of three materials, which include G4 hornfels, Recycled Concrete Aggregates (RCA), and New Concrete (NC). The G4 hornfels material served as the base material, and the NC material helped to assess the degree of self-cementation in the RCA material. Considering the shrinkage properties of the three materials, the results revealed that the cracking potential of the RCA material was very low, so that it could be used in place of G4 hornfels for base/subbase layers construction. In addition, the

results revealed that the latent hydration (due to self-cementation) decreased the pivot-point of optimum percentage cement in the mix, when compared to that of the normal G4 material. The RCA and NC materials tended to reach their maximum shrinkage values at 2.5% cement content.

The evaluation of shrinkage crack-patterns due to shrinkage results indicated that all cement-stabilised materials (all three material types) are classified as materials inducing unacceptable crack-patterns (very severe cracks). For non-stabilised materials, only the NC material is classified as a material inducing unacceptable crack-patterns. The non-stabilised RCA material is classified as a material inducing medium crack-pattern (severe cracks), while the G4 hornfels material is classified as a material inducing acceptable crack-pattern (no cracks). Referring to these crack-patterns, the consideration of methods for mitigating shrinkage cracks is necessary, if these materials are used in pavement layers. Nonetheless, it is evident that specifically RCA, although it has latent self-cementing properties, will not be subject to the same potential for cracking as NC.

OPSOMMING

Die konstruksie van plaveisel kroon- en stutlae vereis hoë gehalte materiale soos natuurlike aggregate. Die gebruik van materiale wat plaaslik beskikbaar is bied verskeie voordele, insluitend die afname in die nodigheid vir steengroewe en vervoer, wat die koste van konstruksie verminder. Ongelukkig reageer die plaaslike materiaal nie altyd voldoende vir strukturele doeleindes nie en benodig stabilisering. Sement word gesien as 'n bindmiddel wat alle tipe materiaal kan behandel en goeie resultate kan lewer. Alhoewel sementstabilisering die materiaaleienskap versterk, is sementgestabiliseerde materiale geneig om te krimp, wat erken word as die grootste bron van verskillende vorms van krake, geïdentifiseer as die ergste probleem vir plaveisels met sement-gestabiliseerde lae (SGL). As gevolg van wrywing vanaf die onderste laag word hoë trekspanning geïnduseer in SGL en krake volg wanneer hierdie spanning die trekspanning van die materiaal oorskry.

Die gebruik van lae sementinhoud was oorweeg as basiese maatreël om inkrimping te beperk, maar dit is nie noodwendig die geval vis al die materiale nie. Die bykomende gebruik van polimeersement bymiddels was oorweeg om sodoende die krimping in plaveisellae te verminder. Die super-absorberende polimere (SAP) kan die krimping verminder, a.g.v. hul hoë kapasiteit om groot hoeveelhede water te behou. Albei hierdie faktore; die byvoeging van polimeersement, sowel as die byvoeging van SAP na Hornfels, was ondersoek.

Die tekort aan natuurlike materiale en streng wetgewing oor die opening van nuwe leengroewe en stortingsterreine het die herwinning van afval een van die hoogste vereistes in menige lande gemaak. 'n Aantal lande het die gebruik van Herwinde Konstruksie en Slopingsafval (RCM) as ongebonde kroon- en stutlae materiale vir plaveiselkonstruksie aangeneem. Herwinde Konstruksie en Slopingsafval (CDW) sluit herwinde beton en messelwerk en herwinde beton aggregate in. Vorige navorsing het egter slegs sementstabilisering vir natuurlike materiaal oorweeg. Die oorweging van sementstabilisering vir hierdie materiale, wat selfsementering eienskappe a.g.v. hul aard aanbied, is noodsaaklik.

Hierdie navorsing het die krimp-eienskappe van drie materiale vergelyk, om sodoende die uitwerking van self-sementeringseienskappe op die materiaalkrimpingspotensiaal te evalueer, insluitend G4 Hornfels, Herwinde Beton Aggregate, en Nuwe Beton (NC). Die G4 Hornfels materiaal het as die basis-materiaal gedien en die Nuwe Betonmateriaal het gehelp om die graad van selfsementering in die Herwinde Beton Aggregate materiaal te assesseer. Wanneer die krimpingseienskappe van die drie materiale in ag geneem word, het die uitslae onthul dat die kraakpotensiaal van die Herwinde Beton Aggregate baie laag was, sodat dit in plaas van

die G4 Hornfels gebruik kon word vir kroon- en stutlae konstruksie. Die resultate het ook onthul dat, in vergelyking met die normale G4 materiaal, die latente hidrering (a.g.v. self-sementasie) die spilpunt van optimale persentasie sement in die mengsel verminder het. Die materiale was geneig om hul maksimum krimpingswaardes by 2.5% sementinhoud te bereik.

Die evaluering van krimping-kraakpatrone a.g.v. krimping resultate het aangedui dat alle sementgestabiliseerde materiale (al drie materiaaltipes) geklassifiseer is as materiale wat onaanvaarbare kraakpatrone (baie ernstige krake) veroorsaak. Vir ongestabiliseerde materiaal word slegs die Nuwe Betonmateriaal geklassifiseer as 'n materiaalinduserende onaanvaarbare kraakpatroon. Die ongestabiliseerde Herwinde Beton Aggregate word geklassifiseer as 'n materiaalinduserende medium kraakpatroon (ernstige krake), terwyl die G4 Hornfels materiaal geklassifiseer word as 'n materiaal wat aanvaarbare kraakpatrone induseer (geen krake). Met verwysing na hierde kraakpatrone, is die oorweging van metodes om die krimp van krake te vermindes nodig wanneer hierdie materiaal in plaveisellae gebruik word. Nietemin is dit duidelik dat spesifiek Herwinde Beton Aggregate, alhoewel dit latent self-sementeringseienskappe het, nie onderworpe sal wees aan dieselfde potensiaal vir krimping nie.

ACKNOWLEDGMENTS

TABLE OF CONTENTS

LIST OF FIGURES

LIST OF TABLES

LIST OF ABBREVIATIONS

CDW   Construction and Demolition Waste

C-S-H   Calcium- Silicate- Hydrates

CSL   Cement Stabilised Layers

CSM   Cement-Stabilised Materials

CSPL   Cement-Stabilised Pavement Layers

CSPM   Cement-Stabilised Pavement Materials

CTNC   Cement-Treated New Concrete

CTRCA   Cement-Treated Recycled Concrete Aggregates

MDD   Maximum Dry Density

NC   New Concrete

OMC   Optimum Moisture Content

RCA   Recycled Concrete Aggregates

RCM   Recycled Concrete and Masonry

RH   Relative Humidity

SAP   Super-Absorbent Polymers

SU   Stellenbosch University

CHAPTER 1. INTRODUCTION

1.1   Background

The construction of pavement base/subbase layers necessitates quality materials such as natural aggregates. Availability of these natural materials involves different activities including quarrying, crushing, and transporting. These activities disrupt the environment and deplete natural resources. The use of locally available materials offers numerous advantages, such as reduction in the need for quarrying and transporting, which reduces the cost of construction. Unfortunately, these local materials don't always perform adequately for structural purposes, and hence, require mechanical or chemical stabilisation. Chemical stabilisation involves addition of chemicals to the material, whereas mechanical stabilisation requires compaction or introduction of fibrous and additional non-biodegradable reinforcements to the material (Das, 2003).

All over the world, stabilisation of inferior materials has been considered as a successful activity. Stabilisation involves numerous cementitious binders such as cement, lime and fly ash, which can be mixed to achieve some specific properties. The main objective of using these binders is to increase the strength of the host material, and the load spread capacity, as well as to improve its durability and workability. Different influential factors determine the choice of the binder. These factors include the design requirements, laboratory test results, site conditions, availability and economic concerns (TRH 13, 1986).

At the same time, the shortage of natural materials and strict laws on opening new borrow pits and landfills have made the recycling of wastes, one of the highest requirements in many countries. The recycling of Construction and Demolition Waste (CDW) has gained a considerable importance since the Second World War. A number of countries such as the Netherlands, Germany, USA, Japan, Brazil, China, and Australia adopted the use of recycled CDW as unbound base/subbase materials for pavements construction (Hansen, 1992). For example, the Netherlands, since the late 1970s, has made use of recycled waste from concrete and masonry in the base course, as unbound material, and has become a very common practice (Molenaar and van Niekerk, 2002). Nowadays, in the Netherlands, more than 80% of the road base materials are crushed concrete and masonry granulates (Molenaar, 2010). Cement treatment of these recycled materials improves their quality, and enhances their use as base/subbase layers for heavily loaded pavements (Xuan, 2012).

1

Despite all these advantages associated with cement-stabilisation, Cement-Stabilised Pavement Layers (CSPL) are prone to some engineering problems, resulting from their nature. The load- induced fatigue cracking and shrinkage cracking are the primary distresses affecting the performance of pavements with cement-treated layers. Fatigue cracks are due to traffic load and material strength, and originate from the bottom of Cement Stabilised Layers (CSL), while shrinkage cracks appear at the surface of CSL, and are caused by the volume change (George, 1990).

Shrinkage of CSL includes autogenous shrinkage, drying shrinkage, thermal shrinkage, and carbonation shrinkage; which are respectively due to hydration, loss of moisture, low temperature contraction, and chemical reaction with atmospheric carbon dioxide (Xiaojun, 2014). Drying shrinkage is the major reason of shrinkage cracking of pavements (Little, 1992). Shrinkage cracking of CSL can cause infiltration of water, which leads to reflecting cracking in the layers above. Due to this constraint to cement-stabilisation, methods for mitigation in the magnitude of shrinkage cracking are required, in order to expand the use of these natural and recycled materials.

1.2   Problem statement

Shrinkage has been recognized as the major source of different forms of cracking, and identified as the most severe distress for pavements consisting of cement stabilised layers. Shrinkage cracking is considered as an inherent behaviour of stabilised materials that cannot be avoided, and could even be a cause of concern for materials prone to self-cementing effects (George, 1990). High tensile stresses are induced in a CSL, if it is fully or partially restrained by friction from the layer below. Cracks occur when these stresses exceed the tensile strength of the material. Mitigating methods are necessary for the alleviation of these cracks. Significant information regarding the shrinkage of Cement-Stabilised Materials (CSM) is essential for choosing an appropriate mitigating method, and to understand if this is an issue in all cases.

Drying shrinkage, which is believed as directly related to the moisture loss, is considered as the main cause of shrinkage cracking of CSPL. This type of shrinkage is due to different mechanisms such as surface tension, capillary tension, movement of interlayer water, and disjoining pressure Hansen (1987). Additional factors to cement content have an influence on the degree of shrinkage of CSM. The use of low cement content has been considered as basic measure to mitigate shrinkage, but it is not necessarily the case of all materials. Moreover,

studies have shown that the quality of the host material, with associated intrinsic properties, can play a major role in CSL cracking than the use of low cement content.

In addition, following practice and proficiency from USA, Brazil, Australia, different countries of Europe and Asia, the use of recycled CDW has also proven to offer structural viability, to be used as pavement layer materials. In South Africa, the use of these recycled materials is still restricted, due to the lack of enough information on their properties and performance. Due to their nature, these types of materials have got a potential for latent hydration, and as for the natural materials, they can be treated with cement to improve their quality, for their use in heavily loaded pavements. A disregard to evaluate the shrinkage of these recycled materials presents a knowledge-gap regarding their suitability and layer cracking, which could lead to wrong choice of a mitigating method.

The key focus of this study is to research the influence cement has on the shrinkage properties of the material. At the same time the potential for latent hydration, and cement influence are investigated for materials with self-cementing properties.

1.3   Research objectives

The majority of research focussing on CSPL has investigated natural aggregates as the material to be stabilised. However, a significant advantage of using recycled aggregates was considered, as stated in previous statements. These recycled materials can be used in the pavement construction, since they are proven to offer structural viability. The question is; do self-cementing materials pose a challenge due to their latent hydraulic properties? Also, does quality improvement of these materials through cement treatment increase the risk of increased shrinkage and ultimate cracking?

The main objective of this study is to investigate the effects of drying and cement hydration on the properties related to shrinkage and cracking of pavement construction materials.

To achieve this main objective, the following specific secondary objectives were defined:

1. Identification of the factors and mechanisms that influence shrinkage of pavement construction materials, through literature study.
2. Characterisation and evaluation of tensile and compressive strengths of research materials, conforming to South African road construction material guidelines, and evaluate their comparison to standard road materials.

3

3. Evaluate previous literature for validation of a specimen preparation procedure that offers the most representative shrinkage results.

4. Determine if Super-Absorbent Polymers (SAP) are able to reduce shrinkage of material and thus mitigate the potential for cracking within layers.

5. Determine whether Recycled Concrete Aggregates exhibit the potential for cracking (with and without stabilisation) by evaluating its shrinkage properties.

1.4   Scope and limitation

Characterisation of the research materials was limited to various standard tests recommended by SAPEM (2014) and TRH 13 (1986) for gravel-crushed aggregate (G4 Hornfels), since recycled aggregates are not defined in South African road construction material guidelines. These tests included materials gradation, Atterberg limits and linear shrinkage, MDD and OMC, as well as CBR determinations. For the evaluation of strength of materials, the two tests considered (UCS and ITS), were limited to the use of one cement percentage (4%) in the sample.

The laboratory shrinkage assessment considered cylindrical specimens, and the measurement was limited to the use of dial gauges. Shrinkage in the circumferential direction was not considered, with cement content and type of material being the only variables, due to the availability of instruments.

1.5   Thesis outline

Chapter 1: Introduction

The first chapter gives a brief background of stabilisation of pavement materials. The chapter discusses shrinkage due to cement-stabilisation and highlights where the knowledge gap is. It also outlines the research objectives, scope and limitation.

Chapter 2: Literature review

The second chapter provides a detailed literature review about stabilisation of materials, with a special attention given to cement-stabilisation. The chapter gives an extensive review of previous studies on cement-stabilisation of pavement materials, as well as cement-treatment of recycled materials. The chapter discusses the factors and mechanisms that influence shrinkage, and reviews the methods previously used for shrinkage evaluation at laboratory level. The chapter also discusses the effect of SAP on shrinkage.

4

Chapter 3: Research methodology

This chapter describes standard tests conducted to characterise research materials. The chapter presents the procedures followed for shrinkage testing, where an experimental design is provided.

Chapter 4: Material characterisation and strength tests results discussion

Following South African road construction material guidelines, this chapter discusses the results obtained from characterisation and strength of materials used for this study.

Chapter 5: Shrinkage test results discussion and interpretation

This chapter discusses and interprets the results obtained from shrinkage tests, through the comparison of the three materials used in this research.

Chapter 6: Implications of shrinkage results

The chapter discusses the implications of shrinkage results in a pavement structure through comparison with existing results.

Chapter 7: Conclusions and recommendations

This chapter presents general conclusions from the findings of this study, and provides recommendations for further research.

CHAPTER 2. LITERATURE REVIEW

2.1   Introduction

This chapter mainly discusses the reviewed literature regarding stabilised materials, as there is very little work on the shrinkage cracking of Recycled Concrete Aggregates (RCA). It is acknowledged that what manifests in these stabilised materials can potentially be the same cause of mechanisms that could create problems in RCA.

Several countries have been using cement-stabilised (treated) materials extensively as pavement base and/or subbase. Pavement materials treated with cement vary from course-grained aggregates, recycled aggregates to fine-grained soils (Terrel et al. 1979). Generally, well-graded granular materials are the most suitable materials to be treated with cement (TRH 13, 1986). Cement Treated Granular Materials (CTGM) can be defined as a mixture in which a small quantity of cement is used as a binder of course granular materials, and which requires appropriate water content for compaction and cement hydration. Figure 2-1 shows the family of cement treated materials (Williams, 1986).

Figure 2-1: The family of cement treated materials (Williams, 1986)

In addition, during the last decades, recycled Construction and Demolition Waste (CDW), comprising of Recycled Concrete Aggregates (RCA) and Recycled Concrete and Masonry (RCM), has been effectively produced and used as aggregates for pavement construction (Hansen, 1992, Xuan et al. 2010 and Van Niekerk, 2002). It can also be treated with cement for the improvement of different required properties (Xuan, 2012).

6

The application of cement as a stabiliser for the material has different advantages such as improving the workability, increasing the strength of the mixture, improving the durability and increasing the load spread capacity (TRH 13, 1986). Despite all these advantages, cement- stabilised layers still have weaknesses due to their nature. The main problems caused by these weaknesses are shrinkage and associated reflective cracking, together with the load induced fatigue cracking (Adaska and Luhr 2004). For pavement layers with untreated RCA, shrinkage can result from latent hydration properties of the material. An appropriate mixture design and a suitable construction procedure can limit and control these problems.

The main objective of this chapter is to provide a detailed overview of the properties and behaviour of Cement-Stabilised Pavement Materials (CSPM) and materials with self-cementing properties, such as the RCA. For this objective, the chapter provides an extensive description of different types and mechanisms of shrinkage, shrinkage cracks and mitigating methods, as well as the effect of Super-Absorbent Polymers (SAP) on shrinkage. Furthermore, it reviews the characteristics and recycling of Construction and Demolition Waste (CDW), and finally discusses shrinkage testing in laboratory.

2.2   Properties and behaviours of cement stabilised layers

Consideration of the factors that influence the properties of Cement-Stabilised Materials (CSM) is essential for an understanding of the properties and behaviour of Cement Stabilised Layers (CSL). This arises of the fact that the influence of the properties of CSM on the behavioural states of a cement-stabilised layer, affects the overall pavement structure as it works in unity (Mbaraga, 2015).

2.2.1   Stabilisation of pavement materials

According to TRH 13 (1986) stabilisation can be defined as the treatment of granular materials with chemicals or any other means for the improvement of engineering properties. There is a need of a clear clarification of the two objects of stabilisation, namely Cementation and modification.

Stabilisation associated with an increase in compressive or tensile strength is referred to as "cementation". The term "cemented material" may be used. When the object of stabilisation is not necessarily to increase compressive or tensile strength, the term "Modification" is used. In this case, the main objective is to reduce the Plasticity Index (PI) and to increase the California Bearing Ratio (CBR). The term "Modified material" may be used.

2.2.1.1 Mechanisms of stabilisation

Stabilisation involves several stabilising agents such as cement, lime, blends of milled granulated blast furnace slag, and blends of fly ash with lime. The choice of a stabilising agent involves many influential factors such as design requirements, laboratory test results, site conditions, availability of stabilisers and economics. For the use of materials in pavement layers, cement is mostly effective for the stabilisation of medium to low plasticity materials. Due to the high cement content required and the complications with pulverizing and mixing, cement is difficult to treat fine, clayey materials (TRH 13, 1986).

According to Freeman and Little (1998), the mechanisms of stabilisation involving cement, lime and fly ash as stabilising agents are as follows:

- **Cation exchange:** amongst other cations, sodium and magnesium are replaced by calcium cations from calcium hydroxide
- **Flocculation and agglomeration:** it consists of an increase in the effective grain size and reduction in plasticity due to flocculation of the clay particles. This results in an increase of strength of the matrix.
- **Pozzolanic reaction:** silicates and aluminates are soluble at clay surface due to the creation of the high pH environment by the available calcium hydroxide. The reaction of silicates and aluminates with calcium ions form cementitious products, which are composed mainly of calcium silicate hydrates or calcium aluminate hydrates, or both.
- **Carbonate cementation:** cementation of the soil particles is caused by the formation of calcium carbonate precipitates, which result from a reaction of calcium oxide with carbon dioxide from the atmosphere.
- **Cementitious hydration reaction:** the production of Portland cement clinker and the coal burning (fly ash) process are initiated by the chemical combination of calcium silicates and/or calcium aluminates, which hydrate rapidly to form calcium silicate hydrates and/or calcium aluminate hydrates.

2.2.1.2 Factors affecting properties of stabilised pavement materials

The main factors that affect the properties of stabilised pavement materials comprise of the host materials, amount and type of stabilising agent, moisture content, compaction, mix uniformity, curing conditions, and the age of the compacted mixture (Xiaojun, 2014)

a) Host Materials

The properties of the host materials significantly affect the performance of stabilised materials. The active participation of soil components in the hydration process, has dominated the traditional consideration that the soil itself is inert. The strength, which is the main object of stabilisation, results from cementitious bonds between the hydration products and soil particles. This means that the choice of the binder type depends on the properties of the host material (Xiaojun, 2014).

According to TRH 13 (1986), cement can be suitable for the treatment of all types of soils but yields best results on well-graded granular materials with sufficient fines, which form a floating aggregate matrix. On the other hand, lime is suitable for stabilisation of medium, moderately fine, and fine-grained soils to increase strength and workability and to reduce swell and plasticity. Fly ash acts as pozzolans and/or fillers to reduce the air void content in the mixture. Little et al. (1987) stated that clay is mostly pozzolanic in nature. Therefore, it does not need addition of pozzolans.

Shrinkage cracking usually occurs for fine-grained materials, particularly those with uniform gradation, since it requires more binder to achieve the required strength. On the contrary, stabilisation of well-graded granular soils requires low binder content, and rarely exhibit shrinkage cracking (Bofinger and Sullivan, 1971). The presence of fine-grained soil negatively affects the shrinkage property of stabilised materials, and has an influence on the possibility of cracking (Kodikara & Chakrabarti, 2005).

In the case of RCA, there might still be a significant amount of latent unhydrated products sitting around these host materials. Houben (2011) revealed that the host materials quality can have an influence as it restrains shrinkage cycles. This behaviour can be a problem in RCA as they get their original state from concrete.

b) Stabilising agents

The type of stabilising agent used has a considerable effect on the properties of stabilised materials for the pavement performance. Stabilised materials with cement as the stabilising agent offer higher stiffness, more shrinkage and are more prone to fatigue, compared to those containing lime, fly ash, or blended stabilising agents (cement blended with lime and/or fly ash). Stabilisation with blended cement is disposed to less shrinkage effects than using a single stabilising agent. More time is required for stabilisation with blended cement, to achieve the same long-term strength and stiffness (TRH 13, 1986).

The reduced heat generated during the hydration process explains why stabilisation with lime and/or fly ash lessens shrinkage, than stabilisation with cement or blended cement. However, Hodgkinson (1991) revealed that stabilisation with lime and/or fly ash takes a long time, and provides lower strength and stiffness. Their use is generally limited in Australia.

c) Amount of stabilising agent

The amount of stabilising agent is another influential factor to the properties of stabilised materials. An increase in the quantity of stabilising agent in the stabilised material leads to an increase in strength, stiffness and shrinkage. Chakrabarti et al. (2002) indicates that in Australia, the contents of stabilising agents used in stabilised materials vary from 0% to 8% by dry mass. This range is much less, compared to the percentages used for concrete, which can be over 15%.

Different authors recommended various amounts of stabilising agents for material stabilisation. Hodgkinson (1991) recommended 3.4% as cement content for the stabilisation of in situ recycled pavement materials. He recommended that in the presence of high clay/fines content, the cement content could increase up to 4.6%. Chakrabarti and Kodikara, (2003) indicated that for stabilisation of crushed rock with blended cement, a decrease in shrinkage was achieved by increasing this stabilising agent up to 4%, but later on, the shrinkage increased again. Bofinger and Sullivan (1971) reported that an increase in crack spacing results from an increase in cement content for a given soil. In the case of RCA, the latent unhydrated products inherently increase the amount of active cement.

To confirm that the amount of active stabiliser is not unsatisfactorily lessened by the early cation exchange and flocculation reactions, as described in Section 2.2.1.1, it is essential to determine the "Initial Consumption of Lime (ICL)" or "Initial Consumption of Cement (ICC)" (Paige-Green, 2008). The ICL can be explained as a measure of how much lime is required to raise and keep the pH of the soil up to 12.4, which is considered as a point where any further addition of lime will not raise the pH, but instead will start the stabilisation process (Ventura, 2003). The Eades and Grim (1966) test was used to perform this technique, and it is currently specified as BS 1924-2 (BSI, 1990) (Paige-Green, 2008).

d) Moisture content and compaction

It is common knowledge that during compaction, the moisture content of stabilised materials has a strong influence on the achieved density for a given compactive effort. The density increases with an increase in moisture content, attains a maximum value, and then starts to

10

decrease with any further increase in moisture content. Holtz and Covacs (1981) state that the above statement is due to the fact that excess moisture limits the soil particles from getting closer to each other. The highest achieved dry density is referred to as "Maximum Dry Density" (MDD), and the moisture content corresponding to this value is known as "Optimum Moisture Content" (OMC) (Figure 2-2). The density considerably affects the fatigue behaviour of stabilised materials.

The required moisture content is very important during the mixing and forming stages of cement mixture. Insufficient moisture content causes inadequate hydration, while excessive moisture content causes the reduction in final setting strength (Montgomery, 1998).

Figure 2-2: Determination of the MDD and OMC of a cement-stabilised crushed limestone (Beckett and Ciancio, 2014)

In the figure above, L-series, O-series, and H-series, respectively indicate -2% OMC, OMC, and + 2% OMC. S_r indicates the degree of saturation.

e) Curing conditions

The curing conditions, which include temperature and moisture, considerably affect the performance of stabilised materials. As specified in the previous statement, adequate moisture supply is required for the hydration of stabilised materials during the curing process. When

11

the curing of stabilised materials is under dry conditions, the shrinkage, which is due to drying occurs, and can cause microcracks, followed with a reduction of the elastic modulus. In laboratory, the use of plastic sheets to cover stabilised material samples can avoid moisture loss (Little et al., 2002).

Higher temperatures accelerate the curing process of stabilised materials and can cause microcracks. Little et al. (2002) reported that accelerated curing at 113^0F (45^0C) for 28 days simulates nearly curing for 100 days at approximately 73^0F (23^0C), while curing for around 40 to 45 days at 113^0F (45^0C) approximately corresponds to curing for 6 months at 73^0F (23^0C).

In his investigation, Mbaraga (2015) obtained definite answers for stabilised materials cured to higher temperature. He considered a curing temperature of 70^0C, and cured for 3 days (72 hours), which seemed to be too excessive. However, Dumbleton and Ross (1960) indicated that for the majority of cohesive materials, an increase in material strength associated with the curing temperature is greater at higher temperatures, compared to lower temperatures. Ruff (1965) agrees with Dumbleton and Ross (1960).

Figure 2-3: Unconfined Compressive Strength vs curing temperature at various curing times (Ruff, 1965)

f) Age

The increase of strength and stiffness of stabilised materials continues for long time after mixing and compaction. TSA (1998) states that for cementitiously stabilised materials, over 80% of the strength gained for the first 30 days, and the successive increase in strength, can continue even after 50 days. This period could be much longer when blended cement, lime and/or fly ash were used as stabilisers.

Little et al. (2002) reported on the long-term strength gain of base layers stabilised with lime-cement-fly ash. The strength increase doubled between six-month and ten-year period. This gain in strength was caused by pozzolanic reactions.

2.2.1.3 Cement properties and stabilisation

Standards SANS 50196 (2006) parts 1 to 7 and SANS 50197 (2013) parts 1 and 2, provide the full specifications and testing procedures for common cement types used in South Africa. Table 2-1 summarises the chemical composition of Portland cement with the corresponding nomenclature.

Table 2-1: Chemical composition of Portland cement (Wainwright, 2005)

Name	Chemical compound	Nomenclature
Calcium oxide	CaO	C
Silicon dioxide	SiO_2	S
Aluminium oxide	Al_2O_3	A
Iron oxide	Fe_2O_3	F
Magnesium oxide	MgO	M
Alkali (Sodium, Potassium)	Na_2O_2, K_2O	-
Sulphur Trioxide	SO_3	-
The four main compounds in cement		
Compound name		**Symbol**
Tricalciumsilicate		C_3S
Dicalciumsilicate		C_2S
Tricalciumaluminate		C_3A
Tetracalciumaluminoferrite		C_4AF

Wainwright (2005) states that the hydration reaction of water and cement comprises the following:

13

a) an increase in temperature due to the heat released, since the reaction is exothermic

b) the four main compounds react with water, where tricalciumsilicate and dicalciumsilicate reactions are similar and different from the two others

c) the reactions happen at the surface of cement particles and at different rates

d) stability of hydration products in water

e) no existence of the resultant composites in pure state

Due to its complexity, it is not easy to illustrate the chemical reaction of Portland cement by simple chemical equations. According to Tazawa et al. (1995), for every compound with concurrent gypsum, the chemical reactions that happen during the hydration process include but are not limited to the following equations:

$$2C_2S + 6H_2O \quad \rightarrow \quad C_3S_2H_3 + 3Ca(OH)_2$$

Equation 2-1

$$2C_2S + 4H_2O \quad \rightarrow \quad C_3S_2H_3 + Ca(OH)_2$$

Equation 2-2

$$C_3A + 3(CaSO_42H_2O) + 26H_2O \quad \rightarrow \quad C_3A3CaSO_432H_2O$$

Equation 2-3

$$2C_3A + C_3A3CaSO_432H_2O + 4H_2O \quad \rightarrow \quad 3[C_3ACaSO_412H_2O]$$

Equation 2-4

$$C_3A + Ca(OH)_2 + 12 H_2O \quad \rightarrow \quad C_3ACa(OH)_212H2O$$

Equation 2-5

$$C4AF + 3(CaSO42H_2O) + 27H_2O \quad \rightarrow \quad C_3(AF)3CaSO_432H_2O + Ca(OH)_2$$

Equation 2-6

$$2C_4AF + C_3(AF)3CaSO_432H_2O + 6H_2O \quad \rightarrow \quad 3[C_3(AF))CaSO_412H_2O] + 2Ca(OH)_2$$

Equation 2-7

$$C_4AF + 10H_2O + 2Ca(OH)_2 \quad \rightarrow \quad C_3AH_6-C_3FH_6 \text{ (solid solution)}$$

Equation 2-8

Figure 2-4 illustrates five stages of the hydration process, which comprise mixing, dormancy, hardening, cooling, and densification.

The monitoring of heat produced during the reactions involved in the hydration process is essential and manifests as follows (Taylor et al. 2007):

a) production of a short-term heat during mixing

b) no heat generated during dormancy

c) stable rise in heat during hardening

d) The heat reaches the peak and drops continuously during cooling

e) minor heat is generated during densification

Figure 2-4: Different stages of hydration (Taylor et al., 2007)

Following is the description of five stages of hydration (Taylor et al., 2007)   :

- **Mixing:** this stage lasts for about 15 minutes. Silicates, which dissolve very slowly, react with water to produce compounds that strengthen the concrete but their effect is not instantaneous. Aluminates and gypsum, which react within very short time (minutes) and have an immediate effect, generate considerable heat by creating new compounds. There is creation of a gel-like substance.

- **Dormancy:** this stage takes 2 to 4 hours. The material is plastic and there is no generation of heat. It behaves as if nothing is happening to the mixture but cement is still dissolving and water becomes saturated with calcium and hydroxyl (OH) ions.

- **Hardening:** this stage also lasts about 2 to 4 hours. There is formation of Calcium-Silicate-Hydrate (C-S-H) chains by silicate reactions. Tricalciumsilicate controls the early strength-gain, while dicalciumsilicate controls the long-term strength-gain.

- **Cooling:** the material shrinks due to changes in temperature and moisture content. There is creation of internal tensile stresses and these may cause the material to separate or crack.

15

- **Densification:** this final stage continues for years depending on the available moisture within the material matrix. Hydration will continue as long as water and cement are present.

Amongst others, the following are the factors that influence the process of hydration of Portland cement (Stutzman, 1999 and Copeland et al. 1960) :

a) chemical composition

b) water/cement ratio

c) presence of mineral admixtures and fineness

d) curing temperature

Uchikawa et al. (1996) studied the hydration reactions, hydration products, and pore structure of concrete, by replacing fine aggregates with a large amount of mineral admixtures comprising fly ash, slag, limestone and silicious stone. They revealed that the fluidity of concrete decreases and the viscosity increases due to the increase in fine particles. They observed a higher strength caused by the densification from the effect of filled mineral admixtures and additional C-S-H created by Pozzolanic reactions. They concluded that the increase of cement paste in concrete caused a slight increase of the creep of the concrete for the fly ash concretes, and a reduction of the dynamic Young's modulus.

Helmuth and Verbeck (1968) stated that high temperature curing creates changes in the microstructure of cement paste. It also has an influence on porosity, bound water and ionic pore solutions of the material matrix. The rapid initial rate of hydration, attributed to higher temperatures, results in a non-uniform distribution of the products of hydration within the material microstructure. Due to the low solubility and diffusivity of the products of hydration, the time available for these products to diffuse away from the cement particles is not sufficient, which leads to their non-uniform precipitation within the hardened cement paste. This non-uniformity of products of hydration has an influence on the mechanical properties of stabilised materials.

2.2.2 Benefits and problems associated with cement-stabilised pavement layers

The main objective of using cement-stabilised materials is to increase the strength of pavement layers (base or subbase) to obtain CSL that provide an excellent support for the pavement structure due to their good load-spreading properties. In comparison with equivalent un-stabilised materials, CSM are more resilient, water resistant, and uniform.

16

Although CSL are strong, this does not automatically guarantee good long-term pavement performance. These layers are prone to shrinkage cracking. It is therefore necessary to provide acceptable strength, while minimizing shrinkage and maximizing durability. Reduction of the binder content, which limit the shrinkage and increase the durability, can improve the long-term pavement performance (Little et al. 1995).

2.2.2.1   Benefits

Cement stabilisation improves stability and strength of pavement materials. The presence of cement stabilised layers in pavement, significantly reduces the vertical pressure on the subgrade (Freeman and Little, 1998).

The most significant advantages of stabilisation include the following (TRH 13, 1986):

a) increase of the material strength

b) enhancement on the durability and resistance on water effects

c) drying out of wet soils

d) upgrading of the workability of clayey materials

According to Little et al. (1987), the following are some of the engineering advantages of soil stabilisation:

a) working platform purpose

b) dusting reduction

c) soil waterproofing

d) improvement of borderline aggregates or soils

e) strength improvement

f) durability improvement

g) control of volume changes

h) upgrading of soil workability

i) drying of wet soils

j) reduction in pavement thickness necessities

k) aggregates conservation

l) reduction in construction and haul costs

m) energy preservation

n) provision of a transitory or permanent wearing surface

The purpose of cement stabilisation for the consideration in pavement improvement is as follows (Little et al. 1987):

a) limit subgrade stresses in order to prevent rutting and plastic deformation

b) deliver required support to the wearing course, so as to retard fatigue cracking and limit transient deflections

c) provide a working platform to accelerate construction

d) provide an impermeable layer (base or subbase) to prevent moisture changes in the subgrade.

2.2.2.2   Problems

Achieving an adequate strength for the performance of pavements with cement stabilised layers, does not always guarantee consideration of the properties that characterise shrinkage and durability potential. George (1990) states that load-induced fatigue cracking and shrinkage cracking are the primary distresses that affect the performance of pavements with cement-treated layers. While fatigue cracks originate from the bottom of CSL and caused by traffic load and material strength, shrinkage cracks appear at the surface of CSL and are due to the volume change.

Despite the fact that the main objective of stabilisation is to ensure adequate (high) strength and stiffness, Little et al. (1995) revealed that a heavily stabilised base frequently leads to premature failure in the form of severe shrinkage cracking followed by accelerated fatigue cracking. This means that an emphasis on shrinkage potential is vital, the same as strength and stiffness.

Freeman and Little (1998) revealed that shrinkage cracking in stabilised layers, has very little effect on riding quality of the pavement at the time of occurrence, but the "secondary deterioration" effects, including deflection and resultant weakening of the subgrade, are harmful to the performance of the pavement structure.

At the beginning, shrinkage cracks appear as single isolated cracks. With the development of the shrinkage and the application of traffic loads, they can meet and form connected multiple cracks. At this time, they reduce the entire stiffness of the pavement, which influence water infiltration and capillary rise into the bottom layers, and therefore, provide pathways for erosion of cement-stabilised materials (Chakrabarti and Kodikara, 2003). However, SAPEM (2014) reveals that for cement stabilised layers, the micro-cracks can result in reduction of layer stiffness, when these layers have reached the equivalent granular state (present a

18

comparable effective stiffness to an unbound granular layer). In this case, as cracks are still working together, there is a good interlock and no influence to water infiltration. The layer stiffness is still supporting the pavement structure very well.

The size and spacing of the shrinkage cracks significantly affect the performance of the pavements with cement stabilised layers. Closely-spaced and small cracks are less effective to reflect through the surface than widely-spaced and large cracks. The more the penetration of cracks through the surface is, the more the effect on the performance of the pavement will be, since there is an increase in the ingress of the surface water to the bottom layers (Bofinger and Sullivan, 1971).

Freeme (1984) revealed that cement stabilised layer modulus reduces due to the occurrence of shrinkage cracks alongside repeated loading. In order to clarify this reduction in layer modulus, Freeme assessed the changes in elastic modulus of a material class C2 (South African material classification system). Figure 2-5 illustrates these changes.

Figure 2-5: Change in elastic modulus of a cement stabilised layer (Freeme, 1984)

Figure 2-5 indicates three phases; precracked phase, postcracked phase, and influence of excess porewater pressure (EPWP). These phases represent the trends a stabilised layer experiences. The effective modulus is reasonably high in the precracked phase. The stabilised layer is undamaged. In the postcracked phase, the layer modulus reduces due to crack propagation, which creates a poor load-transfer. This is actually the phase where most structural and functional life of the stabilised layer takes place. In Phase 3, the layer modulus reduces again due to water infiltration into the underlying layer pavements. This layer modulus reduction is more pronounced for poor quality materials because of their higher potential for cracking.

2.3   Construction and Demolition Waste (CDW)

2.3.1   Introduction

The growing need for sustainable development has made recycling of waste one of the highest requirements in many countries. The recycling of CDW started after the Second World War. Different countries such as Netherlands, Germany, USA, Japan, Brazil, China, and Australia used them as unbound base/subbase materials for pavements construction. The shortage of natural materials and strict laws on opening new borrow pits and landfills are the main cause of this need of recycling in pavement engineering (Hansen, 1992).

Practically, recycled CDW is generally composed of recycled concrete and masonry with different variations in composition. Depending on the countries, different terminologies denote Recycled Concrete and Masonry (RCM). Some studies consider RCM as Recycled Crushed Aggregates (RCA), while some others consider it as Recycled Construction and Demolition Waste (RCDW) or Recycled Debris.

However, recycled concrete can be separated to recycled masonry as referred to the definition of Hansen (1992). This author has defined Recycled Concrete Aggregates (RCA) as materials obtained from the crushing of old concrete, with limited quantity of brick and masonry. He has also defined Recycled Masonry (RM) as aggregates obtained from the crushing of masonry rubble. He indicated that masonry resulted from the demolition of building and other civil structures mainly composed by ordinary concrete, clayey materials, and concrete blocks. The material (RCA) used in this study refers to this definition.

Bester et al. (2004) define RCM as aggregates obtained by the crushing of residual materials remaining from buildings or any other structures under construction, renovation and demolition. This definition includes haul-backs and overruns, with the former materials meaning excess from produced concrete that have not been supplied to users, while the latter materials are excess concrete supplied to users.

The quality control of recycled CDW is essential. For example the Dutch specifications have established the requirements of recycled CDW to be used as base course material (Table 2-2). The specification considers three types of recycled CDW, which depend on the main component. Furthermore, the other types of stony materials, contaminants and organic materials are carefully controlled (Xuan, 2012).

20

Table 2-2: Dutch specifications for recycled CDW (Xuan, 2012)

Type of recycled CDW	Masonry granulates	Mixed granulates	Concrete granulates
Dry density of crushed masonry, kg/m³	≥ 1600	≥ 1600	
Dry density of crushed concrete, kg/m³		≥ 2100	≥ 2100
Crushed masonry and stony materials by mass, %	≥ 85	≤ 50	≤ 10
Crushed concrete and stony materials by mass, %	-	≥ 50	≥ 80
Other types of stony materials (asphalt, glass, slag, light weight concrete etc.) by mass, %	≤ 15	≤ 10	≤ 10
Contaminants (gypsum, metals, plastic, etc.) by mass, %	≤ 1	≤ 1	≤ 1
Organic materials (wood, rope, paper, etc.) by mass, %	≤ 0.1	≤ 0.1	≤ 0.1

2.3.2 Recycling of CDW

The main proportion of construction and demolition waste is concrete rubble and brick rubble (Figure 2-6 (a) and Figure 2-6 (b)). Literature confirms that with appropriate processes of recycling of CDW, it is likely to produce aggregates having enough potential for use in pavement construction, such as the present practice in the Netherlands (Xuan, 2012).

Figure 2-6: Construction and Demolition Waste (a) Concrete rubble (b) Masonry rubble

Figure 2-6 shows that before CDW can be reused, it has to be crushed. This can be done on site, by mobile crushing machines; or off site, at a crushing plant. After this activity, the material will be free of unwanted components such as iron, wood, paper and plastics. It will then display a suitable particle size distribution, which has an influence on shrinkage of the material.

The treatment of CDW includes the following activities (Xing, 2004):

    a) removal of non-stony materials, such as wood, plastics, paper and course materials

    b) size reduction

    c) separation of ferrous metals, such as iron and steel

    d) separation of non-ferrous metals, such as aluminium

    e) obtaining different size groups (classification by sieving)

    f) removal of contaminants, such as organics, heavy metals and soluble salts

Figure 2-7 illustrates this treatment process:

Figure 2-7: Preliminary separation for the removal of unwanted materials (Xing, 2004)

The removal of unwanted components from CDW needs suitable separation techniques. This removal considers the main assets of separation such as particle size, shape, density, magnetic susceptibility and colour. In relation to differences in size, the removal of fine materials is by screen. Associating size and density, the separation of light- weight materials such as wood, paper, and plastics, from stony materials is by hand sorting and wind-sifting. Separation of stony materials from each other is by differences in density. Magnetic separation removes ferrous metals whereas removal of non-ferrous metals is by eddy current separation. The consideration of colour separation is necessary, when there is notable colour difference between particles. It should be noted that dry methods are always cheaper than wet methods, due to the need of expenses for discarding of slurry, left in case of wet separation. Table 2-3 illustrates these suitable separation techniques (Xing, 2004):

Table 2-3: Separation techniques for Concrete and Demolition Waste (Xing, 2004)

Technique	Type	Input of material	Feed properties	Parameters
Aquamator system	wet	containing lighter and heavier materials	weight/density	water flow speed
Coal-spiral	wet	materials with different densities (<3mm)	density	water speed, amount of feed
Colour separation	dry	materials with different colours	colour	
Eddy current separation	dry	non-magnetic metals	non-magnetic metal	electric current
Fluidised bed separation (with water)	wet	materials with different densities	density	particle size and density, water supply
Fluidised bed separation (with sand)	wet	materials with different densities	density	particle size and density, air flow speed
Grab crane	dry	large and light material	particle size	particle size
Hand-sorting	dry	large and light material	particle size	particle size
Humphrey spiral	wet	materials with different densities (<3mm)	density	particle density, amount of feed, water supply
Jigging	wet	materials with different densities (<3mm)	density	particle size, speed and frequency of water flow
Magnetic separation	dry	containing ferrous metals or iron oxide	Magnetic susceptibility	electric current
Screen	dry/wet	material with different particle sizes	particle size	the size of material to be removed
Thermal method	dry		thermal property (shrinkage)	temperature and time
Wind-sifting	dry	light material	weight	wind strength

The following is a flow chart that summarises these separation techniques:

23

Figure 2-8: Concrete and Demolition Waste treatment flowchart (Xing, 2004)

2.3.3   Performance of recycled CDW

The physical characteristics and chemical composition of aggregates have a strong influence on their strength and durability, and therefore, on the overall pavement performance. Dukatz (1989) has assessed some pavement performance indicators related to the impact of aggregate

properties. Recycled aggregates from CDW are prone to different contaminants, which can negatively affect their performance, and thus, display less mechanical performance than needed.

Table 2-4: Impact of aggregate properties on pavement performance (Dukatz, 1989)

Property	Permanent Deformation	Fatigue	Low Temperature Cracking	Moisture Damage
Physical				
Shape	5	4	3	2
Surface	3	1	3	4
Absorption	3	3	1	4
Specific gravity	3	3	3	1
Morphology	3	4	3	4
Gradation	5	4	3	4
Chemical				
Composition	3	3	2	5
Solubility	3	3	1	5
Surface charge	1	2	2	5
Mechanical				
Strength	3	4	2	1
Durability	5	5	2	1
Toughness	5	5	2	1
Hardness	3	5	1	1

Note: 5 denotes significant impact and 1 denotes minor impact

Different investigations, such as Poon et al. (2006); Singh and Kumar (2014); Edil and Schaertl (2009), and Chai et al. (2009) reveal that the particle size distribution of RCA materials vary according to the crushing methods. These investigations state that these materials display a lower particle density and a greater angularity, compared to natural subbase/base course materials. The surface of RCA shows some residual mortar, cement paste and contaminants from CDW. The presence of this mortar has an influence on the properties of RCA, such as rougher surface texture, lower specific gravity, and higher water absorption, in comparison to natural aggregates.

The self-cementing ability of RCA is an important characteristic that contributes to their performance, as shown by the above investigations. This self-cementation (re-cementation behaviour) occurs when unhydrated cement particles, present in RCA materials, are exposed to water, permitting the continuation of hydration. This has an impact on the increase of stiffness compared to the use of natural aggregates, and therefore, contributes to the long-term performance of the material in the pavement. An investigation from Chai et al. (2009) reveals that this characteristic does not have any effect on shrinkage cracking. All these investigations believe that self-cementing extent depends on parameters such as age, grade and mix-proportions of the RCA, but they recommend further studies to establish a clear relationship.

Molenaar (2008) investigated the fatigue performance of self-cementing base courses. He used a mixture of crushed concrete and crushed masonry with addition of 10% of pulverised blast furnace slag, as the materials for the investigation. He concluded that, although these materials tested showed an increase of stiffness and strength in time due to self-cementation; repeated loading disturbed the self-cementation process, which resulted in a considerable lower strength and stiffness, in comparison to the values found for undisturbed samples and section. No cracks were observed in tested samples or section, which was interpreted as if the materials weakened from a bound state to an unbound one, without developing any noticeable cracks. It was therefore, not possible to describe a fatigue relation for the materials tested. However, design guidelines were proposed, which include keeping the ratio σ_1/σ_{1f} at the top of the base course, below 0.4; and the horizontal tensile strain at the bottom of base courses, below 10^{-4} m/m.

2.4   Types and mechanisms of shrinkage of pavement layers with cement stabilised or latent hydraulic behaviour

Different forms of cracking, identified as the most severe distresses for pavements with Cement-Stabilized Layers, result from shrinkage of CSL. CSPL are prone to different types of shrinkage and these are caused by several mechanisms. The following section explains the types and mechanisms of shrinkage associated with CSPM. Several researchers indicated that drying shrinkage is the major reason of shrinkage cracking for pavements.

2.4.1   Shrinkage types

Shrinkage of CSL includes autogenous shrinkage, drying shrinkage, thermal shrinkage, and carbonation shrinkage; which are respectively due to hydration, loss of moisture, low temperature contraction, and chemical reaction with atmospheric carbon dioxide (Xiaojun, 2014). The following section provides more details on each type of shrinkage.

2.4.1.1   Autogenous shrinkage

The source of autogenous shrinkage is hydration. This type of shrinkage does not usually imply important moisture loss from the hydration of cement. During the hydration of cement, which involves the movement of water, there is a need of more water to replace the consumed one. Water moves from high to low saturation zones (George, 1973).

Hydration of CSM leads to shrinkage due to the phenomenon known as "Le Chatelier contraction". This phenomenon relies on the fact that the volume of hydrated products is smaller than the original total volume of the binder material and water. According to Tazawa et al. (1995), the volume reduction of the hydrated products, from the volume of the original input material can reach 8% to 10%, depending on the main chemical reaction involved in hydration.

The chemical reactions involved in hydration consume moisture and results in the drying of the specimen. There is a macroscopic volume reduction under a constant temperature without any exchange in moisture to and from the specimen (Tazawa et al. 1995). As for the drying shrinkage, in the early stages, when the material has not gained enough strength, tensile stresses develop, which pull the material particles closer and generate some dimensional changes (George, 1973; Hansen, 1987). Autogenous shrinkage due to the phenomenon of the Le Chatelier contraction is very little, in comparison to shrinkage induced by the loss of internal moisture resulting from hydration (Xiaojun, 2014).

2.4.1.2   Drying shrinkage

Drying shrinkage is caused by the moisture loss at a given temperature and humidity conditions. This has an influence on the material stability as it generates change in volume of the material. Hansen (1987) states different factors that simultaneously have an influence on the magnitude of volumetric change of a material. Those factors include time-scale deformations, hydration of cement, as well as internal and external restraints.

The identification and explanation of volume reduction in cementitious materials is very complex. Tazawa and Miyazawa (1992) revealed that volumetric changes in cementitious materials comprise material expansion and contraction. Material expansion is due to the hydration, whereas material contraction is due to drying out and/or moisture loss. There is moisture evaporation from the microstructure of a material when subjected to a given temperature and relative humidity. This moisture evaporation leads to the desiccation and therefore, reduction in volume (Bisschop, 2002 and Hansen, 1987).

Kodikara and Chakrabarti (2006) believe that there is a direct relationship between drying shrinkage and moisture loss from cement-stabilised pavements. According to them, from any porous material, the moisture loss depends generally on the surface area, the lengths of the moisture migration pathways, and the drying environment. Consequently, the moisture loss magnitude and the shrinkage potential are different at a given drying time for one-dimensional (1-D) and for three-dimensional (3-D) drying. One-dimensional (1-D) and three-dimensional (3-D) conditions, refer to the faces drying is taking place. One dimensional shrinkage was considered for this research, because shrinkage in the circumferential direction was not measured, and the bottom face was placed on the rigid frame.

Figure 2-9 and Figure 2-10 respectively illustrate the results of drying shrinkage and moisture loss at a given drying time, for crushed basaltic aggregate stabilised with general-purpose Portland cement (GP) (Kodikara and Chakrabarti, 2006).

Figure 2-9: Drying shrinkage against drying time (after Kodikara and Chakrabarti, 2006)

Figure 2-10: Measured and predicted moisture loss against drying time (after Kodikara and Chakrabarti, 2006)

It is clear from Figure 2-9 and Figure 2-10 that at a particular binder content, the drying shrinkage was higher for the specimen dried under 1-D drying conditions than the ones dried under 3-D drying conditions. The moisture loss was higher for the specimen made from material stabilised with less binder content.

The following points are a summarised comparison of drying and autogenous shrinkage by (Mbaraga, 2015):

a) drying shrinkage results from moisture loss through evaporation to the outside environment whereas autogenous shrinkage is due to the consumption of water by hydration reaction

b) humidity and temperature are the main influential factors to both shrinkage types

c) the same mechanism such as capillary tension theory apply to both shrinkage types

d) mitigation of drying shrinkage comprises water retention (prevention of diffusion) or water supply whereas mitigation of autogenous shrinkage involves the reduction of the micro-pore structure

e) the mineral composition of cement has an influence on the magnitude of both shrinkage types

2.4.1.3 Thermal shrinkage

Thermal shrinkage is caused by contraction at low temperature (Wang, 2013). Temperature is also an important factor of shrinkage when cement hydration is considered. Williams (1986) revealed that with a typical thermal coefficient of 10µs (microstrains) per degree Celsius, reserved for cement-stabilised granular material, only a temperature fall of a few degrees would induce enough strain to cause fracture in a brittle material at the initial stage of curing, when the tensile strength is low. Luckily, during the early age of CSM, the tendency of hydration heat is to increase the temperature. This heat generated by hydration in CSM depends on the binder content and rate of hydration.

Holt (2001) states that due to cement hydration, the concrete temperature changes during early ages. The early heat of hydration is normally 5 to 8^0C (10 - 15^0F) of adiabatic temperature rise per 45kg of cement. Without any existence of retarding conditions, the heat rise naturally happens in the first 12 hours. There is contraction or shrinkage in the following stages when concrete is cooling. Some of the thermal expansion is elastic, which means that the concrete can return to its original dimensions when cooling. Any non-elastic portion results in permanent thermal shrinkage.

Williams (1986) reports that for gravel lean concrete, cracking is unavoidable under conditions of full restraint in case of seasonal temperature fall of 30^0C. Nevertheless, George (1969) indicates that contraction caused by temperature in stabilised soils is less important compared to the one resulting from drying, due to the need of low binder content in stabilised soils.

2.4.1.4   Carbonation shrinkage

Carbonation shrinkage is mostly a characteristic of concrete material, but the same mechanisms may apply to CSM in lesser degree. It happens for concrete exposed to air containing carbon dioxide. Holt (2001) revealed that this reaction between cement paste of the hardened concrete, moisture, and carbon dioxide from the air, results in decrease in pH of the concrete and a minor shrinkage.

Claisse et al. (1999) define carbonation of concrete as the chemical reaction between the products of hydration and atmospheric carbon dioxide. They state that during the process of carbonation of concrete, the porosity of the exposed concrete reduces since the volume of product from reaction ($CaCO_3$) is greater than the original volume of reactants. There is an increase in the weight of concrete and irretrievable carbonation shrinkage. Erlin and Hime (2004) agree with this definition and add that hydration resulting compounds chemically react with carbonic acid, formed after dissolution of atmospheric carbon dioxide in water.

According to Claisse et al. (1999), the following are the chemical reactions between atmospheric carbon dioxide and the products of hydration during the carbonation of concrete process:

$$Ca(OH)_2 + CO_2 \quad \rightarrow \quad CaCO_3 + H_2O \qquad \qquad \text{Equation 2-9}$$

$$CSH + 3CO_2 \quad \rightarrow \quad (3CaCO_3 \cdot 2SiO_2 \cdot 3H_2O) \qquad \qquad \text{Equation 2-10}$$

$$C_3S + 3CO_2 + vH_2O \quad \rightarrow \quad SiO_2 \cdot vH_2O + 3CaCO_3 \qquad \qquad \text{Equation 2-11}$$

$$C_2S + 2CO_2 + vH_2O \quad \rightarrow \quad SiO_2 \cdot vH_2O + 2CaCO_3 \qquad \qquad \text{Equation 2-12}$$

Different researchers such as Netterberg and Paige-Green (1984), Paige-Green et al. (1990) and Bagonza et al. (1987) investigated on carbonation of lime and cement-stabilised pavement layers. They all agree that carbonation is one of the factors that contribute to failure

and occurs mainly during curing and under the following exposure to the atmosphere prior to sealing. Particularly for lime-stabilised pavement layers, during carbonation process, lime reverts to the limestone it resulted from. In this case, lime becomes unavailable for the completion of stabilisation process, and therefore, for the preservation of the cementing compounds.

2.4.2   Shrinkage mechanisms

According to different researchers such as Hansen (1987), Bazant (1988), Brandt and Li (2003), Soroka (1993) and Kovler and Zhutovsky (2006); the four main noticeable shrinkage mechanisms are surface tension, capillary tension, movement of interlayer water, and disjoining pressure.

Even though until now, no unified theory has explained the drying shrinkage behaviour over the entire range of relative humidity, the general believe is that this involves more than one mechanism. This complexity is largely due to the extensive range of the pore size distribution in concrete mixes. Figure 2-11 indicates the pore size range of concrete as revealed by (Mehta and Monteiro, 2006).

Figure 2-11: Typical size range of pores in a hydrated cement paste (Mehta and Monteiro, 2006)

Following is a brief description on these mechanisms as explained by (Idiart, 2009):

2.4.2.1 Surface tension

Attraction and repulsive forces, present in all directions from close molecules, maintain the equilibrium in a solid material. For molecules lying on the material surface, the absence of symmetry results in a force perpendicular to the surface, inducing compressive stresses that stimulates the material contraction. Surface tension refers to the tension resulting in this surface (Idiart, 2009).

Moisture content and adsorbed water layers on the material surface are the main factors that affect the extent of induced compressive stresses. The presence of these adsorbed water layers indicates a decrease in compressive stresses and thus, surface tension. This results in an increase in volume (swelling). On the other hand, when drying happens, these layers disappear and there is an increase in surface tension, which results in a decrease in volume (shrinkage). Brandt and Li (2003) revealed that this mechanism is valid for RH < 40%

2.4.2.2 Capillary tension

In drying porous media, when hardened cement paste is ready for drying, a meniscus forms in its capillaries (capillary pores). This meniscus creates surface tension forces, which causes tensile stresses in the capillary water. The presence of compressive stresses in the nearby solid, balances these tensile stresses, and leads to the formation of elastic shrinkage strains as illustrated in Figure 2-12 (a). Brandt and Li (2003) stated that this mechanism cannot explain shrinkage deformations at low RH. It is only active in the high RH range (< 50% RH).

Equation 2.13 (Kelvin equation) predicts the recovery of these shrinkage strains for further stage of drying process.

$$\ln(H) = \frac{M_V}{RT}\gamma\left(\frac{1}{r_1} + \frac{1}{r_2}\right) \qquad \text{Equation 2-13}$$

Where;

H = RH

γ: Surface tension force

r_1 and r_2: Radii of the meniscus ($r_1 = r_2$ for a cylindrical pore)

T: Temperature

M_V: Molar volume of water

R: Universal gas constant

Equation 2.14 (the Laplace equation) calculates the force applied on the pore walls (σ).

$$\sigma = \gamma \left(\frac{1}{r_1} + \frac{1}{r_2} \right)$$

Equation 2-14

2.4.2.3 Movement of interlayer water

Bazant (1988) illustrated that this mechanism is due to the CSH layered-structure for the cement gel. Normally, interlayer water can migrate out of the CSH sheets following a reduction of RH to about 10%. This migration of water results in a decrease in the distance between these layers, which induces macroscopic shrinkage strains (Figure 2-12 (d)). In this case, any small amount of water loss contributes to large volume reductions.

2.4.2.4 Disjoining pressure

An increase in the local RH creates an increase in the thickness of the adsorbed water layer. When varied surfaces are very close to each other, inside the material, these layers do not completely develop under the nearby RH, and form zones (areas of hindered adsorption) where disjoining (swelling) pressures develop. These pressures cause the swelling of the material as they separate the two surfaces.

When drying occurs, disjoining pressures decrease and result in shrinkage strains as the separation of close particles reduces. Beltzung and Wittmann (2005) state that this is the main mechanism that explains hygral volume changes above 50% RH, as the pore solution cannot form a capillary meniscus at the nano-scale.

Figure 2-12 illustrates theses mechanisms:

Figure 2-12: Schematic representation of mechanisms acting on drying of concrete. (a) Capillary tension (b) Surface tension (c) Disjoining pressure (d) Movement of interlayer water (Idiart, 2009)

2.4.3   Factors influencing shrinkage

Various text books such as Soroka (1993) and Kovler and Zhutovsky (2006) have discussed the factors influencing drying shrinkage in concrete. The following section gives a brief description on the main factors, which include cement content, curing time, moisture content, compaction and soil type.

2.4.3.1   Cement content

The cement paste in concrete results from the cement content used. The cement paste content defines the shrinking part of the material, as aggregates are normally inert. Increasing the cement content will increase the cement paste content and consequently, the shrinkage. Cement stabilisation can reduce shrinkage due to the tendency of the cement matrix to restrain

34

the movement of the soil, but the moisture loss during the hydration process will still cause some shrinkage.

George (1968) investigated soil-cement mixtures (such as montmorillonite and kaolinite) using ten different soil samples. He concluded that shrinkage first decreased with the small amount of cement used, attained a minimum value, and finally increased with increasing cement content (Figure 2-13). The behaviour in these clayey types of materials can differ to the one in the current materials, since shrinkage is considerably influenced by the amount and kind of clay in these materials.

Figure 2-13 Effect of cement content on shrinkage of soil-cement mixes (after George, 1968)

2.4.3.2   Curing time

Generally, shrinkage cracks increase with time. Bahar et al. (2004) analysed the effect of compaction and cement stabilisation (ordinary Portland cement) on the performance of earth blocks. It was revealed that shrinkage increased rapidly during the first 4 days, and then after

35

shrinkage increase rate decreased. After 22 days, the shrinkage rate was almost constant. Therefore, the first 4 days of curing were important to minimise drying shrinkage and cracks (Figure 2-14).

Figure 2-14: Shrinkage development during the first 28 days (Bahar et al. 2004)

Nakayama and Handy (1965) investigated the linear shrinkage of soil-cement using four different types of soil. Clay soil-cement specimens with no moist curing began to shrink immediately when dried out. After moist curing (curing in the presence of moisture), for clay soil-cement, shrinkage delayed up to approximately one day. This delay was for shrinkage tension build up and overcoming of internal restraints in the hydrated cement gel. The same as the investigation done by Bahar et al. (2004), the shrinkage rate at around 28 days was almost constant (Figure 2-15), which emphasises why 28 days were considered as the curing time for this research.

Figure 2-15: Shrinkage data for typical mix under different curing conditions (after Nakayama and Handy 1965).

In his investigation, George (1968) also agreed with the two first researchers, that the increase in shrinkage was small when it took place after 28 days of moist curing compared to when it took place directly after de-molding.

2.4.3.3   Moisture content

The moisture content is an important factor for the control of the extent of shrinkage of stabilised materials, since this is mainly due to the moisture loss caused by cement hydration and/or evaporation.   Increasing the moisture content leads to the presence of high amount of moisture to evaporate, and therefore, a greater extent to suffer shrinkage strains.

An investigation by Kenai et al. (2006) on clay sandy soil stabilised with cement at different moisture contents, revealed that the final shrinkage increased with the increase in moisture content. This was due to excess of moisture not needed for cement hydration in case of the use of greater moisture content. It is, therefore, necessary to control the moisture content and preferably to use the OMC (Figure 2-16).

Figure 2-16: Variation of the final shrinkage with mixing water content (after Kenai et al. 2006).

George (1968) agreed with Kenai et al. (2006), and revealed that shrinkage increase in soil-cement is a power function of moisture content and not a linear function (Figure 2-17).

Figure 2-17: Effect of moisture on shrinkage (after George 1968).

38

2.4.3.4   Compaction

A well-compacted material reduces the potential for shrinkage to occur. This reduction results from the dense package of soil/aggregate particles, which minimises the voids in the material. A good compaction improves the aggregate interlock and plays a role of material structural support when cracks develop (Adaska and Luhr, 2004).

Bhandari (1973) indicated that when compared to compacting cement-stabilised soil to standard proctor density, the shrinkage reduced up to 50% with the compaction at modified proctor. In addition to the reduction of shrinkage, the OMC at modified proctor compaction was low, compared to the one at standard proctor compaction. Adaska and Luhr (2004) state that there is more shrinkage with compacting by vibratory compactors than by static loading or kneading compactors. George (1968) showed that the compaction could improve the shrinkage but a consideration of moisture content was necessary (Figure 2-18). This means that a mode of compaction that gives a high density (Maximum Dry Density) is preferable. In this case, the corresponding moisture content is the Optimum Moisture Content.

Figure 2-18: Effect of density and moisture on shrinkage (after George, 1968)

2.4.3.5   Soil type

The soil type to be stabilised is another important factor that determines the extent of shrinkage that can occur. Researches such as George (1968) and Nakayama and Handy (1965) investigated on shrinkage of cement-stabilised fine-grained soils such as clays, compared with

39

the one of cement-stabilised granular soils. They found that cement-stabilised fine-grained soils showed more shrinkage than cement-stabilised granular soils. This was due to the presence of greater particle surface areas on cement-stabilised fine-grained soils, which necessitates extra moisture content for compaction. Adaska and Luhr (2004) agrees with the first researchers and adds that fine-grained soils need higher cement content for the achievement of a required strength and durability.

George (1968) showed that an increase in clay content results in a shrinkage increase at a faster rate, since aggregates perform as stiff inclusions in the shrinking matrix, and thus, reduces the degree of shrinkage (Figure 2-19).

Figure 2-19: Effect of clay on shrinkage (George, 1968)

2.5   Effect of Super-Absorbent Polymers (SAP) on shrinkage

2.5.1   Introduction

The use of Super-Absorbent Polymers (SAP) is amongst internal curing methods used to mitigate autogenous shrinkage in concrete, particularly in high strength/ performance concrete (HSC/HPC) (Hasholt et al. 2012 and Schrofl et al. 2012).

Siriwatwechakul et al. (2010) define SAP as polymers having a high capacity of retaining a large quantity of water. According to them the two main types of SAP are thermoplastic polymers and thermoset polymers. The former polymers are linear, while the latter are cross-linked. Thermoplastic polymers possess a high molecular weight with polymer chains that overlap and present pseudo-three dimensional structures, through their junctions performing as physical cross-links. Alternatively, thermoset polymers also being three dimensional polymer networks possess chemical cross-links that maintain polymer chains, which prevent them from dissolution while soaked in solvents (Siriwatwechakul et al. 2010).

According to Zohuriaan-Mehr and Kabiri (2008), SAP can be classified in different ways:

a) According to the presence or absence of electrical charge situated in the cross-linked chains; where they count four groups, which are non-ionic, ionic (anionic and cationic), amphoteric electrolyte (both acidic and basic groups) and zwitterionic (polybetaines) that contains both cationic and anionic groups

b) According to the type of monomeric unit used in their chemical structure, where they are cross-linked polyacrylates and polyacrylamides, hydrolyzed cellulose-polyacrylonitrile (PAN) or starch-PAN graft copolymers, and cross-linked copolymers of maleic anhydride.

They reveal that in the industrial production of SAP, the mostly used monomers are principally acrylics (acrylic acid and its sodium or potassium salts) and acrylamides (Figure 2-20)

41

Figure 2-20: Chemical structures of the reactants and general pathways to prepare an acrylic SAP network. (a) Cross-linking polymerization by a polyvinylic cross-linker, and (b) Cross-linking of a water soluble prepolymer by a polyfunctional cross-linker (after Zohuriaan-Mehr and Kabiri, 2008).

2.5.2 Absorption capacity of SAP

Siriwatwechakul et al. (2010) defines SAP absorption capacity (called the swelling rate), as the weight of the swollen SAP (swollen state) to the dried SAP (collapsed state) ratio. SAP absorbs a high amount of water, they get in contact with. This absorption causes water to migrate into the polymer network, where molecules of water diffuse into the void space, resulting in a swollen polymer gel.

Hasholt et al. (2012) state that the word "SUPER" in SAP_s is related to their capacity to absorb high amount of water (more than 1000 times their own weight). They reveal that this absorption capacity depends on the fluid to absorb, with high capacities for pure water (distilled or demineralized water). It reduces with the presence of ions such as divalent ions like Ca^{++}.

In their study, Craeye et al. (2011) assumed the absorption capacity of SAP as 45g/g. Hasholt et al. (2012) state that this value would be very high in fresh concrete due to the presence of ions in the pore solution, and confirmed it to be only 12g/g. However, Schrofl et al. (2012) proposed that the determination of this value should be by the "tea-bag method".

Olawuyi and Boshoff (2013) used the "tea-bag method" for the determination of the SAP absorption capacity. They added this quantity of water in the mixture to examine the affect of SAP addition on the compressive strength of HPC. As summarised in Table 2-5, the values that they found for the two sizes of SAP used (03/08 μm and 06/12 μm), were greater than the value confirmed by Hasholt et al. (2012), but less than the value assumed by (Craeye et al. 2011). It should be noted that they considered values at 10 minutes time intervals of immersion, which is considered as the required time for completion of concrete mixing and casting after addition of water.

Table 2-5: Absorption capacity of SAP (after Olawuyi and Boshoff, 2013)

Time (min)	SAP1 (g/g) Water	Cement Pore Solution	SAP2 (g/g) Water	Cement Pore Solution
0.5	72.34	20.11	65.8	26.61
2	170.29	20.84	180.63	31.49
5	216.17	22.59	233.95	32.02
10	228.44	24.3	258.22	33.93
15	242	31.64	284.49	35.8
30	253.02	35.18	292.95	36.76
60	257.07	38.14	297.54	41.85
180	260.76	41.8	298.22	48.24

They considered the values of 25g/g (SAP1) and 30g/g (SAP2) for the cement pore solution. In the present study, these values were used.

2.5.3   Effect of SAP on strength

Craeye et al. (2011) revealed that internal curing with SAP reduces both the compressive and tensile strengths (Figure 2-21). This reduction is due to the increase in w/b-ratio caused by the added quantity of internal curing water. In addition, the presence of SAP has an influence on the occurrence of a higher quantity of larger pores (up to 200μm), and therefore, a reduction in the amount of smaller pores, where hydration products are supposed to be filled. The creation of air voids in the concrete, by the presence of SAP, affects its strengths (especially the compressive strength). It is believed that it decreases by 5% for every 1% air addition.

Figure 2-21: Influence of SAP on the compressive and tensile splitting strength (after Craeye et al. 2011)

In Figure 2-21, the values after SAP (50, 70, and 90) are the assumed SAP absorption capacities.

Hasholt et al. (2012) has given a summary on the effect of SAP on compressive strength. It was revealed that there is a contradiction in results of different investigators, since some of them report reduction of compressive strength; others unaffected compressive strength or even increased compressive strength. According to these researchers, the conclusion from **Craeye et al. (2011)** should be misleading due to inaccurate assumption of the absorption capacity of SAP. Much water was added for internal curing.

Olawuyi and Boshoff (2013) obtained a linear rate of decrease in compressive strength for an increase of SAP up to 0.4% (0.2%, 0.3% and 0.4%), and a deviation from the trend for 0.6%. The strength loss was ≤ 25% for 0.4% SAP and 40% for 0.6% SAP (Figure 2-22).

Figure 2-22: Compressive strength of HPC with SAP (after Olawuyi and Boshoff, 2013)

Where:

CM: Control Mixture

MS: Mixture containing SAP

1 and 2: the SAP size incorporated as admixture (i.e.03/08μm as "1" and 06/12 μm as "2")

 A, B, C, and D: the SAP content (0.2%, 0.3%, 0.4% and 0.6% respectively)

2.6   Shrinkage cracks and mitigating methods

2.6.1   Introduction

Drying shrinkage, hydration and/or changes in temperature can cause contraction of cement-stabilised pavement layers. High tensile stresses are induced in the layer if it is fully or partially restrained by friction from the layer below. Cracks occur when these stresses exceed the tensile strength of the material. Wide cracks (> 6mm) are due to drying shrinkage rather than hydration or changes in temperature (Penev and Kawamura, 1993 and Halsted, 2010).

As highlighted Xuan et al. (2015), Figure 2-23 illustrates the development of stresses in a cement-stabilised pavement layer, resulting from shrinkage.

Figure 2-23: Stress scheme of a cement-stabilised pavement layer against shrinkage (Xuan et al. 2015)

Where:

L_{t1}: length of cement-stabilised pavement layer

τ: friction experienced by the cement-stabilised pavement layer from the layer below

When crack occurs, the induced tensile stress attains the maximum value, which is greater than the tensile strength of the material.

$$\sigma(t_1) > f_t(t_1)$$
Equation 2-15

Where:

$\sigma(t_1)$: induced tensile stress in the cement-stabilised pavement layer, due to shrinkage at time t_1

$f_t(t_1)$: tensile strength of the base material at time t_1

Several factors have an impact on the cracking and crack spacing of cement-stabilised pavement layers. These factors include material characteristics, construction procedures, traffic loading, and imposed restraint on the stabilised layer by the layer below. These developed cracks are not from pavement structural defects but they are natural characteristics of cement-stabilised pavement layers and can reflect to the pavement surface layer. They are, most of the time narrow and don't have a negative effect on the pavement performance (Figure 2-24 (a)). Unfortunately, when these cracks are wide, they contribute to the pavement deterioration since water infiltrates, resulting in debonding of layers and pumping of the underlying material (Little et al. 1995) (Figure 2-24 (b)).

46

Figure 2-24: Cracks reflected on the pavement surface layer (a) Narrow cracks (b) Wide cracks (Adaska et al. 2004).

Several methods exist for mitigation of shrinkage cracking in cement-stabilised pavement layers and minimize the potential for reflection through the asphalt surface layers. These methods include proper construction and curing of the cement-stabilised pavement layer, Use of pre-cracking to reduce crack size, and use of flexible layers in pavement structure for relief of stress concentrations (Adaska & Luhr 2004). Pre-cutting of the stabilised layer and the use of fly ash and ground granulated blast furnace slag (GGBFS) in cement-stabilised materials, are additional methods for mitigation of shrinkage cracking (George, 2000 and Sebesta, 2005).

2.6.2 Shrinkage cracking

According to TRH 13 (1986); George (1973) and Bofinger et al. (1978), cracking extent is associated with the amount of moisture loss during drying. Due to increased moisture loss and shrinkage, wet materials display high cracking extent. An increase in cement contents for stabilisation leads to high moisture consumption and consequently high shrinkage. This results in extreme shrinkage cracking with wide cracks (Little et al. 1995).

Hwang and Young (1984) indicated that the moisture gradient grows crossways the drying specimen when dried out. This form of growing leads to non-uniform shrinkage due to self-restraint from internal parts of the specimen, causing the microcracking, as they shrink considerably slower than the outer parts. For cement paste, self-restraint leads to the development of cracks that are perpendicular to the dried surface. For cement-stabilised

47

materials, aggregate particles are a source of restraining effects, which leads to radial and circumferential microcracking around them (Goltermann, 1995).

Stress relaxation is an important material property for the developed tensile stresses. For concrete materials, stress relaxation effect causes the reduction of tensile stresses within the time concrete is gaining enough strength. For cement-stabilised materials, the stress relaxation effects differ from those in concrete, aiming from differences in characteristics and properties. Additionally, the presence of a low cement content in cement-stabilised materials is to be taken into consideration (Houben, 2011). Figure 2-25 illustrates the shrinkage cracking mechanism (TRH 13, 1986).

Figure 2-25: Shrinkage cracking resulting from interrelationship between shrinkage stress, strength and time (TRH 13, 1986)

Figure 2-25 suggests that it is possible to prevent shrinkage cracking. However, for cement-stabilised materials, shrinkage is followed by cracking, which can differ according to the type of material stabilised. The use of low cement content contribute to the reduction of potential for cracking.

2.6.3   Methods for mitigating shrinkage cracks

The methods for mitigating shrinkage cracking in cement-stabilised pavement layers include proper construction and curing of the cement-stabilised pavement layer, use of pre-cracking for crack size reduction, use of flexible layers in pavement structure for relief of stress

concentrations, pre-cutting stabilised layer, and use of fly ash and Ground Granulated Blast Furnace Slag (GGBFS) (Adaska & Luhr 2004; George, 2000 and Sebesta, 2005). The following section briefly describes these methods:

2.6.3.1   Pre-cracking

The main objective of pre-cracking is to reduce wide shrinkage cracks by development of several micro-cracks as a replacement for single transverse cracks. The process implicates numerous passes of a massive vibratory roller above the cement-stabilised layer, one to two days after its placement. This creates a network of fine cracks and delivers a crack pattern that minimizes any further expansion of wide shrinkage cracks (Adaska and Luhr, 2004).

Brandl (1999) stated that pre-cracking is the most appropriate procedure for mitigating shrinkage cracks. Scullion (2002) used this technique for a project comprising several streets in a residential zone in Texas. He applied the technique on three different street sections and kept the fourth street as a control section. After six months, the results showed that for all the three pre-cracked sections, the stiffness was equal or higher than the prime stiffness, indicating that there was strength gain with time. With regards to shrinkage cracking, the results showed that the amount of cracking was considerably reduced in all the three pre-cracked sections in comparison with the un-pre-cracked section as indicated by Table 2-6.

Table 2-6: Summary of shrinkage cracking six months after surfacing (adapted from Scullion, 2002)

Street	Crack length in meters per 30 meters of pavement (223 m²)
Salzburg Court	1.9
Von Trapp	1.1
Neuburg Court	0.7
Control Section	8.2

2.6.3.2   Stress relief

Stress relief is a technique used to minimize reflection of shrinkage cracking in the asphalt surface layers from cement-stabilised pavement layers. The main objective of the technique is to relieve the stress concentrations resulting from cracks in cement-stabilised pavement layers (Adaska and Luhr, 2004). Figure 2-26 gives an example of three pavement designs with reduction of stresses that would cause cracking reflection from a cement-stabilised base to surface layers.

Figure 2-26: Pavement designs for stress relief to minimize shrinkage cracking reflection (Adaska and Luhr, 2004)

2.6.3.3   Pre-cutting

The leading purpose of pre-cutting stabilised layers was to control crack width by introducing grooves or cuts at close intervals (Colombier and Marchand, 1993). However,   George (2001) indicates that currently, pre-cutting is used to preclude the presence of occasional but comparatively wide and damaging cracks, which can reflect through surfacing layers.

According to Lefort (1996), the most benefit of pre-cutting is to alleviate wide shrinkage cracks at indicated spacing. Shalid and Thom (1996) investigated a course grained soil-cement using this technique and found that the system induced numerous cracks of less than 0.5 mm width in a cement-stabilised base layer, while the width of natural cracking was more than 1 mm related to the type of aggregate. They also noted that the stiffness was not greatly affected.

Factors such as materials characteristics and thermal effects govern the pre-cutting period of a stabilised layer. Therefore, this period is not easy to be specified. However, it can vary from some hours to a few days after placement, depending on strength of the layer at the cutting time. For pre-cutting of a stabilised layer, the cut-depth can vary from one-third to one-half of the stabilised layer thickness (George, 2001).

2.6.3.4   Use of fly ash and GGBFS

Investigations by different researchers reported that replacing a part of cement (for material stabilisation) with fly ash or Ground Granulated Blast Furnace Slag (GGBFS), results in narrow shrinkage cracks without mislaying the long-term strength of the material.

For example, George (2001) states that the setting rate of a mixture of cement and fly ash is abridged with a resultant reduction in cracking. El-Rahim and George (2001) reported that for stabilised base layers, by replacing a part of cement with fly ash, shrinkage cracks were narrow, compared to when fly ash was not used. Regarding the use of GGBFS with cement, George (2001) reports that replacing about 50% of cement with GGBFS in concrete, results in change of physical properties. A slower rate of strength-gain is obtained with any increase in slag (especially at early ages), which influences drying shrinkage and cracking criteria (Gress, 2001).

2.7   Shrinkage testing in laboratory

Various shrinkage test methods exist and different setups, measurement criteria, specimen geometry, as well as curing conditions and procedures are used. Nakayama and Handy (1965) considered cylindrical specimens, dynamically compacted with microscopic slide for shrinkage measurement.   Bofinger et al. (1978) also considered cylindrical specimens, and noted some degree of anisotropy resulting from the differences in measured total shrinkage of the specimens.

However, Grobler (1994) favoured beam specimens over cylindrical ones and states that cylindrical specimens with the used compaction methods do not simulate field condition. He preferred horizontally positioned and vertically compacted beam specimens, which would simulate field criteria. George (1970) shares the same intuition with Grobler (1994). They both used rectangular beam specimens to measure the shrinkage.

The method of compaction and curing conditions influence the degree of shrinkage as recognised by Bofinger et al. (1978). Compared to specimens compacted using static compaction methods, the ones compacted using dynamic, impact and kneading compaction methods showed higher shrinkage. Compared to sealing off surfaces, evaporation from unprotected surfaces produced higher volume changes. Nakayama and Handy (1965) states that many researchers consider shrinkage as higher in the direction perpendicular to compaction. In fact, during compaction, there is some degree of anisotropy that is produced in the specimens, and the particles tend to align at right angles to the direction of compaction.

51

When the internal suction is developed, it is easier for particles to move in the direction perpendicular to compaction, and therefore inducing higher potential for shrinkage in that direction (Bofinger et al. 1978).

This high magnitude of shrinkage explains the preference of measuring shrinkage perpendicular to the direction of compaction. However, for this research, cylindrical specimens were used, and shrinkage was measured in the direction of compaction. This consideration was based on various advantages of cylindrical specimens, such as providing greater and representative shrinkage results through large exposed surface area.

Researches related to shrinkage were focused on the drying shrinkage measurement for specimens firstly cured in moist conditions during a specified period (Nakayama and Handy, 1965 and Bofinger et al. 1978). These researchers indicate that with this approach, there is no consideration of volumetric changes occurring immediately after completion of compaction and during the early stages of curing. This reveals the importance of shrinkage measurement immediately after compaction of specimens.

Table 2-7 provides a summary on a comparison of beam and cylindrical shrinkage testing methods (Campher, 2015):

Table 2-7: Comparison of beam and cylindrical shrinkage testing methods (adapted from Campher, 2015)

	Shrinkage method type	
	Beam shrinkage testing	**Cylindrical shrinkage testing**
Advantages	• Shrinkage measurements are taken in the direction simulating a pavement layer situation. Practically, shrinkage causes horizontal tensile stresses in adjacent layers. These stresses induce shrinkage cracks.	• With thicker compaction layers, a more realistic aggregate packing is realised • Cylindrical specimens offer the most representative shrinkage results. Providing greater shrinkage values than beam specimens, a better idea of the material shrinkage is achieved • With large exposed surface area, shrinkage is kept continuous • Easy and repeatable method

Disadvantages	• Probable discontinuities in shrinkage measurement caused by one curved surface throughout testing • Less realistic aggregate packing due to thin compaction layers • With a high risk of manifestation of shrinkage cracks, the method is less repeatable and erroneous	• In practice, shrinkage measurements are taken perpendicular to the direction of compaction. This is not the case for this method

Figure 2-27 (a), Figure 2-27 (b), Figure 2-28 (a) and Figure 2-28 (b) respectively indicate the direction of compaction for beam specimens, the direction of shrinkage testing for beam specimens, the direction of compaction for cylindrical specimens, and the direction of shrinkage testing for cylindrical specimens

Figure 2-27: Direction of compaction and shrinkage testing for beam specimens (a) direction of compaction (b) direction of shrinkage testing

Figure 2-28: Direction of compaction and shrinkage testing for cylindrical specimens (a) direction of compaction (b) direction of shrinkage testing

2.8   Summary of the literature review

The properties of Cement-Stabilised Materials (CSM) influence the behaviour of Cement stabilised layers (CSL) and hence the overall pavement structure since it works in unity. The factors that influence these properties include, amongst others, the host materials, binder type and content, moisture content, compaction, mix uniformity, curing conditions, and the age of the compacted mixture. This chapter provided an overview of how these factors affect CSM. In addition, their effects on Cement-Stabilised Pavement Layers (CSPL) were reviewed, and finally the benefits and damages of these types of layers were presented.

CSPL improve the pavement strength due to their good load-spreading properties. They also increase the workability and the durability of the pavement. Unfortunately, due to their nature, they reveal some weaknesses and are prone to problems. Several researchers reported that the main problems related to CSPL are shrinkage and associated reflective cracking, together with the load induced fatigue cracking. This chapter revised the types and mechanisms of shrinkage of CSPL.

Most of the first literature considered CSPL with the combination of natural aggregates only. Later on, due to the shortage of natural materials and strict laws on opening new borrow pits and landfills, recycled aggregates were considered. These recycled aggregates are formed of Recycled Concrete Aggregates (RCA) and Recycled Concrete and Masonry (RCM), which are produced from Concrete and Demolition Waste (CDW). Recycled aggregates can be treated with cement to achieve desired properties. Therefore, they become disposed to the same problems of shrinkage and cracking as cement treated natural aggregates. In case these materials are used without any cement treatment, shrinkage can still happen, resulting from latent hydration properties. A review of the recycling of these materials was provided, together with the performance of recycled CDW.

The types of shrinkage of CSPL include autogenous shrinkage induced by hydration, drying shrinkage due to loss of moisture, thermal shrinkage due to low temperature contraction and carbonation shrinkage due to chemical reaction with atmospheric carbon dioxide. A particular emphasise was put on drying shrinkage since it is the main source of shrinkage and cracking of CSPL. The mechanisms of shrinkage of CSPL include surface tension, capillary tension, movement of interlayer water, and disjoining pressure. The chapter explained the process of these mechanisms. Factors influencing shrinkage of CSPL were also discussed and these include cement content, curing time, moisture content, compaction, and soil type. Cement content was highlighted. For shrinkage reduction, Super-Absorbent Polymer (SAP) was

discussed. This is an additive which is one of internal curing methods to mitigate autogenous shrinkage. It exhibits a high capacity of retaining large quantity of water.

Drying shrinkage, hydration and/ or changes in temperature can cause contraction of cement-stabilised pavement layers. High tensile stresses are induced in the layer if it is fully or partially restrained by friction from the layer below. Cracks occur when these stresses exceed the tensile strength of the material. Wide cracks (> 6mm) are due to drying shrinkage rather than hydration or changes in temperature. The methods for mitigating shrinkage cracking in CSPL were discussed. These methods include proper construction and curing, use of pre-cracking, stress relief, pre-cutting, and use of fly ash and GGBFS.

Various shrinkage test methods exist. They use different setups, measurement criteria, specimen geometry, curing conditions and procedures. Some researchers have considered cylindrical specimens, some others beam specimens. They always considered different compaction methods. The ones who considered beam specimens stated that cylindrical specimens, with the used compaction methods, do not simulate field condition. Unfortunately, with beam specimens, the occurrence of cracks within specimens negates any reliable measure of shrinkage. These cracks are due to the friction located at the interface between the beam and mould surfaces.

Factors that influence shrinkage of pavement materials were discussed. This research compares the effects of drying and hydration on shrinkage and cracking of the layers, for the three materials used. The effect of SAP is considered for a G4 hornfels material, and the potential for latent hydration, which results from self-cementing properties, is evaluated for both the RCA and NC materials. The differences in the characteristics and behaviours of the three materials lead to different Optimum Moisture Contents, which significantly influence the magnitude of shrinkage.

CHAPTER 3. RESEARCH METHODOLOGY

3.1   Introduction

This chapter discusses the methodology used to achieve the research objectives. It is divided into four main parts. The first part describes the research materials, the cement type used for stabilisation, and the quantity of the Super-Absorbent polymers (SAP) used for shrinkage reduction measure. The second part discusses the material characterisation, the third part discusses the material strength evaluation, and the last part describes the shrinkage testing. The material characterisation and strength tests results are presented in Chapter 4, while shrinkage tests results are presented in Chapter 5. The determination of potential for cracking is presented in Chapter 6, and finally conclusions and recommendations are presented in Chapter 7.Figure 3-1 illustrates the schematic layout of the Research study.

Figure 3-1: Schematic layout of the research study

3.2   Research materials, cement type and polymer quantity

3.2.1   Research materials

Three types of materials were used in this research: crushed hornfels stone (G4), Recycled Concrete Aggregates (RCA; old concrete) produced from CDW, and New Concrete (NC). G4 hornfels material selection was based on recommended materials for base/subbase layers of a typical South African pavement structure (SAPEM, 2013 and TRH 14, 1985). RCA presented crushed concrete material from an old building, typically more than 30 years old, that can also be used as a material for base/subbase layers, as stated in Chapter 2. The NC material selection was to assess the cement activity from new to old concretes. The NC material was approximately six months old, but was cured according to the statement in the next paragraph, so that moisture was available for the hydration process.

All these materials were collected from different areas in South Africa. The G4 hornfels was collected from Tygerberg quarry. The RCA was a mix between CDW from Helderstroom (a demolished access road to the Department of Agriculture at Stellenbosch University), and crushed material received from Murray & Roberts. The NC, with strength of 30 MPa, was collected from structural engineering laboratory of Stellenbosch University. To avoid any environmental effects, such as moisture evaporation, the NC was packed in sealed plastic bags, which were then sealed in plastic containers.

Figure 3-2 shows the G4 hornfels material pile.

Figure 3-2: G4 hornfels

Figure 3-3 (a) and Figure 3-3 (b) respectively show the RCA material for course fractions, and the RCA material fine fractions.

Figure 3-3: Recycled Concrete Aggregates (a) Course fractions (b) Fine fractions

Figure 3-4 (a) and Figure 3-4 (b) respectively show the NC material in sealed plastic bags during the "curing" period of six months before it was crushed.

Figure 3-4: New concrete (a) Sealed plastic bags (b) Closed plastic containers

A vibratory hammer (Figure 3-5 (a)) was used to break big size materials into small sizes, which were crushed into suitable sizes using the SU laboratory jaw crusher (Figure 3-5 (b)). After sieving, the required fractions of the same material were carefully mixed (according to the grading) before being used for any test. The process is detailed in Section 3.3.1.

Figure 3-5: Equipment for the preparation of material suitable fractions (a) Vibratory hammer (b) SU laboratory jaw crusher

3.2.2 Cement type

The Portland cement type used for stabilisation is CEM II A-M 42.5N. The consideration of this type of cement is based on recent trends of research in the road industry. The nomenclature for this type of cement is given as follows:

CEM II A-M 42.5N

Sub Class N, indicating normal early strength

Standard strength class

The second main constituent, and in this case a composite

The proportion of cement clinker, and in this case higher

The main cement type, and in this case Portland composite cement

59

It should be noted that this nomenclature complies with SANS 50197 (2013), Part 1.

3.2.3 SAP quantity

The quantity of SAP used in this research is 0.3% by weight of cement (b_{woc}). Its absorption capacity used is 25g/g. The consideration of these quantities is based on a study done by Olawuyi and Boshoff (2013), in comparison with other researchers as discussed in Sections 2.5.2 and 2.5.3, where they confirmed that these values would not affect the material strength.

3.3 Material characterisation

Material characterisation is required for the evaluation of the material suitability. According to the South African road construction materials guideline, material characteristics and properties are identified through various techniques and index tests. With respect to SAPEM (2014) and TRH 14 (1985) requirements, this section presents the methods followed for various standard characterisation tests performed.

Material porosity was not measured, which is a limitation for the results of this research. Porosity is a measure of the void spaces in a material. It is a fraction of volume of voids over the total volume. According to Kaufmann, E. N (2012), the main techniques for determination of material porosity include gas sorption, liquid intrusion, microscopy, and x-ray and neutron scattering. The choice of technique depends on the expected range of pore sizes, material properties, instrument availability, sample geometry requirements, and final application.

Recycled Concrete Aggregates (RCA and NC) not only contain the original aggregates, but also hydrated cement paste, which reduces the specific gravity and increases the porosity in comparison to similar natural aggregates. This higher porosity leads to a higher absorption resulting in higher OMC that increases the potential for shrinkage, because higher moisture content is available for evaporation during drying. In addition, the higher porosity leads to low crushing resistance, especially during compaction in wet conditions.

3.3.1 Grading

Material grading is a classification process that determines the particle size distribution. It offers information associated with the particle packing, which has an influence on the material density. In order to get the material for specimen preparations, all the three materials used in this research were sieved into thirteen different fractions. A picture of the set of sieves used is shown in Figure 3-6.

Figure 3-6: Sieve set for the three materials

For all the three materials, the same grading was used; and the maximum fraction was 19mm. The choice of this material maximum size was based on the cylindrical mould used for the preparation of specimens. The size of this mould was 300mm in height and 100mm in diameter (Figure 3-7).

61

Figure 3-7: Split cylindrical mould used for the preparation of specimens

The material blend composition was designed using Fuller's equation shown in Equation 3-1.

$$P = \left(\frac{d}{D}\right)^n \qquad\qquad \text{Equation 3-1}$$

Where;

P: % passing a sieve with aperture d

D: Maximum particle size, and

n: ranging between 0.25 and 0.45. For this study 0.45 was considered, since it was found to give densest packing (SAPEM, 2014).

The Grading Modulus (GM), which is shown in Equation 3-2, indicates the quality of the material for pavement construction purpose. A higher GM (>2) indicates that the material is coarsely graded and of good quality, while a lower GM indicates that the material contains more fine grain sizes and is of poor quality (SAPEM, 2014).

$$GM = \frac{P2.00\ mm + P0.425\ mm + P0.075\ mm}{100} \qquad\qquad \text{Equation 3-2}$$

Where;

$P2.00\ mm$ etc.: Percentage retained on the indicated sieve size

3.3.2   Atterberg limits & Linear Shrinkage

The Atterberg limits tests (PL and LL) provide a measure of the critical water contents of the material, and give basic information regarding the plasticity. The Plasticity Index (PI) offers a clear indication of the material's performance, with a low PI indicating a better material performance. The PI is obtained by subtracting the Plastic Limit (PL) from the Liquid Limit (LL). The Linear Shrinkage (LS) provides insights related to the material's sensitivity to water.

For this study, TMH1 (1986) Method A2, Method A3 and Method A4 were followed, respectively for the determination of the Liquid Limit, the Plastic Limit and Plasticity Index, and finally, the Linear Shrinkage.

3.3.3   Maximum Dry Density (MDD) and Optimum Moisture Content (OMC)

The material density and moisture content are important factors that have an impact on the material mechanical properties. The packing of material particles, which determine the material void ratio, influence the strength and permeability of the material. It is essential to understand the material grading as it determines the highest achievable dry density (MDD), and the corresponding moisture content (OMC). In this study, two methods were used for the determination of the MDD and OMC. For the Modified AASHTO compaction test, TMH1 (1986) Method A7 was followed. This method was compared to the vibratory hammer compaction method.

The vibratory hammer compaction method is a much better simulation of reality, since it allows for translation and rotation of the particles through vibration, which results in a better (higher) compaction and densies. It was, therefore, used for shrinkage and material strength (UCS and ITS) specimen preparation. On the other hand, the Modified AASHTO compaction method was used for CBR determination. Figure 3-8 (a) and Figure 3-8 (b) respectively illustrate the apparatus for Modified AASHTO compaction and vibratory hammer compaction.

Figure 3-8: Apparatus for MDD and OMC determination (a) Modified AASHTO compaction (b) Vibratory hammer compaction

3.3.4   California Bearing Ratio (CBR)

The California Bearing Ratio (CBR) is a standard test for the evaluation of the strength of G4 and lower quality materials, in order to be used as road construction materials (SAPEM, 2013). The test compares the material bearing capacity to that of a reference material. It is carried out on a 4 days soaked compacted specimens of the tested material. In this study, the procedure in TMH1 (1986) Method A8 was followed. Figure 3-9 illustrates the CBR test equipment with a 4 days soaked compacted specimen of the tested material.

Figure 3-9: CBR test equipment with a 4 days soaked compacted specimen

3.4   Material strength evaluation

The tensile and compressive strength tests are used to evaluate the strength of stabilised road construction materials. For this study, a minimum strength corresponding to material class C4 was required, because it is the one that can be used as a base/subbase layer material (TRH4, 1996). In addition, the results from these standard tests were compared to results from shrinkage specimens (cured for 28 days), in order to assess shrinkage influence on the material strength.

3.4.1   Unconfined Compressive Strength (UCS)

The UCS test was done following the procedure described in TMH1 (1986) Method A14. The method states that specimens are axially loaded with a displacement controlled loading up to failure, and the force causing failure is noted. This study considers seven days cured cylindrical specimens as stated in the procedure, but with a different height of 152 mm and a diameter of 152 mm. It should also be reminded that the study considers compaction with the

vibratory hammer. In addition, two different loading rates were compared, as the standard loading rate (153KN/min) broke shrinkage specimens before a reading could be made. We decided to consider the ITS test standard rate (40KN/min) for comparison with the UCS test standard rate. Figure 3-10 illustrates the UCS testing equipment.

Figure 3-10: UCS testing equipment

Equation 3-3 shows how to determine the compressive strength.

$$\text{Compressive strength (kPa)} = \frac{P}{\pi \times r^2}$$ Equation 3-3

Where;

P: Force causing failure (kN)

r: Radius of specimen (m)

3.4.2   Indirect Tensile Strength (ITS)

The ITS test was done following the procedure described in TMH1 (1986) Method A16T. Contrary to the UCS test, the specimens were loaded diametrically, and the force causing failure was noted. As for the UCS test, the study considers seven days cured cylindrical specimens, but with a different height of 75 mm and a diameter of 152 mm. The compaction was also done by the vibratory hammer. Only the standard loading rate (40KN/min) was used. Figure 3-11 illustrates the ITS testing equipment.

Figure 3-11: ITS testing equipment

Equation 3-4 shows how to determine the tensile strength.

$$Tensile\ strength\ (kPa) = \frac{2 \times P}{(\pi \times d \times h)} \times 10000 \qquad \text{Equation 3-4}$$

Where;

P: Maximum applied load (kN)

h: Height of specimen (cm)

d: Diameter of specimen (cm)

Note: For both UCS and ITS tests, three specimens were tested for the same cement content, to increase result accuracy. For standard tests, only 4% cement content was considered. However, all the cement contents used in this study (0%, 2.5%, and 4%) were used for shrinkage specimens. This means that comparisons between standard and shrinkage specimens were done for only 4% cement content, and for the other cement contents, shrinkage specimens were considered.

3.5   Shrinkage testing

3.5.1   Introduction

A comparison of different methods of shrinkage testing at laboratory level was provided in Chapter 2. According to previous studies, this study preferred cylindrical specimens to beam specimens due to various advantages, such as providing higher and representative shrinkage results, and keeping shrinkage continuous through their large exposed surface area. In addition, the method is easy and repeatable. To increase result accuracy, each specimen type was repeated three times and an average was retained.

During this study, some of the factors that influence shrinkage, see Chapter 2 (section 2.4.3), were fixed and some others were variable. Apart from the three different materials used, the variation in cement content (% in the sample) was another significant factor for shrinkage evaluation. For shrinkage reduction and control of cracks, only one percentage of SAP (0.3% b_{woc}) was considered, with a fixed absorption capacity (25g/g). Table 3-1 summarises shrinkage influential factors considered in this study. It also provides the reasons why they were fixed or allowed to vary.

Table 3-1: Variability of shrinkage influential factors considered

Shrinkage influential factor	Variability		Reason for variability
	Fixed	Variable	
Cement content [C] (%)		0	To assess the effect of change in cement content on shrinkage
		2.5	
		4	
Temperature (⁰C)	22-25		To simulate field conditions and to minimize the initial expansion due to increase in temperature
Curing period (days)	28		Previous studies revealed that shrinkage stabilises in 28 days at ambient temperature
Moisture content	OMC		To minimise void contents, which influence material shrinkage
Density	MDD		
SAP	0.3% b_{woc}		Only to assess the effect of SAP on shrinkage. The change in SAP content was not considered
	25g/g		

Table 3-2 provides the identification of specimens.

Table 3-2: Identification of specimens

Cement content (%)	SAP content (%C)	Amount of specimens	Specimen identification		
			G4 hornfels		
			Specimen 1	Specimen 2	Specimen 3
0	0	3	**A1**	**A2**	**A3**
2.5	0	3	**B1**	**B2**	**B3**
4	0	3	**C1**	**C2**	**C3**
4	0.3	3	**D1**	**D2**	**D3**
			RCA		
			Specimen 1	Specimen 2	Specimen 3
0	0	3	**E1**	**E2**	**E3**
2.5	0	3	**F1**	**F2**	**F3**
4	0	3	**G1**	**G2**	**G3**
			New concrete		
			Specimen 1	Specimen 2	Specimen 3
0	0	3	**H1**	**H2**	**H3**
2.5	0	3	**I1**	**I2**	**I3**
4	0	3	**J1**	**J2**	**J3**

It is essential to note that shrinkage influential factors that are not cited in this table are always picked and fixed.

3.5.2   Shrinkage experimental plan

This section presents the shrinkage test experimental plan. In the present study, shrinkage measurement was done in 28 days (from day one), and thereafter, the specimen were cut to the required sizes, which were used for strength tests (UCS and ITS). These strength results were compared to the standard ones as indicated in Section 3.4 of this chapter. Details on preparation and curing of specimens, and shrinkage measurement are presented in the next sections of this chapter. It is necessary to note that the polymer quantity is evaluated by weight of cement (b_{woc}).

69

SHRINKAGE TEST EXPERIMENTAL PLAN

G4 HORNFELS   **RCA**   **NEW CONCRETE**

CEMENT (C):   **0%   2.5%   4%**   **0%   2.5%   4%**   **0%   2.5%   4%**

POLYMER: **0% C   0% C   0 and 0.3% C**   **0% C   0% C   0% C**   **0% C   0% C   0% C**

3 repeats

SHRINKAGE TESTS: | 28 days | 28 days | 28 days | | 28 days | 28 days | 28 days | | 28 days | 28 days | 28 days |

1 each repeat

UCS TESTS: | After 28 days | After 28 days | After 28 days | | After 28 days | After 28 days | After 28 days | | After 28 days | After 28 days | After 28 days |

1 each repeat

ITS TESTS: | After 28 days | After 28 days | After 28 days | | After 28 days | After 28 days | After 28 days | | After 28 days | After 28 days | After 28 days |

Figure 3-12: Flowchart of shrinkage test experimental design

70

3.5.3   Preparation of specimens for shrinkage testing

Previous sections of this chapter described the steps involved in the material sample preparation. These includes breaking of the big sizes with the vibratory hammer, crushing into suitable sizes with the crusher, sieving into required fractions with a set of sieves, and finally grading according to Fuller's equation. The cylindrical mould used in compaction of specimens was also described in section 3.3.1.

This section briefly describes the steps involved in the preparation of specimens, after the materials were graded. Those steps are as follows:

a) Determination of the Optimum Moisture Content (OMC) and the Maximum Dry Density using the vibratory hammer, since it was the one used in the compaction of specimens. This was described in section 3.3.5.

b) According to the specimen size required (300mm in height and 100mm in diameter), the total mass of the material was calculated based on the density found. Referring to the grading, the required mass for each fraction was calculated. All these fractions were carefully mixed before any addition of water, and stored in closed bags. The required mass of cement was calculated according to the material total mass, and was evenly added to the mixed fractions.

c) When the SAP was required, its mass was calculated according to the mass of cement in the mix. It was also added to the mix before any addition of water.

d) The required quantity of water (OMC) was calculated according to the total mass of the material, but when SAP was used, some additional water was required. This additional water was related to the absorption capacity of SAP, as described in Chapter 2 of this research.

e) The required quantity of water was carefully mixed with the material sample and compaction could start.

f) The vibratory hammer was used for the compaction of specimens. This compaction was done in five layers (layer by layer), which means that the total mix was divided into five equivalent portions. For layer bonding, a scarified tool was used to roughen each compacted layer.

3.5.4   Curing and shrinkage measurements

3.5.4.1   Curing of specimens

A cylindrical split mould was used to facilitate the demoulding of the specimens. Since shrinkage starts immediately after compaction, the time between testing and compaction was minimised. Thus, after compaction, the mould was immediately taken to the temperature control room, and the specimens were de-moulded at 22^0C - 25^0C. The Relative Humidity (RH) was constant. The height and the weight of the specimens were measured to check the real density achieved during compaction. The specimens were finally placed on the two rigid frames located in the temperature control room, where curing took place. In order to minimise the time, these frames were mounted with six dial gauges each, which means that twelve specimens could be placed at the same time (Figure 3-13).

Figure 3-13: Rigid frames located in the temperature control room

3.5.4.2   Laboratory shrinkage measurement

The dial gauges, with a revolution of 0.01 mm each, were used to take the measurements for the dimensional changes, and these were divided by the height of specimens to get shrinkage or swelling values. The first reading, called the zero reading, was considered as a benchmark for other readings, and dial gauges were adjusted to reflect this reading. Any reading in the clockwise direction compared to the zero reading shows swelling, and is indicated by a positive sign. Anti-clockwise readings show shrinkage, and are indicated by a negative sign. Perplex squares were glued on top of specimens to ensure that the readings are taken on a flat surface.

Shrinkage value readings were taken at different time intervals, with more readings taken at early stages of the curing period, since these would indicate if there was initial expansion, and specify other phases of changes within the shrinkage cycles. In addition, the specimens required some time to stabilise when they were placed on frames. These shrinkage readings time intervals are presented in the Appendices. Figure 3-14, Figure 3-15 and Figure 3-16 show the specimens placed on the frames, the perspex squares, and the dial gauges used for shrinkage value readings for all the three materials used in this study. The Perspex squares were glued on top of the specimens with the epoxy glue. Only the middle part of the perspex squares was glued, which allowed moisture loss at the surface. Although the squares were only provided with one dial gauge, the plane rotation (that could result when the specimen deforms during setting) was insignificant. Therefore, there was no danger. The small values obtained for standard deviation between shrinkage results of the specimens explain this insignificance of the plane rotation.

Figure 3-14: Curing and shrinkage measurement of G4 hornfels

Figure 3-15: Curing and shrinkage measurement of RCA

Figure 3-16: Curing and shrinkage measurement of NC

3.6   Summary of the research methodology

The main purpose of this chapter was to provide the methodology used to achieve the research objectives. The chapter described the research materials used (G4 hornfels, RCA, and NC), and gave reasons why they were selected. The cement type used for stabilisation, and the polymer (SAP) used for shrinkage reduction measure were described in this chapter.

For the evaluation of the material suitability, material characterisation is essential. This chapter described the various standard characterisation tests to be done, as recommended by the South African road construction material guideline. These characterisation tests included the Atterberg limits and linear shrinkage, the MDD and OMC, and the CBR and swell. For the material gradation the Fuller's equation was used, and was described in this chapter. The chapter also described the UCS and ITS tests, which were done for the evaluation of the material strength.

Lastly, the shrinkage testing was described in this chapter, where the preparation of shrinkage specimens, the curing of specimens, and the laboratory shrinkage measurement were detailed.

CHAPTER 4. MATERIAL CHARACTERISATION AND STRENGTH TESTS RESULTS DISCUSSION

4.1 Introduction

This chapter presents and discusses the characterisation and strength test results obtained for all the three materials used in this study. In order to evaluate their suitability and performance as pavement construction materials, these results (for all the three materials) were compared to standard values as recommended by SAPEM (2014) and TRH 14 (1985) for gravel-crushed aggregate (G4 Hornfels). It should be noted that the two other materials used (RCA and NC) are not established in South African road construction material guidelines.

4.2 Material characterisation tests results

4.2.1 Grading

The same grading was used for the three materials in this study, in order to keep the same influence on shrinkage, during the comparison of materials. The TRH 14 (1985) provides the grading envelope for G4 materials (Table 4-1). From the provided grading envelope, the Fuller's equation (as shown in Equation 3-1) was used to determine the grading of the three materials.

Table 4-1: Grading envelope for the G4 materials (TRH 14, 1985)

G4 ENVELOPE		
Sieve size (mm)	Lower Limit (%)	Upper Limit (%)
53.00	100	100
37.50	85	100
19.00	60	90
4.75	30	65
2.00	20	50
0.425	10	30
0.075	5	15

Figure 4-1: Grading of the three materials used (G4 hornfels, RCA, and NC)

The calculated Grading Modulus is 2.41, and according to SAPEM (2014), the materials are coarsely graded, and of good quality for pavement construction.

4.2.2 Atterberg limits and Linear Shrinkage

The laboratory Atterberg limit tests performed showed that all the three materials were non-plastic. In fact, the determination of the Plastic Limit (PL) could not be attained because the moist samples were cohesionless. The samples could not be moulded into balls.

For the Linear Shrinkage (LS), SAPEM (2014) states that the material is considered as "non-plastic" if it has a LS that is below 0.5%. The three materials did not shrink, and are therefore, considered as "non-plastic".

4.2.3 Maximum Dry Density (MDD) and Optimum Moisture Content (OMC)

Two types of compaction were used for the determination of the MDD and the OMC; the Modified (Mod) AASHTO compaction and the vibratory hammer compaction. The results from the two types were compared. The vibratory hammer is a better simulation of reality, since it allows for translation and rotation of the particles through vibration, resulting in higher compaction and densities. It was therefore, preferred for shrinkage and material strength (UCS and ITS) specimens preparation. Table 4-2 and Table 4-3 show the results for the Mod AASHTO compaction and the vibratory hammer compaction, respectively. Figure 4-2 shows the typical compaction curves for the Mod AASHTO and the vibratory hammer compactions.

Typical compaction curves

Figure 4-2: Typical compaction curves for the Mod AASHTO and the vibratory hammer compaction methods

The MDD of the G4 hornfels material was the highest of the three materials. The MDDs of the RCA and NC were similar, with a higher OMC.

Table 4-2: Mod AASHTO compaction results for research materials

Material type	MDD (kg/m³)	OMC (%)
G4 hornfels	2264	6.3
RCA	1984	11.9
NC	1988	12.3

Table 4-3: Vibratory hammer compaction results for research materials

Material type	MDD (kg/m³)	OMC (%)
G4 hornfels	2285	4.9
RCA	2084	10.2
NC	2068	10.7

The decrease in MDD and OMC between the vibratory hammer and the Mod AASHTO compaction methods was analysed. It should be clarified that the OMC deceased from the Mod AASHTO to the vibratory hammer, while the MDD decreased from the vibratory

78

hammer to the Mod AASHTO. Figure 4-3 illustrates these decreases for all the three materials.

Figure 4-3: Decrease in MDD and OMC between the vibratory hammer and the Mod AASHTO compaction methods

Figure 4-3 shows the decrease (in percentage) in MDD and OMC between the vibratory hammer and the Mod AASHTO compaction methods. It is clear that a higher decrease in OMC, with a smaller decrease in MDD were registered for the G4 hornfels material. The decreases in OMC for RCA and NC materials were similar and smaller, and were associated with higher decreases in MDD, which were also similar. For a small decrease in OMC, the vibratory hammer produced higher densities for these latter materials, and this was related to their potential for self-cementation. This statement means that self-cementation, which is related to cement activity in the material, caused higher densities when the vibratory hammer was used for compaction; although a small decrease in OMC from the Mod AASHTO to the vibratory hammer was noted for both RCA and NC.

4.2.4 California Bearing Ratio (CBR)

The results of CBR tests for the three materials are presented in Table 4-4. These results are established at 100% Mod AASHTO relative compaction. The CBR values at 2.54 mm penetration are presented against this relative compaction. According to SAPEM (2014) and TRH 14 (1985) recommendations, the CBR value for a typical G4 material should not be less than 80% at 98% Mod AASHTO density. It should be noted that very high values were obtained for both RCA and NC as expected, and could potentially be as a result of the hydration. Appendix A shows the CBR curves of the three materials.

All the three materials showed non-swelling behaviour. In fact, swell results were less than 0.2%, which is the maximum swell recommended by TRH 14 (1985) for a typical G4 material.

Table 4-4: CBR and Swell results of the three materials at 100% Mod AASHTO relative compaction

Material type	CBR at 2.54 mm penetration (%)	Swell (%)
G4 hornfels	93.7	0.024
RCA	198.6	0.016
NC	331.2	0.031

Table 4-5 summarises the material characterisation tests results for G4 hornfels, RCA, and NC.

Table 4-5: Summary of material characterisation test results

Grading	G4 hornfels, RCA, and NC		
Sieve Size (mm)	% Passing		
37.5	100		
26.5	87		
19	78		
13.2	69		
9.5	60.5		
6.7	52		
4.75	46		
2.36	34.5		
1.18	26		
0.6	20		
0.425	17.5		
0.3	15		
0.15	10.5		
0.075	7		
Property	**G4 hornfels**	**RCA**	**NC**
Maximum Aggregate Size (mm)	19	19	19
Grading Modulus	2.41	2.41	2.41
Liquid Limit (%)	Non-Plastic	Non-Plastic	Non-Plastic
Plastic Limit (%)	Non-Plastic	Non-Plastic	Non-Plastic
Plasticity Index	Non-Plastic	Non-Plastic	Non-Plastic
Linear Shrinkage (%)	Non-Plastic	Non-Plastic	Non-Plastic
[1]MDD (kg/m3)	2264	1984	1988
[2]MDD (kg/m3)	2285	2084	2068
[3]OMC (%)	6.3	11.9	12.3
[4]OMC (%)	4.9	10.2	10.7
CBR @ 100% Mod AASHTO	93.7	198.6	331.2
Swell @ 100% Mod AASHTO	0.024	0.016	0.031

[1] Dry Density based on the AASHTO Modified Compaction Method

[2] Dry Density based on the Vibratory Hammer Compaction Method

[3] Optimum Moisture Content based on the AASHTO Modified Compaction Method

[4] Optimum Moisture Content based on the Vibratory Hammer Compaction Method

4.3   Strength test results

In order to evaluate the compressive strength and tensile strength of the research materials, the Unconfined Compressive Strength (UCS) and Indirect Tensile Strength (ITS) tests were performed, respectively. Amongst four standard categories of cement stabilised materials used in South African pavement structures (C1, C2, C3, and C4), C3 or C4 was selected for this study. This selection was based on the TRH 14 (1985) recommendation for subbase/base materials. According to TRH 14 (1985), the recommended values range from 0.75 to 1.5 MPa UCS at 100% Mod AASHTO, along with a minimum ITS of 200 kPa, and 1.5 to 3.5 MPa UCS at 100% Mod AASHTO, along with a minimum ITS of 250 kPa, for C4 and C3, respectively.

Table 4-6 shows the average standard (7 days) UCS and ITS results with 4% cement stabilisation for the three materials. It is clear from this table that very high results were obtained for both UCS and ITS. Therefore, the materials were suitable for subbase/base layers construction, but an adjustment of cement content is to be considered. It should also be reminded that the vibratory hammer was used for compaction, which contributed to these high values.

Table 4-6: Average standard (7 days) UCS and ITS results with 4% cement stabilisation

Material type	Average UCS (MPa)	Relative Standard Deviation for the UCS	Average ITS (kPa)	Relative Standard Deviation for the ITS
G4 hornfels	11.7	5.0	1184.3	4.2
RCA	10.1	12.6	1136.8	17.9
NC	9.9	35.6	872.4	6.2

Table 4-6 shows that there was consistency in the three repeats made for each type of material, with the highest deviation to the average registered for the NC material, where the Relative Standard Deviation is ± 35.6%. Appendix A shows all the UCS and ITS values obtained for the three repeats made. Figure illustrates the average standard (7 days) UCS and ITS results with 4% cement stabilisation, where the recommended limits for a C4 and C3 material are marked. The standard deviations are also shown on each average.

Figure 4-4: Average standard UCS results vs C4 and C3 recommended value ranges

Figure 4-5: Average standard ITS results vs recommended minimum values

As mentioned in Section 3.4.1, for the UCS test, the standard loading rate (153kN/min) broke shrinkage specimens before reading could be made. Therefore, a different loading rate (40kN/min) was considered and the results were compared. When this loading rate was used for G4 hornfels material with 4% cement stabilisation, a very similar UCS result (11.6 MPa) as the standard one was obtained, and hence, this latter loading rate was used for shrinkage specimens strength testing after the curing period (28 days).

Appendix A shows the tables and graphs of strength tests (UCS and ITS) results for the shrinkage specimens of the three materials used. The lower values were obtained for the NC material specimens. Comparing to very high shrinkage values obtained for this latter material, more cracking effect will occur, following the creation of high tensile stresses against these low tensile strengths.

4.4   Summary

This chapter discussed the characterisation and strength results obtained for the three materials used in this study. The South African road construction material guidelines were considered in order to evaluate the suitability and performance of these materials for pavement construction, especially for base and subbase layers construction. Comparing to recommended standard values, the results obtained confirmed that the three materials could be used for the specified purpose, with an adjustment of cement when stabilisation is required.

CHAPTER 5. SHRINKAGE TEST RESULTS DISCUSSION AND INTERPRETATION

5.1 Introduction

This chapter presents and discusses shrinkage results obtained from all specimens that were tested in laboratory. Initially, for the three materials used in this study, the shrinkage measurements for each specimen type (all the three repeats for the same mix) were compared on the same graph to evaluate the consistency of the test results. To this end, an average of the three repeats is considered for comparison between different specimen mixes. Also, the standard deviation is shown for each of the averages considered. A layout for clarification of this chapter is presented in Table 5-1.

Table 5-1: Chapter organisation

Item	Discussion	Section
G4 Hornfels	Introduction	5.2
	General description of phase division	5.2
	Observations made for specimens A, B, C, and D	5.2.1
	Comparison of specimens A, B, C, and D	5.2.2
	Averages of final shrinkages	5.2.2.1
	Coefficient of Variation (CV)	5.2.2.2
	Variation in curing temperature	5.2.2.3
	Trends of the averages of shrinkage	5.2.2.4
RCA	Introduction	5.3
	Observations made for specimens E, F, and G	5.3.1
	Comparison of specimens E, F, and G	5.3.2
	Averages of final shrinkages	5.3.2.1
NC	Introduction	5.4
	Observations made for specimens H,I, and J	5.4.1
	Comparison of specimens H, I, and J	5.4.2
	Averages of final shrinkages	5.4.2.1
G4, RCA, and NC	Comparison of the three materials	5.5
	Trends of the averages of shrinkage	5.5.1
	Magnitudes of changes for all specimen types	5.5.2
	Averages of final shrinkage of all specimens	5.5.2.1
	Averages of the highest shrinkage value	5.5.2.2
	Averages of shrinkage magnitude at pivot-point	5.5.2.3
	Averages of shrinkage results vs UCS and ITS	5.5.3

Appendix B shows dial gauge readings, with calculated axial shrinkages for the three materials used in this study.

A number of aspects are considered for comparison between different specimen mixes. The same aspects are used for comparison between same specimen mixes of different materials. These aspects are the final shrinkage, the time to pivot-point (explained in Section 5.2) and its shrinkage magnitude, the highest shrinkage measurement, and the potential influence of temperature variation as given in Table 5-1.

Additionally, the coefficient of variation (CV) is also considered in the analysis of results.

5.2   G4 hornfels analysis

Four different specimen mixes were considered for the G4 hornfels material. These include specimens A, where no cement and no SAP were used, specimens B with 2.5% cement and no SAP, specimens C with 4% cement and no SAP, and specimens D with 4% cement and SAP.

Figure 5-1 illustrates the shrinkage measurements for all G4 hornfels specimens tested. The discussion and interpretation of the results are done thereafter. It should be noted that clear differentiated shrinkage measurements phases were present, and these are visually identified and discussed.

Figure 5-1: Shrinkage measurements for all G4 hornfels specimens

Figure 5-1 indicates 4 phases for specimens A and B, and 3 phases for specimens C and D. These latter specimen types don't present phase 2. On the other hand, specimens B present phase 2 for only specimen B1 (only one repeat). Herewith a general description of phase division:

- **Phase 1**

This phase starts immediately after the zero reading was made, up to the beginning of initial swelling. It denotes **the early and sudden shrinkage**, which was due to the setting of specimens (time it took for specimens to get stable) after the zero reading was made. It should be noted that for specimens that did not present Phase 2, this phase connects directly to Phase 3. It should be noted that the immediate setting was shown in the results to explain the trends of shrinkage results. In fact, this immediate setting resulted from the time it took for specimens to get stable on the frames, and for this reason it was decided not to be eliminated from the usual results.

- **Phase 2**

This phase denotes **the initial swelling**, which can be influenced by different factors such as cement quantity, material type, maximum aggregate size, and temperature. In this study, the maximum aggregate size is not considered since it was kept the same for all types of materials used and for all specimens. The material type is considered for comparison between same specimen mixes of different materials.

- **Phase 3**

This phase denotes **the ordinary shrinkage** that is due to different causes of shrinkage as discussed in Section 2.4.1. Shrinkage magnitude distinguishes the shrinkage discussed in this phase from the one discussed in Phase 1. The end of this phase is marked by the Pivot-point. The pivot-point is defined as the time when the ordinary shrinkage stabilises. After this point, there is a notable decrease in the gradient of shrinkage.

- **Phase 4**

This last phase starts from the pivot-point up to the end of the curing period. It denotes **the shrinkage behaviour after the pivot-point**. It is also due to different causes of shrinkage as discussed in Section 2.4.1.

5.2.1   Observations made for specimens A, B, C, and D

Phase 1

Figure 5-1 reveals an early and sudden shrinkage for all specimen types (all repeats), which is due to the setting of the specimens after the zero reading was made. As indicated by the dial gauge readings in Appendix B, this shrinkage only lasted one day for specimens A and B, and 2 days for specimens C and D.

Phase 2

The initial swelling (expansion) occurred for specimens where cement was not used in the mixture (specimens A and B). This initial swelling was due to the difference between the aggregate temperature (before specimens were made), and the curing temperature (22^0C - 25^0C). The average aggregate temperature that was measured before the preparation of specimens was 14.5^0C. The aggregates expanded due to increase in temperature, which resulted in change in internal moisture distribution.

However, specimen B1 presented initial swelling even if cement was used in the mixture. The other two repeats of specimen B (specimens B2 and B3) did not swell. This occurrence of initial swelling for specimens B1 could possibly be due to the very low aggregate temperature (11^0C) compared to the others (18^0C).

On the other hand, specimens where cement was used in the mixture (specimens B, C, and D) did not present the initial swelling, and therefore Phase 1 connected directly to Phase 3. This absence of Phase 2 was due to the increase in autogenous shrinkage that was caused by the presence of cement in the mixture, in addition to drying shrinkage. These two types of shrinkage dominated the thermal expansion.

Phase 3 and Phase 4

Specimens A

For specimens A, the shrinkage is attributed to moisture loss through evaporation, as there is no cement in the mixture to cause hydration reactions. After six days (144 hours), drying shrinkage stabilised. The shrinkage gradient decreased considerably, and soon after almost flattened completely. This flattening implies that the material was stable after nine days (216 hours), and this point is referred to as the pivot- point.

Specimens B

The pivot-point occurred between 11 days (264 hours) and 14 days (336 hours) for the three repeats. After this period, the shrinkage gradient decreased and the material results exhibited less variation. There was still some swelling after the material had stabilised, and this swelling was due to hydration process of cement. As discussed in Chapter 2, Section 2.2.1.3, during hydration process, exothermic chemical reactions occur. These reactions create heat that increases the internal temperature of the material, and therefore, causes expansion.

Specimens C

The pivot-point occurred after 5 days (120 hours) for all the three repeats. After this period, the shrinkage gradient decreased, but the material only stabilised for a period of time ranging between 1 and 2 days. For the remaining time, the material presented inconsistent periods of shrinkage followed by swelling. These periods are called shrinkage-swelling cycles. The swelling is due to a more active hydration process initiated by a high content of cement, which generates more heat. Because this swelling is counteracted by shrinkage due to moisture loss through evaporation, and that hydration process continues as long as moisture is present in the mixture; the two simultaneous processes result in creation of the mentioned cycles.

Specimens D

The pivot-point occurred between 3 days (78 hours) and 5 days (120 hours) for all the three specimens. After this period, the shrinkage gradient decreased for another 2 to 3 days, and tended to stabilise for the rest of the time. Some expansion associated with the hydration process happened before the end of the test period, but presented a smaller gradient compared to specimens C. Furthermore, this expansion was more consistent and closer to linear. Obviously, this consistency was due to the use of SAP.

It should be noted that even if specimen D2 presented some shrinkage-swelling cycles, they were few and less disporite compared to specimens C. This behaviour could be a potential advantage regarding the possible formation of cracks in the material, and hence, in the pavement layers. The larger the disparity of shrinkage-swelling cycles the more potential fatigue induced by cracks can happen.

5.2.2   Comparison of specimens A, B, C and D

Figure 5-2 illustrates the averages and standard deviations for the three repeats of each G4 hornfels specimen type, according to the aspects that were considered in the comparison between specimens with different cement percentages in the mixture. Their interpretation was given thereafter. Appendix C shows the values of all repeats for these aspects. The coefficient of variation (CV) was considered to avoid any possible misinterpretation of the results.

5.2.2.1   Averages of shrinkages

Average final shrinkage

Figure 5-2 indicates that the final shrinkage increases with increase in cement content. This is in accordance to the literature, since more cement content needs an increased amount of moisture for the hydration process, and therefore, causes more shrinkage. On the other hand, the use of SAP was not beneficial for shrinkage reduction as expected. It is recommended to use different quantities of SAP, and to vary the absorption capacity, in order to evaluate SAP effect in terms of shrinkage reduction. However, the material strength is to be evaluated for any change in SAP quantity, as discussed in Chapter 2, Section 2.5.2.

Average time to pivot-point

Figure 5-2 reveals that the presence of cement in the mixture decreased the time to pivot-point for specimens C and D when compared to B. This outcome is in confirmation with the fact that the presence of cement in the mixture induces hydration reactions, which consume the material moisture and increase the ordinary shrinkage. Further increase in cement content creates higher dispority in shrinkage-swelling cycles, as discussed in Section 5.2.1. These cycles affect the time required to keep the same shrinkage gradient.

When SAP was used (specimens D), the time to pivot-point was slightly lower, compared to when it was not used (specimens C). This decrease in time could be due to the ability of SAP to retain water, and therefore, delayed the loss of moisture; but as it is only a slight decrease, it could also be as a result of material variability.

Figure 5-2: Averages of the three repeats for the aspects of shrinkage comparison (G4 hornfels)

Average shrinkage magnitude at pivot-point

Figure 5-2 reveals that shrinkage magnitude at pivot-point increases with increase in cement content. This increase is due to the moisture loss through hydration process, as discussed in previous sections. The figure also indicates that, at this point, shrinkage magnitudes are greater than final shrinkage values for specimens containing cement in the mixtures (specimens B and C), but an exception occurred for specimens D, and it resulted from the presence of SAP in the mixture. SAP has the capacity to retain water, which delays the hydration reactions, and therefore, the final shrinkage value was closer to shrinkage magnitude at pivot-point, than when there was no SAP in the mixture. When cement was not added to the mixture (specimens A), these two values of shrinkage were also very close because there were no hydration reactions to cause swelling.

Average highest shrinkage value

Figure 5-2 reveals that for all specimens, the highest shrinkage values registered increased with increase in cement. This increase in the highest shrinkage values with increase in cement emphasises the interpretation given previously; that cement induced moisture loss through hydration process, and therefore, increased shrinkage. Once again, the use of SAP was not beneficial for reducing this highest shrinkage value as expected. The same recommendation as provided in Section 5.2.2.1 (Average final shrinkage) can be given here.

5.2.2.2   Coefficient of variation (CV)

In order to regulate the interpretations recognised for previous aspects of comparison of shrinkage results, the coefficient of variation (CV) between repeats of the same specimen mix was considered. Figure 5-3 shows these coefficients of variation, and interpretations are given thereafter. Appendix D summarises the coefficients of variation.

Figure 5-3: Coefficients of variation (CV) of three repeats for aspects of shrinkage comparison (G4 hornfels)

CV of final shrinkage

Figure 5-3 shows that the CV of final shrinkage of specimens B is the greatest of all CV of the other specimens. This greatest CV, which indicates more inconsistency in final shrinkage results, could have affected the results, and therefore, the final shrinkage of specimens B was closer to the one for specimens A, although cement was not used in the mixture. The CV of final shrinkage of specimens C is very similar to the one of specimens D. This similarity does not contribute to the explanation of the fact that even with the use of SAP, the final shrinkage of specimens D was still greater than the one of specimens C. The recommendation given in section 5.2.2.1 is therefore, still valuable.

CV of time to pivot-point

Figure 5-3 shows that only variation of time to pivot-point occurred for specimens B, and D. There was consistency in the results obtained for specimens A, and C. The resultant CV of specimens B could have influenced the very high time to pivot-point that happened for these specimens. On the other hand, the resultant CV of specimens D could have influenced their low time to pivot-point compared to specimens C.

CV of shrinkage magnitude at pivot-point

As for time to pivot-point, Figure 5-3 indicates a higher CV of shrinkage magnitude at pivot-point for specimens B, and D. This higher CV for specimens B could have influenced their insignificant difference between shrinkage magnitude at pivot-point and highest shrinkage value (refer to Figure 5-2). Moreover, the higher CV for specimens D could have influenced their lower shrinkage magnitude at pivot-point.

CV of highest shrinkage value

Figure 5-3 indicates a higher CV of highest shrinkage value for specimens B, and D. The high CV for specimens B could have affected their magnitude of highest shrinkage value, and the one for specimens D, to their very high magnitude of highest shrinkage value compared to the one of specimens C.

Following the interpretation given on coefficients of variation for the aspects of comparison, it was concluded that the variations in shrinkage measurements for the three repeats of the same specimen type, did not affect the general outcomes. These variations only influenced the extents in which the shrinkage measurements compared between different specimen types of the same material, and/or the same specimen types of different materials.

5.2.2.3 Variation in curing temperature

Figure 5-4 shows the slight variation in curing temperature, in comparison with average shrinkage results of all specimen types. This variation was small (22-25^{0}C), as the temperature control room was used for curing of specimens.

Figure 5-4 shows that shrinkage results of specimens A, B, and D; are smooth, while the curing temperature was slightly varying, and therefore, the slight variation in temperature did not have any effect on shrinkage results of these specimens. On the other hand, there is an inconsistency in what should be the influence of this slight variation in temperature on shrinkage results of specimens C. The selected point (a), shows that when the temperature increased, shrinkage increased. This increase in temperature continued even when the temperature decreased. The selected point (b), shows that while the temperature was almost constant, shrinkage decreased and then increased. The selected point (c), shows that both the temperature and shrinkage were almost constant. Finally, the selected point (d), shows that while the temperature was constant, shrinkage decreased. Considering this inconsistency, the slight increase in temperature was also concluded not to affect shrinkage results.

This same analysis of the effect of variation in curing temperature on shrinkage results was done for the two other materials (RCA and NC), and the same conclusion was made, that the slight variation in temperature did not have any effect on shrinkage results. The figures can be found in Appendix E.

Figure 5-4: Temperature variation vs shrinkage results of G4 hornfels specimens

5.2.2.4   Trends of the average shrinkage for specimens A, B, C, and D

Figure 5-5 illustrates the averages of shrinkage for specimens A, B, C, and D. A comparison of these specimens is done based on the graphs, and a table summarising their shrinkage trends is given in Table 5-2.

Figure 5-5: Averages of shrinkage results of specimens A, B, C, and D

Table 5-2: Summary of shrinkage trends of specimens A, B, C, and D (G4 Hornfels)

Shrinkage trends (G4 hornfels)				
Sudden and early shrinkage, and ordinary shrinkage	**Initial swelling**	**Further shrinkage or swelling after pivot-point**	**Shrinkage-swelling cycles**	**Shrinkage extents**
• Early and sudden shrinkage for all the specimen types • The Ordinary shrinkage occurred for all the specimen types since there was loss of moisture	• Only specimens A presented an initial swelling • Specimens with cement stabilisation (B, C, and D) did not present an initial swelling. Drying and autogenous shrinkage dominated thermal expansion	• The shrinkage gradient of specimens A almost flattened after ordinary shrinkage. • Hydration reactions caused further shrinkage and swelling for specimens with cement stabilisation (B, C, and D)	• Not presented in specimens A. No hydration reactions • Not presented in specimens B due to low extent of the hydration process • Occurred in specimens C, and D. Higher extent of the hydration process due to higher cement content • Controlled by SAP use in specimens D	• Shrinkage increases with increase in cement • The use of SAP did not reduce shrinkage as expected. The recommendation given in Section 5.2.2.1 is considered here

5.3   Recycled concrete aggregates (RCA) analysis - old

Only three different specimen compositions were considered for RCA materials as explained before. These include specimens E (0% cement, 0% SAP), specimens F with 2.5% cement and 0% SAP, and specimens G with 4% cement and 0% SAP.

Figure 5-6 illustrates shrinkage measurements for all RCA specimens tested. The discussion and interpretation of the results were done thereafter. The RCA shrinkage measurements were divided into phases, which relate to the same definitions as given in Section 5.2.

5.3.1   Observations made for specimens E, F, and G (RCA)

Phase 1

Figure 5-6 reveals that all specimen types showed an early and sudden shrinkage due to the setting of specimens after the zero reading was made. This shrinkage only lasted one day for all the specimens.

Phase 2

Specimens E showed initial expansion that lasted one day for all three repeats. As explained in Section 5.2.1, the main cause of this initial swelling was the difference between aggregate temperature (12^0C - 17^0C for this case) and the curing temperature (22^0C - 25^0C).

No initial swelling was experienced for specimens with cement in the mix (specimens F and G), and therefore, drying and autogenous shrinkage dominated the thermal expansion.

Phase 3 and Phase 4

Specimens E

After initial expansion, shrinkage started and its gradient changed (pivot-point) after a period of 17 days (408 hours) for all three specimens, where it became closer to flat up to the last testing day, except from some small swelling periods observed in specimen E2.

Specimens F

The specimens presented some inconsistencies, but the shrinkage gradient reduced during the whole period and at the pivot-point almost flattening out. Nevertheless, specimen F3 still presented some shrinkage and swelling periods after this point. The pivot-point occurred after 16 days (384 hours) for the three repeats.

Figure 5-6: Shrinkage measurements for all RCA specimens

Specimens G

The pivot-point occurred after 5 days (126 hours) for all the three repeats. After the pivot-point, shrinkage gradient decreased, whilst the material only stabilised for 5 days (interim phase 4a), followed by shrinkage-swelling cycles. Section 5.2.1 (Phase 3 and Phase 4) gives explanation about the origin of these cycles.

5.3.2   Comparison of specimens E, F and G

Figure 5-7 shows the averages of the three repeats along with the standard deviations for each RCA specimen type, according to the aspects of comparison between different specimen types. The interpretation related to these aspects of comparison is given thereafter. Appendices C and D respectively show the values of all repeats for these aspects and their coefficients of variation (CV). Greater consistency was found in repeats of each RCA specimen type compared to G4 hornfels specimen types.

5.3.2.1   Averages of shrinkages

Average final shrinkage

Figure 5-7 illustrates that the addition of cement increases the final shrinkage of RCA materials. As expected, during hydration process, there is moisture loss in the material through hydration reactions created by the presence of cement in the mixture. However, an increase in cement content (4%) did not increase the final shrinkage of the RCA material. This higher final shrinkage value for small amount of cement content was possibly due to the latent hydration in the material. The accumulation of the latent hydration product in the RCA material seem to saturate the potential for shrinkage, therefore reaching its maximum shrinkage at 2.5% cement content.

Average time to pivot-point

Figure 5-7 indicates that the time to pivot-point is highest for specimens E, where cement was not used. This time reduced slightly for specimens F, and finally, reduced considerably for specimens G. The highest time to pivot-point for specimens E was due to latent hydration that consumed the material moisture in addition to moisture loss during drying of the material. Both these activities increased the ordinary shrinkage time. For specimens F, the addition of small amount of cement increased the presence of small swelling periods in the material, which reduced ordinary shrinkage time. For specimens G, the high amount of cement content created shrinkage-swelling cycles, which considerably reduced the ordinary shrinkage time.

101

Figure 5-7: Averages of the three repeats for the aspects of shrinkage comparison (RCA)

Average shrinkage magnitude at pivot-point

The same observation as given in Section 5.2.2.1 (average shrinkage magnitude at pivot-point) is considered here.

Average highest shrinkage value

Figure 5-7 indicates that the highest shrinkage value that was registered during shrinkage measurement, increased with increase in cement, due to more moisture loss through hydration process as cement increases. The closeness in highest shrinkage values of specimens F and G emphasises the possibility of latent hydration, which contributed to the small difference between lower and higher cement addition.

5.4　New Concrete analysis (NC)

As for RCA materials, three different specimen compositions were considered. These include specimens H (0% cement, 0% SAP), specimens I with 2.5% cement and 0% SAP, and specimens J with 4% cement and 0% SAP.

Figure 5-8 illustrates shrinkage measurements for all NC specimens tested. The discussion and interpretation of the results are done thereafter. The NC shrinkage measurements were divided into phases, which also relate to the same definitions as given in Section 5.2.

5.4.1　Observations made for specimens H, I, and J (NC)

Phase 1

As for G4 hornfels and RCA materials, Figure 5-8 reveals an early and sudden shrinkage due to the same reason as for these previous materials. This shrinkage lasted one day for all the specimens.

Phase 2

Specimens H showed initial expansion that lasted one day for all three repeats due the same reason as for specimens E (refer to Section 5.3.1 Phase 2). For this case, the aggregate temperature varied between 11^0C and 16^0C.

Specimens I and J did not experience initial swelling due to the same reason as for specimens F and G (refer to Section 5.3.1 Phase 2).

Figure 5-8: Shrinkage measurements of all NC specimens

Phase 3 and Phase 4

Specimens H

The initial expansion was followed by shrinkage characterised by an inconsistent gradient, which changed (pivot-point) at a period of 22 days (528 hours) for all the three repeats. After the pivot-point, shrinkage gradient became almost flat, except from specimen H2, where a slight swelling was observed. The main cause of this shrinkage was the moisture loss through evaporation. However, a very high shrinkage magnitude was presented, which is associated to cement activity in the material.

Specimens I

As for specimens F, the material presented some inconsistencies, with shrinkage gradient reduction towards the end of the curing period. The shrinkage gradient became almost flat when the pivot-point was reached. The pivot-point occurred after 24 days (576 hours) for the three repeats.

Specimens J

The pivot- point occurred after 5 days (126 hours) for all the three specimens. After the pivot-point, the shrinkage gradient decreased. The material stabilised for almost 4 days (90 days), followed by another higher shrinkage gradient for 1 day, which was followed by a flat shrinkage period of 7 days (168 days). This flat shrinkage period was followed by shrinkage-swelling cycles.

5.4.2   Comparison of specimens H, I and J

Figure 5-9 shows the shrinkage averages of the three repeats of each NC specimen type, associated with the aspects of shrinkage comparison between different specimen types. Interpretation related to these aspects of comparison is given thereafter. Appendices C and D respectively show the outcomes of measurements for all specimens, and their coefficients of variation (CV). As for RCA material, a greater consistency was found in repeats of each NC specimen type compared to G4 hornfels specimen types.

5.4.2.1   Averages of shrinkages

Average final shrinkage

Similar to RCA material, Figure 5-9 shows that the addition of cement in the mixture increased the final shrinkage, which was due to the hydration reactions that generated

105

moisture loss. The latent hydration increased the final shrinkage of NC material, but the creation of shrinkage-swelling cycles, for specimens with increased cement content (4%), reduced the final shrinkage value.

Average time to pivot-point

Figure 5-9 indicates that the times to pivot-point for specimens H and I were very close and very high compared to the one for specimens J. The similarity of times to pivot-point for specimens H and I was due to the presence of some cement that was still active in NC material before any cement addition. The addition of a small amount of cement did not have a significant influence on hydration process in the material. However, the creation of shrinkage-swelling cycles for specimens with increased cement content (4%) reduced the ordinary shrinkage time.

Average shrinkage magnitude at pivot-point

As for RCA material, Figure 5-9 indicates that the addition of cement increased shrinkage magnitude at pivot-point because hydration reactions were enhanced. The addition of higher cement quantity created shrinkage-swelling cycles, and therefore, reduced shrinkage magnitude at pivot-point. It should be noted that both in specimens H and I, the shrinkage magnitudes at pivot-point, were very close to final shrinkage, which emphasises that the addition of a small amount of cement was dominated by cement activity in NC material itself.

Average highest shrinkage value

As explained previously, an increase in cement quantity in the mixture generates more moisture loss through hydration process, thus, producing higher shrinkage value.

5.5   Comparison of the three materials (G4, RCA and NC)

5.5.1   Trends based on the average shrinkage results

Figure 5-10 illustrates the trends of the averages of shrinkage results for all materials tested. The shrinkage results for the specimens of different materials with the same cement content are put together in the same graphs for a clear comparison. Finally, the shrinkage results for all specimens tested are put in the same graph.

Different observations are made from Figure 5-10:

- **0% cement content:**

For the G4 hornfels and RCA materials, the thermal expansion is dominant at the beginning (after the early and sudden shrinkage), whereas for the NC material the thermal expansion was dominated by shrinkage.

The final shrinkage magnitude is very high for the NC material, whereas for the G4 hornfels and RCA materials this magnitude is low and more or less the same. However, there is still a rate of change for RCA material.

It can be concluded that cement activity is higher for the NC material than for the RCA material.

- **2.5% cement content:**

The behaviours of the G4 hornfels and RCA materials are different here. A significant difference in the final shrinkage magnitudes is notable. In addition, their trends are not the same. Still the NC material presents a highest final shrinkage, but its trend is more or less the same as the one of the RCA material.

It can be concluded that there is a potential for latent hydration in the RCA and the NC materials.

- **4% cement content:**

Again the behaviour of the RCA material becomes more or less the same as the one of the G4 hornfels material. Their final shrinkage magnitudes are similar. It is remarkable that the final shrinkage magnitude of the RCA material is less than for 2.5% cement content. Also the similarity in the final shrinkage magnitudes for 2.5% and 4% cement contents is noted for the NC material.

It can be concluded that the latent hydration dominated and the increase in cement content did not have a great influence

The graphs of rates (horizontal lines) of shrinkage and swelling (Figure 5-11, Figure 5-12, and Figure 5-13) were used to illustrate the observations made on a comparison of the trends of the averages of the shrinkage results of the three materials, and Table 5-3 summarises these observations.

Figure 5-9: Averages of the three repeats for the aspects of shrinkage comparison (NC)

Figure 5-10: Averages of shrinkage results of all specimen types for the three materials tested

Figure 5-11: Rate of shrinkage and swelling for the averages of the results (0% cement content)

Figure 5-12: Rate of shrinkage and swelling for the averages of the results (2.5% cement content)

Figure 5-13: Rate of shrinkage and swelling for the averages of the results (4% cement content)

Table 5-3: Comparison of the trends of shrinkage results of the three materials tested

Shrinkage trends (G4 hornfels, RCA, and NC materials)				
Sudden and early shrinkage, and ordinary shrinkage	**Initial swelling**	**Further shrinkage or swelling after pivot-point**	**Shrinkage-swelling cycles**	**Shrinkage extents**
• All specimen types presented an early and sudden shrinkage • The inevitable moisture loss induced the ordinary shrinkage for all specimen types	• All specimens with 0% cement (A, E, and H) presented an initial swelling • Cement activity dominated thermal expansion in the NC material. Minor initial swelling occurred	• Nonappearance for specimens A (0% cement) • Occurred in specimens E and H. Latent hydration • Occurred for all specimens with cement in the mix (B, F, I, C, G, and J)	• Not presented for specimens A, E, and H. No hydration process for A, and very low extent for E and H • Not presented for specimens B, F, and I due to lower extent of the hydration process • Occurred in specimens C, G, and J. Higher extent of the hydration process resulting from a higher cement addition	• Shrinkage increases with increase in cement for all types of materials • Higher final shrinkage magnitudes for 2.5% cement content in the RCA and NC materials. Increase in cement content dominated by the latent hydration.

113

5.5.2 Magnitudes of changes for all specimen types

At this stage, the magnitudes of changes are addressed based on the aspects of shrinkage comparison between different specimen types. Figure 5-14 illustrates the averages of shrinkage results of all specimen types based on the aspects of shrinkage comparison.

The standard deviations were presented in Sections where the analysis of material by material was done. It should be reminded that the analysis done on coefficients of variation revealed that the variations in repeats of the same specimen types did not affect the general conclusions to be made.

5.5.2.1 Averages of final shrinkage of specimens

Figure 5-14 shows that for the same cement content, the final shrinkage is lesser for the G4 hornfels material, medium for the RCA material and high for the NC material. It increases with increase in cement for the G4 hornfels material, while for the RCA and NC materials, the highest values are found for 2.5% cement content. It can also be seen that the final shrinkage values for the G4 hornfels and RCA materials are similar (1248.5×10^{-6} and 1468.3×10^{-6} respectively) for 4% cement content. Likewise, for these latter materials, these values are similar for 0% cement content. They are very different (almost double) for 2.5% cement content. The reasons for these observations are given in Section 5.5.1.

5.5.2.2 Averages of the highest shrinkage value

Figure 5-14 shows that for the same cement content, the highest shrinkage value is lesser for the G4 hornfels material, medium for the RCA material and high for the NC material. It increases with increase in cement for all the three materials. This magnitude order emphasises the potential for latent hydration for the RCA and NC materials. In addition, higher cement activity for the NC material is emphasised.

The highest shrinkage values of the G4 hornfels and RCA materials are very similar for 4% cement content. A significant difference is noted between 2.5% and 4% cement contents for the G4 hornfels material, while the two values are similar for the RCA material. It can be concluded from this statement, that the RCA material was close to its maximum shrinkage for 2.5% cement content due to the influence of the latent hydration. In fact, compared to the G4 hornfels material, the very high shrinkage at 2.5% cement content for the RCA material resulted from the higher porosity, which increased the absorption, and therefore the moisture content. This higher porosity was caused by the presence of hydrated cement paste in the

RCA material. Additionally, it can be said that the contribution to the magnitude of shrinkage from the latent hydration in the RCA material was compared to the addition of 1.5% cement.

Similarly, for the NC material, the highest shrinkage values are close for 2.5% and 4% cement contents, which emphasises that the increase of cement in the mix was dominated by the latent hydration.

5.5.2.3   Averages of shrinkage magnitude at pivot-point

Figure 5-14 indicates that the shrinkage magnitude at pivot-point increases with increase in cement for the G4 hornfels material. This increase is due to higher moisture loss due to hydration process. For the RCA and NC materials, the highest shrinkage magnitudes at pivot-point are found for 2.5% cement content, which again emphasises the dominance of the latent hydration and the tendency to maximum shrinkage at 2.5% cement content.

5.5.3   Averages of shrinkage results vs UCS and ITS

Based on the aspects of shrinkage comparison between different specimen types, the averages of shrinkage results were compared to UCS and ITS results after the curing period (28 days). Figure 5-15 and Figure 5-16 illustrate this comparison with UCS and ITS results, respectively.

A direct relationship is noted between the increase in both UCS and ITS results, and the increase in the averages of shrinkage results for all the aspects of shrinkage comparison (for all the three materials). In fact, all other factors (such as course/fine aggregate ratio) being equal, an increase of cement for no increase in water demand reduces the water/cement ratio, and increases the material strength (UCS and ITS). At the same time, there is higher moisture loss due to hydration process, which results in an increase of shrinkage magnitude.

Figure 5-15 and Figure 5-16 show that for all the three materials, an increased cement content (from 0% to 4%) resulted in an increased shrinkage magnitude, and an increased UCS and ITS. However, when comparing the three materials, the G4 hornfels material registered the highest UCS and ITS values, with lowest shrinkage values, for the same cement content. Furthermore, the RCA material registered higher UCS and ITS values than the NC material, for the same cement content, but the shrinkage magnitudes were lower. These magnitudes emphasise the potential for latent hydration for the RCA and NC materials in general, and the higher cement activity for the NC material in particular.

Figure 5-14: Averages of shrinkage results of all specimen types

Figure 5-15: Averages of shrinkage results of all specimen types vs UCS

Figure 5-16: Averages of shrinkage results of all specimen types vs ITS

5.6   Statistical analysis

5.6.1   Introduction

The final shrinkage, the shrinkage magnitude at pivot-point, and the highest shrinkage are all dependent on a combination of factors, which are the cement content (%), the moisture content (%), the moisture loss (%), and the density (kg/m^3). These factors are called independent variables.

Using Microsoft excel, a multiple regression analysis was done to analyse the influence of these independent variables on the shrinkage results. This analysis (multiple regression analysis) predicts a dependent variable based on multiple independent variables. Some other software such as SPSS can also be used for this analysis.

To perform this analysis, the means of three or more independent variables are compared using the Analysis Of Variance (ANOVA), which determines if there is a significant relation between variables. The F-value, which tests the overall significance of the model, is computed from the sum of squares. The larger the F, the greater the significance is. To reject the null hypothesis "H_0", the overall p-value (overall significance or significance F) must be less than the considered level of significance (α). The current analysis considers the level of significance of 0.05, which is the most commonly used. The null hypothesis indicates that there is no relation between the independent variables as a group and the dependent variable.

It should be noted that a model can present a global significance with insignificant independent variables or significant independent variables with global insignificance. In case of the latter situation, the model is of no importance.

The three categories of shrinkage results were analysed for material by material, and finally, analysed for all the three materials together. The outputs were then compared. In addition, the influence of the independent variables on the UCS and ITS results was analysed, followed by the influence of the UCS and ITS results on shrinkage results.

The following sections, only present the significance F, the t stat, and the P-value for conclusions. The full summary outputs are presented in Appendix F. The t stat is performed to check if there is a relationship between each independent variable and the dependent variable. The software calculates it by dividing the variable coefficient by its standard error. The higher the t-stat, the most influential the variable is. Table 5-4 illustrates the inputs for independent and dependent variables.

Table 5-4: Inputs for statistical analysis

Material type		INDEPENDENT VARIABLES				DEPENDENT/INDEPENDENT		DEPENDENT VARIABLES		
		Cement content (%)	Moisture content [Vibratory hammer] (%)	Moisture loss [Vibratory hammer] (%)	Density (kg/m³)	UCS - 28 DAYS (MPa)	ITS - 28 DAYS (kPa)	Final shrinkage (X10⁻⁶) [mm/mm]	Shrinkage magnitude at pivot-point (X10⁻⁶) [mm/mm]	Highest shrinkage (X10⁻⁶) [mm/mm]
G4 Hornfels	A1	0	4.876	1.065	2452	1.3	105.6	-434.8	-507.2	-525.4
	A2	0	4.880	0.556	2442	1.2	95.8	-821.8	-763.6	-883.6
	A3	0	4.876	0.834	2447	1.2	85.9	-523.6	-407.3	-523.6
	B1	2.5	4.848	1.307	2444	7.8	738.5	-487.8	-644.6	-662.0
	B2	2.5	4.866	1.426	2456	8.2	757.9	-1157.9	-1964.9	-1964.9
	B3	2.5	4.869	1.536	2460	8.6	716.4	-868.8	-1365.2	-1365.2
	C1	4	4.889	1.702	2474	12.5	1315.8	-1109.2	-1490.5	-1507.8
	C2	4	4.900	1.794	2481	12.3	1214.4	-1590.9	-1783.2	-2307.7
	C3	4	4.900	1.824	2482	11.9	1180.1	-1045.3	-1324.0	-1533.1
RCA	E1	0	10.107	3.341	2170	1.5	109.4	-503.6	-359.7	-503.6
	E2	0	10.113	3.351	2172	1.4	134.2	-1007.2	-791.4	-1007.2
	E3	0	10.106	3.264	2169	1.4	100.9	-1032.6	-887.7	-1032.6
	F1	2.5	10.104	4.700	2198	8.4	747.7	-1459.1	-1227.8	-1459.1
	F2	2.5	10.133	4.753	2205	7.5	610.2	-1766.8	-1580.3	-1837.5
	F3	2.5	10.118	4.714	2201	7	765.9	-1748.3	-1923.1	-1923.1
	G1	4	10.200	5.438	2232	11.1	1282.3	-1358.9	-1550.5	-1689.9
	G2	4	10.152	5.231	2218	10.7	1188	-1431	-913.8	-1810.3
	G3	4	10.188	5.406	2229	11.8	1128.5	-1615.1	-1182.3	-1907.2
NC	H1	0	10.570	4.365	2207	1.5	121.5	-1593.4	-1611.7	-1611.7
	H2	0	10.552	4.639	2206	2	139.6	-1758.9	-1941.4	-1941.4
	H3	0	10.542	4.520	2201	1.9	100.5	-1851.9	-1888.9	-1888.9
	I1	2.5	10.611	4.944	2223	7.5	495.8	-2643.9	-2625.9	-2643.9
	I2	2.5	10.598	5.053	2223	6.5	461.2	-2078.9	-2114.7	-2114.7
	I3	2.5	10.576	5.025	2218	6.9	514.5	-2777.8	-2759.3	-2814.8
	J1	4	10.677	5.538	2248	10.4	952.8	-2035.7	-1910.7	-2285.7
	J2	4	10.697	5.310	2247	9.9	897.6	-2437.5	-1850.5	-2740.2
	J3	4	10.700	5.529	2253	10.5	998.5	-2750	-2642.9	-3089.3

5.6.2   Analysis of material by material

5.6.2.1   Effect of the independent variables on the final shrinkage

Table 5-5 shows the outputs of the effect of the independent variables on the final shrinkage.

Table 5-5: Outputs of the effect of the independent variables on the final shrinkage

Material type	Independent variable	t stat	P-value	Significance F
G4 hornfels	Cement content	-1.349140219	0.248603354	0.171107928
	Moisture content	-0.74126402	0.499691722	
	Moisture loss	-0.735896653	0.502615996	
	Density	0.738402377	0.501249228	
RCA	Cement content	-0.211062893	0.843154968	0.105613246
	Moisture content	-1.062171703	0.348031527	
	Moisture loss	-1.09165468	0.336330571	
	Density	1.0697886	0.344974065	
NC	Cement content	-1.618764843	0.180809598	0.254805549
	Moisture content	-0.546495516	0.613779481	
	Moisture loss	-0.443547088	0.680305313	
	Density	0.703952562	0.520282969	

Table 5-5 shows that the analysis of material by material reveals that there is no significant influence of the independent variables as a group on the final shrinkage, since all significance F values are greater than 0.05. Statistically it implies that none of these independent variables are significant within a 95% confidence interval. However, it is interesting to note that both the G4 Hornfels and NC concrete have the highest significance for cement content (as expected). However, the RCA shows a very small significance to the cement content which is counterintuitive. It is however noteworthy, that the moisture content and the moisture loss has the "most significance of all the parameters for RCA (within a 70% confidence interval).

5.6.2.2   Effect of the independent variables on the shrinkage magnitude at pivot-point

Table 5-6 shows the outputs of the effect of the independent variables on the shrinkage magnitude at pivot-point.

Table 5-6: Outputs of the effect of the independent variables on the shrinkage magnitude at pivot-point

Material type	Independent variable	t stat	P-value	Significance F
G4 hornfels	Cement content	-1.409872643	0.231384116	0.22643769
	Moisture content	-1.164943573	0.308778364	
	Moisture loss	-1.164748788	0.30884875	
	Density	1.164484746	0.308944187	
RCA	Cement content	0.683435079	0.5318666	0.211349056
	Moisture content	-0.582904521	0.591238269	
	Moisture loss	-0.61767286	0.570220719	
	Density	0.585934707	0.589386575	
NC	Cement content	-0.897733213	0.420078815	0.552030341
	Moisture content	-0.039153763	0.970644052	
	Moisture loss	-0.297385173	0.780977324	
	Density	0.249754124	0.815079414	

The same as for the final shrinkage, Table 5-6 shows that there is no significant influence of the independent variables as a group on the shrinkage magnitude at pivot-point due to the same reason. Here again it should be noted that the highest significance is with the cement content of the G4 hornfels, with not the RCA or the NC showing significance in the cement content with the "pivot-point" being a dependent variable. It is in all probability the fact that the long term latent properties has a huge influence on the behaviour not reflected in the pivot-point which is only a "short phase" dependent.

5.6.2.3   Effect of the independent variables on the highest shrinkage

Table 5-7 shows the outputs of the effect of the independent variables on the highest shrinkage.

Table 5-7: Outputs of the effect of the independent variables on the highest shrinkage

Material type	Independent variable	t stat	P-value	Significance F
G4 hornfels	Cement content	-1.033482802	0.359765507	0.241824521
	Moisture content	-0.685853834	0.530491479	
	Moisture loss	-0.684223516	0.531418074	
	Density	0.684414483	0.531309478	
RCA	Cement content	-0.775127662	0.481536673	0.048619929
	Moisture content	-1.276660696	0.270801921	
	Moisture loss	-1.295216916	0.264942073	
	Density	1.281798862	0.269166952	
NC	Cement content	-1.054561106	0.351110643	0.20357385
	Moisture content	-0.718440151	0.512214769	
	Moisture loss	-0.702636528	0.52102044	
	Density	0.793795429	0.471746631	

Table 5-7 only shows a little significant influence of the independent variables on the highest shrinkage for the RCA material. For this material, the significance F value is less but very

close to 0.05. Nevertheless, for the same material, all the individual P-values are greater than 0.05, which means that no independent variable has a significant influence on the highest shrinkage of this material. Again, for the G4 hornfels and the NC materials, the highest significance is with the cement content, while for the RCA material, the highest significance is with the moisture loss.

Due to the non-significant influence of the independent variables on the three categories of shrinkage results, when the materials are analysed separately, it was decided to analyse the influence of the independent variables when the materials are analysed together. This decision was based on the consideration of material characteristics, which caused higher variations of some independent variables, such as the moisture content, the moisture loss, and the density.

5.6.3   Analysis of the three materials together

Table 5-8 shows the outputs of the effect of the independent variables on the three categories of shrinkage results.

Table 5-8: Outputs of the effect of the independent variables on the three categories of shrinkage results

Shrinkage result category	Independent variable	t stat	P-value	Significance F
Final shrinkage	Cement content	-0.495546642	0.625128132	2.87197E-07
	Moisture content	-3.139167791	0.004767248	
	Moisture loss	0.51415901	0.612267131	
	Density	-4.173156366	0.000395287	
Shrinkage magnitude at pivot-point	Cement content	0.112009016	0.911831962	0.000603573
	Moisture content	-1.786175481	0.087862296	
	Moisture loss	-0.087009856	0.931450781	
	Density	-2.941085831	0.007556524	
Highest shrinkage	Cement content	-1.205036424	0.24099212	9.73845E-07
	Moisture content	-2.721453516	0.012463084	
	Moisture loss	0.405136064	0.689290104	
	Density	-3.854202449	0.000860087	

Table 5-8 shows that the analysis of the three materials together reveals that there is a significant influence of the independent variables as a group on all the three categories of shrinkage results, since all significance F values are very small (<<0.05). For all the three categories of shrinkage results, the moisture content and the density are the independent variables that have a great influence. This great influence for these independent variables agrees with the literature, that drying shrinkage is the major reason of shrinkage cracking of

123

pavements. Drying shrinkage is related to the available moisture, which also dictates the achievable density. It is important to note that, although the P-value of the moisture content for the shrinkage magnitude at pivot-point is greater than 0.05 (P-value = 0.08), the confidence that is greater than 90% still shows some significant influence.

Considering the other independent variables, Table 5-8 indicates that the moisture loss does not really have a significant influence on the three categories of shrinkage results, while the cement content shows some significant influence on the highest shrinkage (76% confidence). This confidence indicates that the cement content has some influence on the highest shrinkage, but not the same as the moisture content and the density do. Figure 5-17 illustrates these outputs.

The moisture content and density have the most significance, although you would expect the moisture loss to be the most significant as opposed to moisture content. This is interesting as drying shrinkage is said to be mostly influenced by the moisture loss/migration.

Figure 5-17: Schematic representation of the outputs of the effect of the independent variables on the three categories of shrinkage results

5.6.4   Analysis of the UCS and the ITS

This section analyses the UCS and the ITS results in association with the independent variables and the three categories of shrinkage results. This means that firstly, the UCS and

the ITS results are considered as dependent variables, then after they are considered as independent variables. This analysis was based on the consideration of whether the UCS and ITS influence the shrinkage or not.

5.6.4.1 Effect of the independent variables on the UCS and the ITS results

Table 5-9 shows the outputs of the effect of the independent variables on the UCS and the ITS results.

Table 5-9: Outputs of the effect of the independent variables on the UCS and the ITS results

UCS or ITS	Independent variable	t stat	P-value	Significance F
UCS	Cement content	15.83230488	1.64918E-13	2.4951E-19
	Moisture content	-2.054576574	0.051987375	
	Moisture loss	1.187918044	0.247532748	
	Density	-1.993732975	0.058723722	
ITS	Cement content	9.471348469	3.21272E-09	1.42819E-14
	Moisture content	-2.55656046	0.017991356	
	Moisture loss	1.343699293	0.192741462	
	Density	-2.822204084	0.009921833	

Table 5-9 shows that there is a significant influence of the independent variables as a group on the UCS and ITS results (Significance F < 0.05). Except from the moisture loss, all the other independent variables have a significant influence on the UCS and the ITS results. It is essential to note the greatest influence of cement content on the UCS and the ITS results, which is as expected.

It is important to note that the significance of parameters on the UCS and ITS was much higher than the three shrinkage categories explored in Section 5.6.2 and 5.6.3. Because of this reason, it was then further decided to see what would happen if the significance of the UCS and ITS results is explored on the three shrinkage categories.

5.6.4.2 Effect of the UCS and the ITS results on the three categories of shrinkage results

Table 5-10 shows the outputs of the effect of the UCS and the ITS results on the three categories of shrinkage results.

Table 5-10: Outputs of the effect of the UCS and the ITS results on the three categories of shrinkage results

Shrinkage result category	Independent variable	t stat	P-value	Significance F
Final shrinkage	UCS	-3.292227044	0.003069561	0.005654863
	ITS	2.92659136	0.007383264	
Shrinkage magnitude at pivot-point	UCS	-3.399980822	0.002357705	0.003408725
	ITS	2.976049616	0.006568652	
Highest shrinkage	UCS	-3.342348266	0.002715735	0.000678203
	ITS	2.662030629	0.013641129	

Table 5-10 shows a significant influence of the independent variables as a group on the three categories of shrinkage results (Significance F < 0.05). Both the UCS and the ITS results have a significant influence on the three categories of shrinkage results. This significant influence emphasises the direct relationship noted between the increase in both UCS and ITS results, and the increase in the averages of shrinkage results for all the aspects of shrinkage comparison (for all the three materials), as discussed in Section 5.5.3. The reason postulated for this is that although the UCS is not a true reflection of the performance parameter shrinkage to be measured,   the UCS and ITS to a high degree does encapsulate the interaction of all these parameters into one value.

5.7   Summary

Chapter 5 presented and interpreted the shrinkage results obtained for all the specimens tested in laboratory. To increase consistency, three repeats were performed for each specimen type. A comparison between different specimen types was done using averages of the three repeats, and the standard deviations were shown.

A number of aspects are considered for shrinkage results comparison. These aspects include the final shrinkage, the time to pivot-point and its shrinkage magnitude, the highest shrinkage measurement, and the potential influence of temperature variation. In addition, the coefficient of variation (CV) was considered for the analysis of results. The shrinkage trends were divided into 3 to 4 phases depending on the specimen types. The four phases included the early and sudden shrinkage (Phase 1), the initial swelling (Phase 2), the ordinary shrinkage (Phase 3), and the shrinkage behaviour after the pivot-point.

Comparing the trends of specimen types, it was revealed that all the specimen types (for all the three materials) presented both Phase 1 and Phase 3. The former phase resulted from the setting of specimens (time it took for specimen to get stable) after the zero reading was made,

while the latter phase resulted from the actual causes of shrinkage, especially the moisture loss due to drying. All the specimen types with 0% cement content presented phase 2, due to thermal expansion (difference between the aggregates temperature and the curing temperature). Nevertheless, for the NC material, minor initial swelling (Phase 2) occurred, since cement activity (latent hydration) dominated thermal expansion.

In Phase 4, specimens with 0% cement content (for all the three materials) did not present shrinkage-swelling cycles because there was no cement to cause hydration reactions (G4 hornfels), or a very low latent hydration resulted (RCA and NC materials). Specimens with 2.5% cement content (for all the three materials) also did not present shrinkage-swelling cycles, because lower extent for the hydration process resulted, due to lower quantity of cement added. However, specimens with 4% cement content (for all the three materials) presented the shrinkage-swelling cycles due to the higher extent of the hydration process caused by the higher cement addition.

For all specimen types, shrinkage increased with increase in cement. However, the final shrinkage magnitude of the RCA material is greater for 2.5% cement content than for 4% cement content. In addition, the final shrinkage magnitudes for 2.5% and 4% cement contents were very similar for the NC material. Therefore, the latent hydration dominated the increase in cement content for the RCA and NC materials.

A direct relationship was noted between the increase in both the UCS and the ITS results, and an increase in the averages of shrinkage results for all the aspects of shrinkage comparison (for all the three materials). However, the G4 hornfels material registered the highest UCS and ITS values with lowest shrinkage values, while the RCA material registered the higher UCS and ITS values than the NC material, with lower shrinkage magnitudes. These shrinkage magnitudes indicate the potential for latent hydration in the RCA and NC materials, with a higher degree for the NC materials.

The statistical analysis showed that the moisture content and the density have a great influence on the final shrinkage, the shrinkage magnitude at pivot-point and the highest shrinkage, whereas the cement content has some influence on the highest shrinkage. The UCS and the ITS results are related with the shrinkage results.

CHAPTER 6. IMPLICATIONS OF SHRINKAGE RESULTS

6.1 Introduction

Chapter 5 discussed and interpreted shrinkage results. This interpretation was done in consideration of material characteristics. This chapter intends to analyse the results in consideration of pavement characteristics, especially pavement cracking due to shrinkage. In order to perform this analysis, other research that has linked shrinkage values with crack width and spacing in a constructed layer was considered as a benchmark.

6.2 Background

Factors affecting properties of stabilised materials

The factors that affect the properties of stabilised materials were extensively discussed in Chapter 2, Section 2.2.1.2. These factors include, amongst others, the host materials, amount and type of stabilising agent, moisture content, compaction, mix uniformity, and curing temperature. Affecting stabilised materials implies affecting the pavement layers, where these materials are applied.

A summary of the effects of these factors on stabilised materials used in pavement layers is provided hereafter.

- **Host materials:**
    - The strength that can be achieved is related to cementitious bonds between the hydration products and the host material.
    - The cement can be used for treatment of all types of materials, but provides good results for well-graded granular materials because their sufficient fines form a floating aggregate matrix (TRH 13, 1986).
    - The stabilisation of fine-grained materials is followed by shrinkage cracking because these materials require more cement quantity to achieve the required strength. This shrinkage cracking is, therefore, more pronounced for fine-grained materials with uniform grading.

128

Figure 6-1: Particle bond with and without cement (Mbaraga, 2015)

Figure 6-1 indicates three different situations. Situation A illustrates coarse particles without any fine or medium particles. This situation leads to very poor bond strength. A very high amount of cement would be used to achieve a required bond strength, which would lead to problems cited in previous statements. Situation B illustrates more coarse and medium particles with limited amount of fines. In this situation, there is some degree of bond strength, but cement efficiency is reduced by an unsuitable particle distribution, which has a negative influence on the strength properties of the material. Situation C illustrates a well-graded material. This situation leads to ideal bond strength. The suitable distribution of fines, medium and coarse particles enhances the cement efficiency, which positively influences the strength properties of the material.

- **Amount and type of stabilising agent:** Stabilisation of materials with cement offers high strength and stiffness for the pavement structure but is more prone to shrinkage than other types of stabilising agents. It is, therefore, necessary to balance the achieved strength and shrinkage extent by selecting the required cement content.
- **Moisture content and compaction:**
  - The material moisture content has a great influence on the achieved density for a given compactive effort. The density affects the fatigue behaviour of stabilised materials. Low density leads to short fatigue life of the pavement and consequently to pavement destruction in short time than expected. It is

therefore, necessary to achieve the required density by the use of appropriate compaction method.

- ▪ Insufficient moisture content causes inadequate hydration process, while excess moisture content causes reduction in final setting strength.

- ▪ Higher moisture content leads to higher shrinkage magnitude due to high possibility of moisture loss, especially when the material (or pavement in general) is exposed to the atmosphere.

- **Curing temperature:** Higher temperatures accelerate the curing process and cause the formation of cracks in the pavement stabilised layers.

Shrinkage types and mechanisms

The shrinkage types and mechanisms were discussed in Chapter 2, Section 2.4.1.1. It was revealed that drying shrinkage is the major reason of pavement cracking due to shrinkage. This type of shrinkage is due to moisture loss at a given temperature and humidity conditions. Cement stabilisation requires moisture for hydration process, and hence, increases the need of moisture in the material, which increases the shrinkage magnitude. The moisture loss leads to the reduction of volume of the material (or pavement layers in general), which creates tensile stresses in a pavement. High tensile stresses are created in stabilised materials (or stabilised layers in general) following their high moisture content.

6.3   The concept of shrinkage cracks in cement stabilised layers

The moisture loss due to drying, hydration and/or changes in temperature, altogether can contribute to formation of cracks in cement-stabilised pavement layers. However, the moisture loss due to drying is the main cause of these cracks.

In fact, moisture loss causes contraction of cement-stabilised pavement layers, and hence, induces tensile stresses in these layers. The stabilised layer is fully or partially restrained by friction from the layer below. This friction adds to contraction and high tensile stresses are induced in cement-stabilised pavement layers. Cracks occur when induced stresses exceed the tensile strength in particular zones of the stabilised layer. These zones are recognised as weak in stabilised layers. Figure 2-23, presented in Chapter 2, illustrates the development of stresses in a cement-stabilised pavement layer, resulting from shrinkage.

Cracking is a natural characteristic of cement-stabilised pavement layers. Cracks can reflect to the pavement surface layer. Low shrinkage is associated with closed and narrow cracks. These cracks don't have a negative effect on the pavement performance because they can still allow

aggregate interlock. However, high shrinkage is associated with spaced and wide cracks. These cracks contribute to pavement deterioration because they are the zones of water infiltration, which results in debonding of layers and pumping of underlying material.

6.4   Analysis of shrinkage and strength results

Table 6-1 illustrates the highest shrinkage and strength average results for the three research materials. It is clear from Table 6-1 that for 0% cement content, materials presented some UCS results, but their ITS results were below the minimum value (200kPa for C4) to be classified as cemented materials. These UCS results were influenced by the high curing period (28 days) compared to the TRH 14 (1985), which considers a standard curing period of 7 days. In addition, the method of compaction used (the vibratory hammer compaction method) gives higher density than the TRH 14 (1985) considered standard method (Mod AASHTO compaction method), and therefore, contributed to high strength results.

These two reasons mentioned in the previous statement, also contributed to the high strength results obtained for the stabilised materials, and consequently to their material classes.

Table 6-1 shows that UCS and ITS results of stabilised G4 hornfels material are the highest, followed by those for stabilised RCA material. For the same cement content, these results are similar for these two materials, compared to the lowest results of stabilised NC material. This order of results magnitude is in opposition with shrinkage results, where shrinkage results of NC material are the highest, and the ones of G4 hornfels are the lowest. Again, it should be noted that shrinkage results of G4 hornfels and RCA materials are similar for the same cement content.

This interaction between strength and shrinkage results for the research materials indicates that more cracking effect will result when the NC material is used as a pavement construction material, since high tensile stress will be induced against low tensile strength. Alternatively, the similarity between G4 hornfels and RCA material strength results and shrinkage results on the other hand, for the same cement content, suggests that comparable cracking effect will result if they are used as pavement construction materials. Therefore the two materials can be used interchangeably.

131

Table 6-1: Averages of highest shrinkage and strength results of the research materials in this project

Material type	Cement content[%]	Average of the highest Shrinkage [X 10 $^{-6}$]	UCS (7 DAYS) [MPa]	UCS (28 DAYS) [MPa]	ITS (7 DAYS) [kPa]	ITS (28 DAYS) [kPa]	Material class referred to TRH 14
G4 hornfels	0	644.2		1.2		95.8	N/A
	2.5	1330.7		8.2		737.6	C1
	4	1782.9	11.7	12.2	1184.3	1236.7	C1
	4 (+ SAP)	1989.2		10.8		1312.5	C1
RCA	0	847.8		1.4		114.8	N/A
	2.5	1739.9		7.6		707.9	C1
	4	1802.5	10.1	11.2	1136.8	1199.6	C1
NC	0	1814.0		1.8		120.5	N/A
	2.5	2524.5		7.0		490.5	C1
	4	2705.1	9.9	10.3	872.4	949.6	C1

132

6.5   Comparison with existing results

6.5.1   Categorisation of crack-patterns

In order to perform the crack pattern (crack width and spacing) analysis, Mbaraga (2015) results, obtained for ferricrete and hornfels, were considered, where the Houben Model was used. These results for ferricrete and hornfels materials were put into three categories. These categories include material inducing acceptable, medium or unacceptable crack propagation behaviour. The Houben Model is a numerical analysis method, which provides the development of tensile stresses and strength, and the times of occurrence of transversal cracks, with their spacing and widths (Houben, 2008). The first cracks occur after construction, and the subsequent cracks result from increased load-induced stresses deriving from wide cracks (Figure 6-2).

The model resultant crack pattern depend (but not limited) to the following parameters:

- material strength properties (tensile strength, compressive strength, and modulus of elasticity)
- seasonal data (temperature amplitude)
- material thermal coefficients (coefficient of linear thermal expansion)
- material shrinkage data
- material stress relaxation
- coefficient of friction

The model assumes the appearance of cracks at mid-span between the layer existing cracks. With this model, the appearance of first cracks is at a wider length L_{W1} compared to the second L_{W2}, which also appears at wider length compared to the third L_{W3}. The same order follows with the subsequent series of cracks. The induced cracking in the layer depends on properties of materials used in the layer, the friction at the interlayer, and the climatic conditions. Figure 6-2 illustrates a schematic representation of crack pattern resulting from shrinkage cracking. For more details on the calculation of the model input parameters, Mbaraga (2015) is considered.

Figure 6-2: Schematic representation of crack pattern resulting from shrinkage cracking (Mbaraga, 2015)

Table 6-2 illustrates the categorisation of crack-pattern of Mbaraga's results, obtained for ferricrete and hornfels materials by the use of the Houben Model.

Table 6-2: Categorisation of crack-pattern of Mbaraga (2015) results

Material type	Cement content (%)	With or without polymer	Average axial shrinkage result Pmax 19.0 mm (X 10^{-6})	Crack-pattern category
Hornfels	0	without	11.1	Acceptable (no cracks)
	2	without	250.3	Acceptable (no cracks)
	2	with	209.9	Acceptable (no cracks)
	3	without	475	Acceptable (no cracks)
	3	with	340.1	Acceptable (no cracks)
	6	without	969.7	Unacceptable (very severe cracking)
	6	with	751.9	Medium (severe cracking)

134

Material type	Cement content (%)	With or without polymer	Average axial shrinkage result Pmax 19.0 mm (X 10^{-6})	Crack-pattern category
Ferricrete	0	without	63.3	Acceptable (no cracks)
	4	without	1549	Unacceptable (very severe cracking)
	4	with	411.1	Acceptable (no cracks)
	6	without	3955.5	Unacceptable (very severe cracking)
	6	with	800	Medium (severe cracking)

Table 6-2 indicates that from an average axial shrinkage of 11.1 to 475 [X10^{-6}], the Houben model did not found any crack induced in the pavement. This range is, therefore, categorised as an acceptable crack-pattern. From an average axial shrinkage of 751.9 to 800 [X10^{-6}], the Houben model found severe cracks, and this range is classified as medium crack-pattern. Finally, from an average axial shrinkage of 969.7 to 3955.5 [X10^{-6}], the Houben model found very severe cracks, and the range is classified as unacceptable crack-pattern. Figure 6-3 illustrates the envelopes for the three categories of crack-patterns.

Figure 6-3: Envelopes of the three categories of crack-patterns

Based on the categorisation done in Table 6-2, the average axial shrinkage results of the research materials were also classified. Table 6-3 summarises this classification.

136

Table 6-3: Categorisation of crack-pattern of materials in this research

Material type	Cement content[%]	Average axial Shrinkage [X 10^{-6}]	Crack-pattern category
G4 hornfels	0	644.2	Acceptable
	2.5	1330.7	Unacceptable
	4	1782.9	Unacceptable
	4 (+ SAP)	1989.2	Unacceptable
RCA	0	847.8	Medium
	2.5	1739.9	Unacceptable
	4	1802.5	Unacceptable
NC	0	1814.0	Unacceptable
	2.5	2524.5	Unacceptable
	4	2705.1	Unacceptable

Table 6-3 reveals that in the same conditions as the ones in Mbaraga's modelling, the Houben model would find very severe cracks (unacceptable crack-pattern), for cement stabilised layers, if the research materials were used. For non-stabilised materials, only the NC material would induce very severe cracks. The G4 hornfels material would induce no cracks (acceptable crack-pattern), while the RCA material would only induce severe cracks (medium crack-pattern). Figure 6-4 compares the average axial shrinkages of the research materials with the envelopes of crack-patterns as shown on Figure 6-3.

137

Figure 6-4: Comparison of the average axial shrinkages with the envelopes of crack-patterns

It is clear, from Figure 6-4, that the non-stabilised G4 hornfels exceeds the limit for the acceptable crack-patterns, but does not reach the medium crack-pattern envelope. It is therefore, classified as inducing an acceptable crack-pattern. Similarly, the non-stabilised RCA exceeds the limit for the medium crack-patterns, but does not reach the unacceptable crack-pattern envelope. It is therefore, classified as inducing a medium crack-pattern.

There is no way the non-stabilised G4 hornfels can shrink and induce cracks. The fact that it exceeds the limit for the acceptable crack-patterns (in consideration of Mbaraga's modelling results) can be related to further parameters investigated in Section 6.5.1, and therefore, the envelope could change in this case. In addition, the statement above reveals that it is possible that the non-stabilised RCA material could be classified as inducing an acceptable crack-pattern as well.

Although the Houben model results were proven practically accurate, it is a limitation that the results from this research have not been compared to in-situ results. In addition, Mbaraga's results that could give an indication were also not compared to field experience.

6.5.2 Investigating further parameters affecting shrinkage results

6.5.2.1 Coefficient of linear thermal expansion

At this level, further analysis was done in order to consider the characteristics used in the model. The coefficient of thermal expansion was taken into consideration for this analysis. This coefficient is explained as the extent of dimensional changes resulting per unit length of a stabilised layer, caused by 1 degree change in temperature. It is given by the product of the UCS value material elasticity and the shrinkage coefficient.

According to Mbaraga (2015), Equation 6-1 is used for the computation of the coefficient of linear thermal expansion:

$$\alpha = C_8 \times E_{28-day} \qquad (^0C^{-1})$$

Equation 6-1

Where:

C_8 : Coefficient of shrinkage

E_{28-day} : 28-day Elastic Modulus (MPa) based on the flexural beam test

Figure 6-5 compares the ranges of the UCS results for the research materials with Mbaraga's, for the acceptable, medium, and unacceptable crack-patterns.

Figure 6-5: Comparison of the UCS results with crack-pattern categories

Figure 6-5 shows that the UCS results of the research materials are higher than the ones obtained in Mbaraga's investigation.

Referring to Xuan (2012) established coefficient of linear thermal expansion for cement treated recycled crushed concrete and masonry aggregates for pavements, the same range of shrinkage coefficients for cement-stabilised materials used in Mbaraga's modelling was kept. In this case, the higher values of UCS, obtained for the research materials, denote the assumption of a higher coefficient of linear thermal expansion.

The higher coefficient of linear thermal expansion indicates the induction of higher thermal deformation in the layers where the research materials could be used. Therefore, the potential for cracking could be increased. The comparison between research materials reveals that with the highest UCS results (for the same cement contents); the G4 hornfels material would induce highest potential for cracking, followed by the RCA material, followed by the NC material. However, the induced potential for cracking must consider the other input parameters of the Houben model, and the combination of the entire input parameters dictate the potential for cracking.

6.5.2.2   Tensile strengths

Figure 6-6 compares the ranges of the ITS results for the research materials with Mbaraga's, for the acceptable, medium, and unacceptable crack-patterns.

Figure 6-6: Comparison of ITS results with crack-pattern categories

Figure 6-6 shows that comparing cement contents, the ITS results of the research materials are higher than the ones obtained in Mbaraga's investigation. Considering these higher tensile strengths obtained for the research materials, the potential for cracking could be reduced for layers where the research materials could be used, because cracks are formed when the induced tensile stresses become greater than the tensile strengths.

Comparing the research materials, the NC material is associated with a highest potential for cracking, due to its lowest ITS results (for the same cement contents). Due to its highest ITS results, the G4 hornfels material is associated with a lowest potential for cracking, and the RCA material is associated with a medium potential for cracking. It is necessary to note that the ITS results of the G4 hornfels material is similar to the one of the RCA material. The two materials are therefore, associated with similar potential for cracking.

6.6 Summary

This chapter investigated the shrinkage results implications by considering pavement cracking due to shrinkage. The other research that has linked shrinkage values with crack width and spacing in a constructed layer was considered as a benchmark.

Referring to the results obtained in Mbaraga's investigation on hornfels and ferricrete, by the use of the Houben model, the limits for the three categories of crack-patterns were

established. These categories include the acceptable, medium, and unacceptable crack-patterns. When associating the shrinkage results of the research materials with these limits of crack-pattern categories, it was revealed that only the induced crack-pattern from the G4 hornfels material with 0% cement was classified as an acceptable crack-pattern. The induced crack-pattern from the RCA material with 0% cement was classified as medium crack-pattern, and all the other induced crack-patterns were classified as unacceptable crack-patterns.

In order to consider the actual situation in the current study, further parameters that could have an effect on the shrinkage results were examined. The higher UCS results obtained for the research materials suggest that a higher coefficient of linear thermal expansion could be required, which could increase the potential for cracking. The higher ITS results obtained for the research materials suggest that the potential for cracking could be reduced, since cracks are formed when the induced tensile stresses become greater than the tensile strengths.

CHAPTER 7. CONCLUSIONS AND RECOMMENDATIONS

7.1   Introduction

The application of cement to G4 hornfels, Recycled Concrete Aggregates (RCA) and New Concrete (NC) materials increases their strength properties. The compressive strength and tensile strength were assessed in this study. However, several factors influence the engineering properties of cement-stabilised materials, and these include the type and quality of materials to be stabilised, the curing conditions and the age. Cement-stabilised materials are prone to shrinkage, which is recognised as the major source of different forms of cracking, identified as the most severe distress for pavements with Cement stabilised layers (CSL). High tensile stresses are induced in CSL due to friction from the layer below. Cracks occur when these stresses exceed the tensile strength of the material. Based on the literature review, drying shrinkage is the major reason of shrinkage cracking for pavements.

The main purpose of this study was to compare shrinkage properties of cement-stabilised natural materials and RCA with and without stabilisation, where self-cementing properties of the latter materials were assessed. To achieve the study objectives, various testing methods presented in Chapter 3, and results analyses presented in Chapter 4 and 5, were followed. Chapter 6 served as a key for the evaluation of the shrinkage results in a pavement structure.

This chapter provides a summary of the general conclusions since specific observations are presented in the above-mentioned chapters. The chapter also presents the recommendations for further researches.

7.2   Conclusions

- The characterisation and strength results showed that the research materials can be used as base/subbase construction materials.
- As part of material property evaluation, cylindrical specimens were preferred to beam specimens for shrinkage measurements. In fact, for beam specimens, the friction located at the interface between the beam and mould surfaces causes cracks, which negates any reliable measure of shrinkage.
- The method of compaction used influences the packing of material particles, which determines the material void ratio, and the highest achievable dry density (MDD) with the corresponding moisture content (OMC), influencing the degree of shrinkage. In this study, the Modified AASHTO compaction method, and the vibratory hammer compaction method were compared. The vibratory hammer compaction method was

preferred for shrinkage and material strength (UCS and ITS) specimen preparation, since it simulates the reality, as it allows for translation and rotation of the particles through vibration, which results in a better (higher) compaction and densities. With this method of compaction, the higher MDD was obtained for lower OMC.

- For the trends of shrinkage measurements, all the specimen types (all materials and all cement contents) presented an early and sudden shrinkage, which was due to the setting of materials. This is the time it took for specimens to get stable on the frameworks, and was between 1 and 2 days.

- For comparison, the grading of the three materials was kept the same, so as to minimise its influence on the degree of shrinkage. The three materials exhibited some shrinkage for 0% cement content, mostly due to moisture loss during the curing period (drying). At this cement content, the NC material exhibited very high shrinkage values, whereas the G4 hornfels and RCA materials exhibited lower shrinkage values, with some rate of change for the RCA material. This dissimilarity in shrinkage magnitudes indicates self-cementing properties for the RCA and the NC materials, with a higher degree for the NC materials.

  In addition, the initial swelling (thermal expansion), which occurred for 0% cement content, after the early and sudden shrinkage, was dominant for the G4 hornfels and RCA materials, whereas for the NC material it was dominated by shrinkage. This shrinkage dominance emphasises the higher degree of self-cementing properties for the NC material.

- Due to hydration reactions, the shrinkage magnitude increased with the increase in cement content for the three materials. There was consistency in the shrinkage magnitude increase for the G4 hornfels material. However, the shrinkage magnitudes for 2.5% and 4% cement contents were very similar for the RCA and the NC materials, due to the latent hydration process (caused by self-cementing properties) which dominated the increase in cement. The RCA and the NC materials tended to reach their maximum shrinkage values for 2.5% cement content.

- Higher cement addition in the mixture (4%) produced higher extent of the hydration process, which induced shrinkage-swelling cycles, as it happened simultaneously with drying shrinkage.

- The considered percentage and absorption capacity for the Super-Absorbent Polymer (SAP) did not reduce the shrinkage magnitude as expected. However, due to its ability to retain water, SAP controlled the shrinkage-swelling cycles, and they became more

144

or less smooth, compared to when it was not used. This smoothness could be a potential advantage regarding the possible formation of cracks. The larger the disparity of shrinkage-swelling cycles the more potential fatigue induced by cracks can happen.

- The analysis of the shrinkage results showed that all cement-stabilised materials (all the three material types) are associated with very severe cracks if they are used in base/subbase layers. For non-stabilised materials, only the NC material is associated with very severe cracks. However, the non-stabilised RCA material is associated with severe cracks, while the G4 hornfels material is associated with no cracks. It is, therefore, necessary to consider different methods for mitigating shrinkage cracks, if these materials are used in pavement layers.

In summary, it can be concluded that cement-stabilisation of inferior materials is essential to increase their strength properties, but care should be taken to the induced shrinkage properties, which lead to shrinkage cracking. The RCA material exhibits some self-cementing properties, but these are minor compared to the NC material. The RCA material can, therefore, be treated with cement to improve its properties, in order to be used in base/subbase layers, as any other natural material. In all cases, with cement-stabilisation, the consideration of methods for mitigating shrinkage cracks is essential.

7.3   Recommendations

- This study considered the same grading for all the three material types through the use of the Fuller's equation, to minimise the grading influence on the degree of shrinkage. However the practical approach is to perform a sieve analysis. It is therefore, recommended to perform a sieve analysis and a CT scanning on the research materials, to investigate the grading influence on shrinkage magnitude.

- The RCA and the NC materials were characterised based on the South African specifications developed for natural materials. These specifications can be limiting to these secondary materials. It is recommended to develop test protocols and specifications for the CDW, and to include it in the South African material guidelines.

- Generally, the CDW includes masonry, which has a great influence on the material properties. It is important to investigate the influence it has on the material shrinkage properties.

- The results showed that the considered percentage and absorption capacity for the Super-Absorbent Polymer (SAP) did not reduce the shrinkage magnitude as expected.

It is recommended to use different percentages and absorption capacities, to investigate the effect of SAP. However, for any considered percentage and absorption capacity, it is essential to assess the material strength.

- It is revealed that the RCA and the NC materials tended to have their maximum shrinkage values at 2.5% cement content. To assess this statement, it is important to consider the percentages close to 2.5% (2% and 3% for example).

- It is important to consider circumferential shrinkage, in order to acquire insights regarding the volumetric shrinkage of the specimens, which provides additional information concerning the material shrinkage potential.

- To evaluate the implications of the current shrinkage results in the pavement structure, other research that has linked shrinkage values with crack width and spacing in a constructed layer was considered as a benchmark. However, it was revealed that some input parameters could be different from the ones used in the considered investigation. It is therefore, recommended to perform a complete modelling with the current input parameters.

REFERENCES

Adaska, W.S. & Luhr, D.R., 2004. Control of Reflective Cracking in Cement Stabilized Pavements. In *5th International RILEM Conference*. Limoges, France, pp. 1–8.

Bagonza, S. et al., 1987. Carbonation of Stabilised Mixtures. In *Transport Research Laboratory*. U.K, pp. 29–48.

Bahar, R., Benazzoug, M. & Kenai, S., 2004. Performance of compacted cement-stabilised soil. *Cement and Concrete Composites*, 26(7), pp.811–820.

Bazant, Z.P., 1988. Mathematical modeling of creep and shrinkage of concrete. , p.459. Available at: http://books.google.com/books/about/Mathematical_modeling_of_creep_and_shrin.html?id=wEdkAAAAMAAJ&pgis=1.

Beckett, C. & Ciancio, D., 2014. Effect of Compaction Water Content on the Strength of Cement-Stabilized Rammed Earth Materials. *Canadian Geotechnical Journal*, 51(February), pp.583–590.

Beltzung, F. & Wittmann, F.H., 2005. Role of disjoining pressure in cement based materials. *Cement and Concrete Research*, 35(12), pp.2364–2370.

Bester, J.J., Kruger, D. & Hinks, A., 2004. Construction and Demolition Waste in South Africa. In *Sustainable Waste Management and Recycling: Construction Demolition Waste:Proceedings of the international conference organised by the concrete and masonry research group*. London: Thomas Telford publishing, pp. 63–67.

Bhandari, R.K.M., 1973. Shrinkage of Cement Treated Mixtures. *Journal of The Australian Road Research Board, No. 3*.

Bisschop, J., 2002. Drying Shrinkage Cracking at Early Ages. *RELIM TC 181-EAS: Final Report*.

Bofinger, H.E., Hassan, H.O. & Williams, R.I.T., 1978. The Shrinkage of Fine-Grained Soil-Cement. In *TRRL Supplementary Report 398, Transport and Road Research Laboratory (TRRL)*.

Brandl, H., 1999. Mixed in Place Stabilisation of Pavement Structures with Cement and Additives. *Proceedings of the 12th European Conference on Soil Mechanics and Geotechnical Engineering*.

Brandt, A.M. & Li, V.C., 2003. Drying shrinkage and crack width of Engineered Cementitious Composites (ECC). *Proc. Int. Symp. "Bittle Matrix Composites 7."*

Campher, L., 2015. *Shrinkage and Flexibility Behaviour of Bitumen Stabilised Materials*. Master's thesis Stellenbosch University.

Chai, L., Monismith, C.. & Harvey, J., 2009. Re-Cementation of Crushed Material in Pavement Bases. , (October).

Chakrabarti, S. & Kodikara, J., 2003. Basaltic Crushed Rock Stabilized with Cementitious Additives: Compressive Strength and Stiffness, Drying Shrinkage, and Capillary Flow Characteristics. *Transportation Research Record*, 1819(1), pp.18–26.

Claisse, P.A., Elsayad, H.I. & Shaaban, I.G., 1999. Permeability and Pore volume of Carbonated Concrete. *ACI materials Journal*, 96(No.3), pp.378–381.

Colombier, G. & Marchand, J.P., 1993. The Precracking of Pavement Underlays Incorporating Hydraulic Binders. In *Proceedings of the 2nd International Conference RILEM Conference on Reflective Cracking in Pavements*. London: E and FN Spon.

Copeland, L.E., Kantro, D.L. & Verbeck, G., 1960. Chemistry of Hydration of Portland Cement. *Research and Development Laboratories of thr Portland Cement Association*, I, pp.429–465.

Craeye, B., Geirnaert, M. & Schutter, G.D., 2011. Super absorbing polymers as an internal curing agent for mitigation of early-age cracking of high-performance concrete bridge decks. *Construction and Building Materials*, 25(1), pp.1–13. Available at: http://dx.doi.org/10.1016/j.conbuildmat.2010.06.063.

Das, B.., 2003. Chemical and Mechanical Stabilization. *Transportation Research Board*.

Dukatz, E.., 1989. Aggregate Properties Related to Pavement Performance. In *Proceedings of Association of Asphalt Paving Technologist*. Nashville, Tennessee, pp. 492–502.

Dumbleton, M.J. & Ross, N.F., 1960. Effect of Temperature in the gain of Strength of Soils Stabilised with Hydrated Lime and Portland Cement. *Research Note RN/3655, BS. 438 Road Research Laboratory*.

Eades, J.. & Grim, R.., 1966. A quick Test to Determine Lime Requirements for Lime Stabilization. In *Highway Research Record 139*. pp. 61–72.

Edil, T.. & Schaertl, G.., 2009. *Engineering Properties of Recycled Materials for Unbound Applications*, Madison, USA.

El-Rahim, A. & George, K.P., 2001. Optimum Cracking for Improved Performance of Cement-Treated Bases. In *Proceedings 9th World Conference on Transport Research*. Seoul, Korea.

Erlin, B. & Hime, W., 2004. Carbonation of Concrete. *Concrete Construction-World of Concrete*, 49(8), pp.22–26.

Freeme, C.R., 1984. Symposium on Recent Findings of Heavy Vehicle Simulator Testing. In *ATC 1984 NITRR*.

George, K., 2001. Soil Stabilization Field Trial. *Interim Report). Department of Civil Engineering, The ...*, (April). Available at: http://docs.trb.org/00929218.pdf.

George, K.., 1968. Shrinkage Characteristics of Soil-Cement Mixtures. In *Highway Research Record, No. 255*. Washington, D.C, pp. 42–57.

George, K.P., 1990. Characterization and Structural Design of Cement-Treated Base. *Transportation Research Record*, 1288, pp.78–87.

George, K.P., 1970. Crack Control in Cement-Treated Bases. In *Final Report*. Civil Engineering Department, University of Mississippi. Available at: http://etheses.nottingham.ac.uk/1898/.

George, K.P., 1969. Cracking in Pavements Influenced by Viscoelastic Properties of Soil-Cement. *Presented at the 48th Annual Meeting, Highway Research Record, No. 263*, pp.47–59.

George, K.P., 1973. Mechanism of Shrinkage Cracking in Soil-Cement Bases. In *Highway Research Record 442 HRB National Research Council*. pp. 1–10.

George, K.P., 2000. Minimizing Cracking in Cement-Treated Materials for Improved Performance. *Final Report to Portland Cement Association Hitek Engineering Consultants*.

Goltermann, P., 1995. Mechanical Predictions of Concrete Deterioration ; Part 2: Classification of Crack Patterns. *ACI Materials Journal*, 92(1), pp.58–63.

Gress, D., 2001. Determination of Shrinkage Characteristics of Concretes with Type K Cement, Mineral and Chemical Additives. In *University of New Hampshire and US Department of Transportation Federal Highways Administration*.

Bofinger, H.E. & Sullivan, G.A., 1971. An Investigation of Cracking in Soil Cement Bases for Roads. In *Road Research Laboratory (RRL) Report LR 379*. Crowthorne, Berkshire: Road Research Laboratory.

Halsted, G.E., 2010. Minimizing Reflective Cracking in Cement-Stabilized Pavement Bases. In *Pavement Maintenance and Preservation Session of the 2010 Annual Conference of the Transportation Association of Canada*. Halifax, Nova Scotia, p. 10.

Hansen, T.C., 1992. Recycling of Demolished Concrete and Masonry. In *Report of Technical Committee 37-DRC Demolition and Reuse of Concrete*. London: Taylor & Francis Group.

Hansen, W., 1987. Drying Shrinkage Mechanisms in Portland Cement Paste. *Journal of the American Ceramics Societey*, 70(5), pp.323–328.

Hasholt, M.T. et al., 2012. Can superabsorent polymers mitigate autogenous shrinkage of internally cured concrete without compromising the strength? *Construction and Building Materials*, 31, pp.226–230. Available at: http://dx.doi.org/10.1016/j.conbuildmat.2011.12.062.

Helmuth, G.J. and Verbeck, R.A., 1968. Structures and physical properties of cement paste. *Proceedings of the 5th International Symposium on the Chemistry of Cement.*, 3(1), pp.1–32.

Hodgkinson, J.R., 1991. Long-term Performanceof Local Government Road Pavements Recycled by Cement Stabilisation. *Paper from 6th National Local Government Engineering Conference*, (Hobart), pp.1–10.

Holt, E.E., 2001. Early age autogenous shrinkage of concrete. *VTT Publications*, (446), pp.2–184.

Holtz, R.D. & Covacs, W.D., 1981. *An Introduction To Geotechnical Engineering*, USA: Prentice Hall, Inc.

Houben, L.J.M., 2008. Model for Transversal Cracking (at Joints) in Plain Concrete Pavements. In Faculty of Civil Technology and Geotechnical, Delft University of Technology.

Houben, L.J.M., 2011. *Model for Transversal Cracking in Non-Jointed Plain Concrete Pavements as a Function of the Temperature Variations and the Time of Construction*, Delft University of Technology.

Hwang, C.-L. & Young, J.F., 1984. Drying shrinkage of portland cement pastes I. Microcracking during drying. *Cement and Concrete Research*, 14(4), pp.585–594.

Idiart, A.E., 2009. *Coupled analysis of Degradation Processes in Concrete Specimens at the Meso-level*. Ph.D. Dissertation Polytechnic University of Catalonia.

Kaufmann, E.N., 2012. *Characterization of Materials.* John Wiley & Sons, Inc.

Kenai, S., Bahar, R. & Benazzoug, M., 2006. Experimental analysis of the effect of some compaction methods on mechanical properties and durability of cement stabilized soil. *Journal of Materials Science*, 41(21), pp.6956–6964.

Kodikara, J. & Chakrabarti, S., 2005. Modeling of Moisture Loss in Cementitiously Stabilized Pavement Materials. *International Journal of Geomechanics*, 5(4), pp.295–303.

Kodikara, J. & Chakrabarti, S., 2006. Modelling drying shrinkage of cement-stabilised crushed rock. *Proceedings of the ICE - Construction Materials*, 159(2), pp.67–75.

Kovler, K. & Zhutovsky, S., 2006. Overview and Future Trends of Shrinkage Research. *Materials and Structures*, 39(9), pp.827–847.

Lefort, M., 1996. Technique for Limiting the Consequences of Shrinkage in Hydraulic-Binder-Treated Bases. In *Proceedings of the 3rd International Conference on Reflective Cracking in the Pavements*. London: E and FN Spon.

Little, D., Thompson, M. & Terrell, R., 1987. Soil stabilization for roadways and airfields. Report ESL-TR-86-19, Air Force Engineering and Services Center, Tyndall Air Force Base, Florida. , 19.

Little, D.N. et al., 2002. Characterization of Design Properties (Compressive Strength and Resilient Modulus) of Lime, Cement, Fly Ash Stabilized Structural Recycled Concrete Base as a Function of Curing Time. *Presented for the 2002 Federal Aviation Administration Airport Technology Transfer Conference*, (Texas).

Little, D.N., 1992. Comparison of In-Situ Resilient Moduli of Aggregate Base Courses with and without Low Percentages of Lime Stabilization. *ASTM Special Technical Publication*, (1135), pp.8–22.

Little, D.N. et al., 1995. Identifaication of the structural benefits of base and subgrade stabilisation. In *Research Report 1287-2F, Texas Transportation Institute*. College Station, Texas: Texas A&M university.

Mbaraga, A.N., 2015. *Shrinkage Characterisation, Behavioural Properties and Durability of Cement-Stabilised Pavement Materials*. Ph.D. Dissertation Stellenbosch University.

Mehta, P.K. & Monteiro, P.J.M., 2006. *Concrete: microstructure, properties, and materials*, Available at: http://en.scientificcommons.org/34168511\nhttp://doi.contentdirections.com/mr/mgh_biblio.jsp?doi=10.1036/0071462899.

Molenaar, A., 2010. Cohesive and non-cohesive soils and unbound granular materials for bases and sub-bases in roads. , (September).

Molenaar, A. & van Niekerk, A., 2002. Effects of Gradation, Composition, and Degree of Compaction on the Mechanical Characteristics of Recycled Unbound Materials. *Transportation Research Record*, 1787(1), pp.73–82.

Molenaar, A.A.., 2008. Fatique Performance of Self-Cementing Base Courses. , pp.251–258.

Montgomery, D.E., 1998. How does cement stabilisation work? In *Stabilised Soil Research Progress Report SSRPR2*. University of Warwick, UK.

Nakayama, H. & Handy, R.L., 1965. Factors Influencing Shrinkage of Soil-Cement. In *Highway Research Record, No. 86*. Washington, D.C, pp. 15–27.

Netterberg, F. & Paige-Green, P., 1984. Carbonation of Lime and Cement Stabilized Layers in Road Construction. In *Technical Report, Report No. RS/3/84, National Institute for Transport and Road Research*. CSIR, South Africa.

Van Niekerk, A.., 2002. *Mechanical Behavior and Performance of Granular Bases and Sub-bases in Pavements*. Phd Dissertation, Delft University of Technology.

Olawuyi, B.J. & Boshoff, W.P., 2013. Compressive strength of high-performance concrete with absorption capacity of Super-Absorbing-Polymers (SAP). In Stellenbosch University, Stellenbosch, South Africa, pp. 1679–1683.

Paige-Green, P., 2008. The Durability of Stabilized Materials. In *The 12th International Conference of International Association for Computer Methods and Advances in Geomechanics (IACMAG)*. pp. 3787–3793. Available at: http://www.ascelibrary.org.

Paige-Green, P., Netterberg, F. & Sampson, L.R., 1990. The Carbonation of Chemically Stabilised Road Construction Materials: Guide to its Identificatin and Treatment. In *Division of Roads and Transport Technology*. CSIR, South Africa.

Penev, D. & Kawamura, M., 1993. Estimation of the Spacing and the Width of Cracks Caused by Shrinkage in the Cement-treated Slab Under Restraint. *Cement and Concrete Research*, 23, pp.925–932.

Poon, C.S., Qiao, X.C. & Chan, D., 2006. The cause and influence of self-cementing properties of fine recycled concrete aggregates on the properties of unbound sub-base. *Waste Management*, 26(10), pp.1166–1172.

Ruff, C.G., 1965. Time-temperature-strength-reaction product relationships in lime-bentonite-water mixtures.

Chakrabarti, S., Kodikara, J. & Pardo, L., 2002. Survey Results on Stabilization Methods and Performance of Local Government Roads in Australia. *Road and Transport Research Journal*, 11(ARRB Transport Research, Australia).

SANS 50196, 2006. South African National Standard. Methods of testing cement Part 1 : Determination of strength. In Pretoria, South Africa: SABS Standards Division.

SANS 50197, 2013. *South African National Standard. Methods of Testing Cement Part 1 : Composition , specifications and conformity criteria for common cements*, Pretoria, South Africa: SABS Standards Division.

SAPEM, 2014. South African Pavement Engineering Manual. In *South African National Roads Agency Ltd*. Pretoria, Republic of South Africa.

Schröfl, C., Mechtcherine, V. & Gorges, M., 2012. Relation between the molecular structure and the efficiency of superabsorbent polymers (SAP) as concrete admixture to mitigate autogenous shrinkage. *Cement and Concrete Research*, 42(6), pp.865–873.

Scullion, T., 2002. Precracking of Soil-Cement Bases to Reduce Reflection Cracking: Field Investigation. *Transportation Research Record*, 1787(1), pp.22–30.

Sebesta, S., 2005. Use of Microcrcaking to Reduce Shrinkage Cracking in Cement-Treated Bases,. *Transportation Research Record TRB Journal of the Transportation Research Board No. 1936, Transportation Research Board of the National Academies*, pp.3–11.

Shalid, M.A. & Thom, N.H., 1996. Performance of Cement Bound Bases with Controlled Cracking. In *Proceedings 3rd International RILEM Conference on Reflective Cracking in Pavement*. E and FN Spon.

Singh, E.S. & Kumar, E.N., 2014. Specifications and recommendations for recycled materials used for various applications. , 3(6), pp.86–90.

Siriwatwechakul, W., Siramont, J. & Vichi-Vadakan, W., 2010. Superabsorbent Polymer Structures. In *International RILEM Conference on use of Superabsorbent Polymers and Other New Additives in Concrete*. Technical University of Denmark, Lyngby, Denmark., pp. 253–262.

Soroka, I., 1993. *Concrete in Hot Environments*, E & FN Spon.

Stutzman, P., 1999. Chemistry and Structure of Hydration Products. *Cements Research Progress*, Chapter 2, pp.37–69. Available at: http://gisceu.net/PDF/U603.pdf.

Freeman, T.J. & Little, D.N., 1998. Develop Maintenance Strategy Selection Procedures for Pavements Incorporating Semi-rigid or Chemically Stabilized Layers. In *Report No.*

FHWA/TX-99/1922-2, Texas Transportation Institute. College Station, Texas: Texas A&M university.

Taylor, P.C., Kosmatka, S.H., and Voigt, G.F., 2007. Integrated Materials and Construction Practices for Concrete Pavement: A State-of-the-Practice Manual. In *Federal Highway Administration Publication No. HIF - 07 - 004*. Washington, D.C.: U.S Department of Transportation. Available at: http://www.swcpa.org/pdf files/ccpw093009/California IMCP Presentation 2008.pdf.

Tazawa, E. & Miyazawa, S., 1992. Autogenous Shrinkage of Cement Paste with Condensed Silica Fume. *4th CANMET-ACI International Conference on Fly Ash, Silica Fume, Slag and Natural Pozzolans in Concrete*, pp.875–894.

Tazawa, E., Miyazawa, S. & Kasai, T., 1995. Chemical shrinkage and autogenous shrinkage of hydrating cement paste. *Cement and Concrete Research*, 25(2), pp.288–292.

Terrel, R. et al., 1979. Soil Stabilization in Pavement Structures, a User's Manual-Volume 2: Mixture Design Considerations. In *FHWA-IP-80-2, Federal Highway Administration, Department of Transportation*. Washington DC.

TMH1, 1986. *Standard Methods of Testing Road Construction Materials*, Pretoria, South Africa.

TRH 13, 1986. Cementitious Stabilisers in Road Construction. In Pretoria, South Africa: Committe of State Road Authorities, pp. 1–64.

TRH 14, 1985. Guidelines for Road Construction Materials. In Pretoria, South Africa: Committe of State Road Authorities, pp. 1–57.

TRH4, 1996. *Structural Design of Flexible Pavements for Interurban and Rural Roads*, Pretoria, South Africa.

TSA, 1998. Mechanistic Characterization of Cementitiously stabilized Pavement Materials. In *MTRD Report No 94/MT/89-1, Materials Technology Section, Transport South Australia*. Walkley Heights.

Uchikawa, H., Hanehara, S. & Hirao, H., 1996. Influence of microstructure on the physical properties of concrete prepared by substituting mineral powder for part of fine aggregate. *Cement and Concrete Research*, 26(1), pp.101–111.

Ventura, D.F.., 2003. Durability Testing of LCB and CTB Materials Supplied by Caltrans. *Technical Memorandum Prepared for The California Department of Transportation*, (May).

Wainwright, P.J., 2005. Portland Cement, School of Civil Engineering University of Leeds.

Wang, J., 2013. *Characterisation and Modeling of Shrinkage Cracking of Cementitiously Stabilised Layers in Pavement*. Ph.D. Dissertation Washington State University.

Williams, R.I.., 1986. *Cement-Treated Pavements: Materials, Design and Construction*, London: Elsevier Applied Science Publishers.

Xiaojun, L., 2014. *Shrinkage Cracking of Soils and Cementitiously-Stabilised Soils:Mechanisms and Modeling*. Ph. D. Dissertation Washington State University.

Xing, W., 2004. *Quality Improvement of Granular Secondary Raw Building Materials by Separation and Cleansing Techniques*. Master's thesis Wuhan University of Technology, China.

Xuan, D., 2012. *Cement Treated Recycled Crushed Concrete and Masonry Aggregates for Pavements*. Phd Dissertation, Delft University of Technology.

Xuan, D. et al., 2010. Cement treated recycled demolition waste as a road base material. *Journal of Wuhan University of Technology-Mater. Sci. Ed.*, 25(4), pp.696–699.

Xuan, D.X., Molenaar, A.A.A. & Houben, M, L.J., 2015. Shrinkage cracking of cement treated demolition waste as a road base.

Zohuriaan-Mehr, M.J. & Kabiri, K., 2008. Superabsorbent Polymer Materials: A Review. *Iranian Polymer Journal*, 17(6), pp.451–477.

APPENDICES

APPENDIX A: MATERIAL CHARACTERISATION AND STRENGTH TESTS TABLES AND GRAPHS

A.1: CBR CURVES OF THE THREE MATERIALS AT 100% MOD AASHTO DENSITY

A.2: TABLES OF STRENGTH TESTS (UCS AND ITS) RESULTS FOR THE SHRINKAGE SPECIMENS.

A.3: GRAPHS OF STRENGTH TESTS (UCS AND ITS) RESULTS FOR THE SHRINKAGE SPECIMENS.

A.4: STANDARD (7 DAYS) UCS AND ITS RESULTS WITH 4% CEMENT STABILISATION

APPENDIX B: DIAL GUAGE READINGS AND CALCULATED AXIAL SHRINKAGES

B.1: G4 HORNFELS

B.2: RECYCLED CONCRETE AGGREGATES (RCA)

B.3: NEW CONCRETE (NC)

APPENDIX C: SHRINKAGE RESULTS OF ALL REPEATS OF SPECIMEN TYPES, ACCORDING TO THE CONSIDERED ASPECTS OF COMPARISON

C.1: G4 HORNFELS

C.2: RECYCLED CONCRETE AGGREGATES (RCA)

C.3: NEW CONCRETE (NC)

APPENDIX D: COEFFICIENTS OF VARIATION OF THE THREE REPEATS OF SPECIMEN TYPES

D.1: G4 HORNFELS

D.2: RECYCLED CONCRETE AGGREGATES (RCA)

D.3: NEW CONCRETE (NC)

APPENDIX E: TEMPERATURE VARIATION VS SHRINKAGE RESULTS

E.1: RECYCLED CONCRETE AGGREGATES (RCA)

E.2: NEW CONCRETE (NC)

APPENDIX F: SUMMARY OUTPUTS FOR STATISTICAL ANALYSIS

F.1: ANALYSIS OF MATERIAL BY MATERIAL

F.2: ANALYSIS OF THE THREE MATERIALS TOGETHER

F.3: ANALYSIS OF THE UCS AND THE ITS

APPENDIX A: MATERIAL CHARACTERISATION AND STRENGTH TESTS TABLES AND GRAPHS

A.1: CBR CURVES OF THE THREE MATERIALS AT 100% MOD AASHTO DENSITY

G4 hornfels

157

RCA

NC

A.2: TABLES OF STRENGTH TESTS (UCS AND ITS) RESULTS FOR THE
SHRINKAGE SPECIMENS

G4 HORNFELS

Specimen type	UCS (28 DAYS)		ITS (28 DAYS)	
	Force [kN]	UCS [MPa]	Force [kN]	ITS [kPa]
A1 (0%C)	10.1	1.3	1.2	105.6
A2 (0%C)	9.8	1.2	1.1	95.8
A3 (0%C)	9.2	1.2	1.0	85.9
AVERAGE	**9.7**	**1.2**	**1.1**	**95.8**
B1 (2.5%C)	61.1	7.8	8.7	738.5
B2 (2.5%C)	64.2	8.2	8.9	757.9
B3 (2.5%C)	67.3	8.6	8.4	716.4
AVERAGE	**64.2**	**8.2**	**8.7**	**737.6**
C1 (4%C)	97.8	12.5	15.5	1315.8
C2 (4%C)	96.6	12.3	14.3	1214.4
C3 (4%C)	93.6	11.9	13.9	1180.1
AVERAGE	**96.0**	**12.2**	**14.6**	**1236.7**
D1 (4%C + P)	81.4	10.4	15.9	1352.3
D2 (4%C + P)	88.1	11.2	13.1	1111.3
D3 (4%C + P)	84.9	10.8	17.4	1473.9
AVERAGE	**84.8**	**10.8**	**15.5**	**1312.5**

RCA

Specimen type	UCS (28 DAYS)		ITS (28 DAYS)	
	Force [kN]	UCS [MPa]	Force [kN]	ITS [kPa]
E1 (0%C)	11.7	1.5	1.3	109.4
E2 (0%C)	10.7	1.4	1.6	134.2
E3 (0%C)	11.2	1.4	1.2	100.9
AVERAGE	**11.2**	**1.4**	**1.4**	**114.8**
F1 (2.5%C)	66.3	8.4	8.8	747.7
F2 (2.5%C)	58.7	7.5	7.2	610.2
F3 (2.5%C)	54.8	7.0	9.0	765.9
AVERAGE	**59.9**	**7.6**	**8.3**	**707.9**
G1 (4%C)	87.4	11.1	15.1	1282.3
G2 (4%C)	83.7	10.7	14.0	1188.0
G3 (4%C)	92.5	11.8	13.3	1128.5
AVERAGE	**87.9**	**11.2**	**14.1**	**1199.6**

NC

Specimen type	UCS (28 DAYS)		ITS (28 DAYS)	
	Force [kN]	UCS [MPa]	Force [kN]	ITS [kPa]
H1 (0%C)	12.1	1.5	1.4	121.5
H2 (0%C)	15.9	2.0	1.6	139.6
H3 (0%C)	15.1	1.9	1.2	100.5
AVERAGE	**14.4**	**1.8**	**1.4**	**120.5**
I1 (2.5%C)	58.7	7.5	5.8	495.8
I2 (2.5%C)	51.3	6.5	5.4	461.2
I3 (2.5%C)	54.5	6.9	6.1	514.5
AVERAGE	**54.8**	**7.0**	**5.8**	**490.5**
J1 (4%C)	81.4	10.4	11.2	952.8
J2 (4%C)	77.6	9.9	10.6	897.6
J3 (4%C)	82.7	10.5	11.8	998.5
AVERAGE	**80.6**	**10.3**	**11.2**	**949.6**

A.3: GRAPHS OF STRENGTH TESTS (UCS AND ITS) RESULTS FOR THE SHRINKAGE SPECIMENS

A.4: STANDARD (7 DAYS) UCS AND ITS RESULTS WITH 4% CEMENT STABILISATION

Material type	Force (kN)	UCS (MPa)	Force (kN)	ITS (kPa)
G4 hornfels	218.0	12.0	21.2	1179.0
	220.0	12.1	22.5	1236.6
	200.7	11.0	20.7	1137.4
RCA	169.4	9.3	17.3	905.4
	172.2	9.4	24.1	1288.3
	211.0	11.6	22.4	1216.8
NC	182.1	10.0	16.2	901.4
	115.7	6.3	14.7	809.5
	244.2	13.4	16.3	906.3

APPENDIX B: DIAL GUAGE READINGS AND CALCULATED AXIAL SHRINKAGES

B.1: G4 HORNFELS

SHRINKAGE TESTING RESULTS - G4 Hornfels														
0% Cement; No Polymer (A)														
Specimen Name			**A1**			**A2**			**A3**			**AVERAGE**	
Specimen Height (mm)			**276**			**275**			**275**				
Wet weight (g)			Wet/Dry	5516	5313.5	Wet/Dry	5500.5	5272.5	Wet/Dry	5495.5	5282		
Day	**Time Interval (hours)**	**Cumulative Time (hours)**	**Temperature (^{0}C)**	**Dimensional change (mm)**	**Axial shrinkage (mm/mm)**	**Axial shrinkage [X 10^{-6}] mm/mm**	**Dimensional change (mm)**	**Axial shrinkage (mm/mm)**	**Axial shrinkage [X 10^{-6}] mm/mm**	**Dimensional change (mm)**	**Axial shrinkage (mm/mm)**	**Axial shrinkage [X 10^{-6}] mm/mm**	**Axial shrinkage (mm/mm)**	**Axial shrinkage [X 10^{-6}] mm/mm**
1	0	0	23.3	0	0.00E+00	0.00	0	0.00E+00	0.00	0	0.00E+00	0.00	0.00E+00	0.00
	1	1		-0.03	-1.09E-04	-108.70	-0.12	-4.36E-04	-436.36	-0.005	-1.82E-05	-18.18	-1.88E-04	-187.75
	1.5	2.5		-0.02	-7.25E-05	-72.46	-0.12	-4.36E-04	-436.36	-0.002	-7.27E-06	-7.27	-1.72E-04	-172.03
	1.5	4		-0.02	-7.25E-05	-72.46	-0.118	-4.29E-04	-429.09	-0.001	-3.64E-06	-3.64	-1.68E-04	-168.40
	1.5	5.5		-0.005	-1.81E-05	-18.12	-0.09	-3.27E-04	-327.27	-0.001	-3.64E-06	-3.64	-1.16E-04	-116.34
2	18.5	24	24.3	0.01	3.62E-05	36.23	-0.06	-2.18E-04	-218.18	0.002	7.27E-06	7.27	-5.82E-05	-58.23
	3	27		0.01	3.62E-05	36.23	-0.046	-1.67E-04	-167.27	0.002	7.27E-06	7.27	-4.13E-05	-41.26
	3	30		0.01	3.62E-05	36.23	-0.045	-1.64E-04	-163.64	0.002	7.27E-06	7.27	-4.00E-05	-40.04
3	18	48	23.7	0.008	2.90E-05	28.99	-0.012	-4.36E-05	-43.64	0.01	3.64E-05	36.36	7.24E-06	7.24
	6	54		0.0075	2.72E-05	27.17	-0.0005	-1.82E-06	-1.82	0.015	5.45E-05	54.55	2.66E-05	26.63
4	18	72	23.2	0.005	1.81E-05	18.12	0.036	1.31E-04	130.91	0.024	8.73E-05	87.27	7.88E-05	78.77
	6	78		0.005	1.81E-05	18.12	0.044	1.60E-04	160.00	0.034	1.24E-04	123.64	1.01E-04	100.58

164

				SHRINKAGE TESTING RESULTS - G4 Hornfels										
				0% Cement; No Polymer (A)										
Specimen Name				A1			A2			A3			AVERAGE	
Specimen Height (mm)				276			275			275				
Wet weight (g)				Wet/Dry	5516	5313.5	Wet/Dry	5500.5	5272.5	Wet/Dry	5495.5	5282		
Day	Time Interval (hours)	Cumulative Time (hours)	Temperature (°C)	Dimensional change (mm)	Axial shrinkage (mm/mm)	Axial shrinkage [X 10⁻⁶] mm/mm	Dimensional change (mm)	Axial shrinkage (mm/mm)	Axial shrinkage [X 10⁻⁶] mm/mm	Dimensional change (mm)	Axial shrinkage (mm/mm)	Axial shrinkage [X 10⁻⁶] mm/mm	Axial shrinkage (mm/mm)	Axial shrinkage [X 10⁻⁶] mm/mm
5	18	96	24.1	-0.0025	-9.06E-06	-9.06	0.034	1.24E-04	123.64	0.016	5.82E-05	58.18	5.76E-05	57.59
	6	102		-0.02	-7.25E-05	-72.46	0.011	4.00E-05	40.00	0.005	1.82E-05	18.18	-4.76E-06	-4.76
6	18	120	23	-0.03	-1.09E-04	-108.70	-0.01	-3.64E-05	-36.36	-0.012	-4.36E-05	-43.64	-6.29E-05	-62.90
	6	126		-0.045	-1.63E-04	-163.04	-0.032	-1.16E-04	-116.36	-0.022	-8.00E-05	-80.00	-1.20E-04	-119.80
7	18	144	23.5	-0.08	-2.90E-04	-289.86	-0.086	-3.13E-04	-312.73	-0.044	-1.60E-04	-160.00	-2.54E-04	-254.19
	6	150		-0.08	-2.90E-04	-289.86	-0.089	-3.24E-04	-323.64	-0.048	-1.75E-04	-174.55	-2.63E-04	-262.68
8	18	168	24.1	-0.11	-3.99E-04	-398.55	-0.128	-4.65E-04	-465.45	-0.072	-2.62E-04	-261.82	-3.75E-04	-375.27
	6	174		-0.115	-4.17E-04	-416.67	-0.138	-5.02E-04	-501.82	-0.074	-2.69E-04	-269.09	-3.96E-04	-395.86
9	18	192	24.2	-0.125	-4.53E-04	-452.90	-0.162	-5.89E-04	-589.09	-0.094	-3.42E-04	-341.82	-4.61E-04	-461.27
	6	198		-0.13	-4.71E-04	-471.01	-0.176	-6.40E-04	-640.00	-0.1	-3.64E-04	-363.64	-4.92E-04	-491.55
10	24	216	23.7	-0.14	-5.07E-04	-507.25	-0.21	-7.64E-04	-763.64	-0.112	-4.07E-04	-407.27	-5.59E-04	-559.39
11	24	240	23.4	-0.14	-5.07E-04	-507.25	-0.212	-7.71E-04	-770.91	-0.114	-4.15E-04	-414.55	-5.64E-04	-564.23
12	24	264	23.3	-0.14	-5.07E-04	-507.25	-0.212	-7.71E-04	-770.91	-0.118	-4.29E-04	-429.09	-5.69E-04	-569.08
13	24	288	24	-0.14	-5.07E-04	-507.25	-0.217	-7.89E-04	-789.09	-0.118	-4.29E-04	-429.09	-5.75E-04	-575.14
14	24	312	23.9	-0.14	-5.07E-04	-507.25	-0.222	-8.07E-04	-807.27	-0.118	-4.29E-04	-429.09	-5.81E-04	-581.20
15	24	336	23.7	-0.14	-5.07E-04	-507.25	-0.226	-8.22E-04	-821.82	-0.118	-4.29E-04	-429.09	-5.86E-04	-586.05
16	24	360	23.2	-0.145	-5.25E-04	-525.36	-0.243	-8.84E-04	-883.64	-0.122	-4.44E-04	-443.64	-6.18E-04	-617.55

				SHRINKAGE TESTING RESULTS - G4 Hornfels										
				0% Cement; No Polymer (A)										
Specimen Name				A1			A2			A3			AVERAGE	
Specimen Height (mm)				276			275			275				
Wet weight (g)				Wet/Dry	5516	5313.5	Wet/Dry	5500.5	5272.5	Wet/Dry	5495.5	5282		
Day	Time Interval (hours)	Cumulative Time (hours)	Temperature (^{0}C)	Dimensional change (mm)	Axial shrinkage (mm/mm)	Axial shrinkage [X 10^{-6}] mm/mm	Dimensional change (mm)	Axial shrinkage (mm/mm)	Axial shrinkage [X 10^{-6}] mm/mm	Dimensional change (mm)	Axial shrinkage (mm/mm)	Axial shrinkage [X 10^{-6}] mm/mm	Axial shrinkage (mm/mm)	Axial shrinkage [X 10^{-6}] mm/mm
17	24	384	23.4	-0.14	-5.07E-04	-507.25	-0.243	-8.84E-04	-883.64	-0.122	-4.44E-04	-443.64	-6.12E-04	-611.51
18	24	408	22.9	-0.14	-5.07E-04	-507.25	-0.243	-8.84E-04	-883.64	-0.132	-4.80E-04	-480.00	-6.24E-04	-623.63
19	24	432	23.6	-0.14	-5.07E-04	-507.25	-0.243	-8.84E-04	-883.64	-0.131	-4.76E-04	-476.36	-6.22E-04	-622.42
20	24	456	22.7	-0.14	-5.07E-04	-507.25	-0.243	-8.84E-04	-883.64	-0.131	-4.76E-04	-476.36	-6.22E-04	-622.42
21	24	480	23.1	-0.125	-4.53E-04	-452.90	-0.221	-8.04E-04	-803.64	-0.124	-4.51E-04	-450.91	-5.69E-04	-569.15
22	24	504	23.7	-0.125	-4.53E-04	-452.90	-0.221	-8.04E-04	-803.64	-0.124	-4.51E-04	-450.91	-5.69E-04	-569.15
23	24	528	23.4	-0.13	-4.71E-04	-471.01	-0.222	-8.07E-04	-807.27	-0.128	-4.65E-04	-465.45	-5.81E-04	-581.25
24	24	552	22.8	-0.125	-4.53E-04	-452.90	-0.222	-8.07E-04	-807.27	-0.128	-4.65E-04	-465.45	-5.75E-04	-575.21
25	24	576	24.2	-0.115	-4.17E-04	-416.67	-0.214	-7.78E-04	-778.18	-0.126	-4.58E-04	-458.18	-5.51E-04	-551.01
26	24	600	23.5	-0.11	-3.99E-04	-398.55	-0.207	-7.53E-04	-752.73	-0.125	-4.55E-04	-454.55	-5.35E-04	-535.27
27	24	624	22.8	-0.11	-3.99E-04	-398.55	-0.217	-7.89E-04	-789.09	-0.134	-4.87E-04	-487.27	-5.58E-04	-558.30
28 start	24	648	23.3	-0.12	-4.35E-04	-434.78	-0.226	-8.22E-04	-821.82	-0.144	-5.24E-04	-523.64	-5.93E-04	-593.41
28 end	24	672	23.2	-0.12	-4.35E-04	-434.78	-0.226	-8.22E-04	-821.82	-0.144	-5.24E-04	-523.64	-5.93E-04	-593.41

				SHRINKAGE TESTING RESULTS - G4 Hornfels										
				2.5% Cement; No Polymer (B)										
Specimen Name				B1			B2			B3			AVERAGE	
Specimen Height (mm)				287			285			282				
Weight (g)				Wet/Dry	5702	5507	Wet/Dry	5683.5	5494.5	Wet/Dry	5627.5	5446		
Day	Time Interval (hours)	Cumulative Time (hours)	Temperature (⁰C)	Dimensional change (mm)	Axial shrinkage (mm/mm)	Axial shrinkage [X 10⁻⁶] mm/mm	Dimensional change (mm)	Axial shrinkage (mm/mm)	Axial shrinkage [X 10⁻⁶] mm/mm	Dimensional change (mm)	Axial shrinkage (mm/mm)	Axial shrinkage [X 10⁻⁶] mm/mm	Axial shrinkage (mm/mm)	Axial shrinkage [X 10⁻⁶] mm/mm
1	0	0	22.4	0	0.00E+00	0.00	0	0.00E+00	0.00	0	0.00E+00	0.00	0.00E+00	0.00
	1	1		-0.015	-5.23E-05	-52.26	-0.01	-3.51E-05	-35.09	-0.06	-2.13E-04	-212.77	-1.00E-04	-100.04
	1.5	2.5		-0.015	-5.23E-05	-52.26	-0.01	-3.51E-05	-35.09	-0.06	-2.13E-04	-212.77	-1.00E-04	-100.04
	1.5	4		-0.015	-5.23E-05	-52.26	-0.01	-3.51E-05	-35.09	-0.06	-2.13E-04	-212.77	-1.00E-04	-100.04
	1.5	5.5		-0.015	-5.23E-05	-52.26	-0.01	-3.51E-05	-35.09	-0.06	-2.13E-04	-212.77	-1.00E-04	-100.04
2	18.5	24	22.9	0.025	8.71E-05	87.11	-0.02	-7.02E-05	-70.18	-0.1	-3.55E-04	-354.61	-1.13E-04	-112.56
	3	27		0.04	1.39E-04	139.37	-0.03	-1.05E-04	-105.26	-0.11	-3.90E-04	-390.07	-1.19E-04	-118.65
	3	30		0.06	2.09E-04	209.06	-0.035	-1.23E-04	-122.81	-0.11	-3.90E-04	-390.07	-1.01E-04	-101.27
3	18	48	23.1	0.08	2.79E-04	278.75	-0.1	-3.51E-04	-350.88	-0.15	-5.32E-04	-531.91	-2.01E-04	-201.35
	6	54		0.1	3.48E-04	348.43	-0.12	-4.21E-04	-421.05	-0.165	-5.85E-04	-585.11	-2.19E-04	-219.24
4	18	72	23.2	0.09	3.14E-04	313.59	-0.185	-6.49E-04	-649.12	-0.19	-6.74E-04	-673.76	-3.36E-04	-336.43
	6	78		0.085	2.96E-04	296.17	-0.2	-7.02E-04	-701.75	-0.205	-7.27E-04	-726.95	-3.78E-04	-377.51
5	18	96	24.1	0.06	2.09E-04	209.06	-0.225	-7.89E-04	-789.47	-0.225	-7.98E-04	-797.87	-4.59E-04	-459.43
	6	102		0.055	1.92E-04	191.64	-0.25	-8.77E-04	-877.19	-0.235	-8.33E-04	-833.33	-5.06E-04	-506.30
6	18	120	23	0.025	8.71E-05	87.11	-0.25	-8.77E-04	-877.19	-0.275	-9.75E-04	-975.18	-5.88E-04	-588.42
	6	126		0.025	8.71E-05	87.11	-0.25	-8.77E-04	-877.19	-0.285	-1.01E-03	-1010.64	-6.00E-04	-600.24

				SHRINKAGE TESTING RESULTS - G4 Hornfels											
				2.5% Cement; No Polymer (B)											
Specimen Name				B1			B2			B3			AVERAGE		
Specimen Height (mm)				287			285			282					
Weight (g)				Wet/Dry	5702	5507	Wet/Dry	5683.5	5494.5	Wet/Dry	5627.5	5446			
Day	Time Interval (hours)	Cumulative Time (hours)	Temperature (°C)	Dimensional change (mm)	Axial shrinkage (mm/mm)	Axial shrinkage [X 10⁻⁶] mm/mm	Dimensional change (mm)	Axial shrinkage (mm/mm)	Axial shrinkage [X 10⁻⁶] mm/mm	Dimensional change (mm)	Axial shrinkage (mm/mm)	Axial shrinkage [X 10⁻⁶] mm/mm	Axial shrinkage (mm/mm)	Axial shrinkage [X 10⁻⁶] mm/mm
7	18	144	23.5	0.025	8.71E-05	87.11	-0.25	-8.77E-04	-877.19	-0.3	-1.06E-03	-1063.83	-6.18E-04	-617.97
	6	150		0.02	6.97E-05	69.69	-0.3	-1.05E-03	-1052.63	-0.3	-1.06E-03	-1063.83	-6.82E-04	-682.26
8	18	168	24.1	0.005	1.74E-05	17.42	-0.325	-1.14E-03	-1140.35	-0.3	-1.06E-03	-1063.83	-7.29E-04	-728.92
	6	174		-0.0025	-8.71E-06	-8.71	-0.31	-1.09E-03	-1087.72	-0.305	-1.08E-03	-1081.56	-7.26E-04	-726.00
9	18	192	24.2	-0.02	-6.97E-05	-69.69	-0.34	-1.19E-03	-1192.98	-0.335	-1.19E-03	-1187.94	-8.17E-04	-816.87
	6	198		-0.01	-3.48E-05	-34.84	-0.365	-1.28E-03	-1280.70	-0.35	-1.24E-03	-1241.13	-8.52E-04	-852.23
10	24	216	23.7	-0.03	-1.05E-04	-104.53	-0.39	-1.37E-03	-1368.42	-0.345	-1.22E-03	-1223.40	-8.99E-04	-898.78
11	24	240	23.4	-0.07	-2.44E-04	-243.90	-0.48	-1.68E-03	-1684.21	-0.365	-1.29E-03	-1294.33	-1.07E-03	-1074.15
12	24	264	23.3	-0.105	-3.66E-04	-365.85	-0.52	-1.82E-03	-1824.56	-0.385	-1.37E-03	-1365.25	-1.19E-03	-1185.22
13	24	288	24	-0.14	-4.88E-04	-487.80	-0.53	-1.86E-03	-1859.65	-0.345	-1.22E-03	-1223.40	-1.19E-03	-1190.29
14	24	312	23.9	-0.16	-5.57E-04	-557.49	-0.56	-1.96E-03	-1964.91	-0.345	-1.22E-03	-1223.40	-1.25E-03	-1248.60
15	24	336	23.7	-0.185	-6.45E-04	-644.60	-0.54	-1.89E-03	-1894.74	-0.345	-1.22E-03	-1223.40	-1.25E-03	-1254.25
16	24	360	23.2	-0.19	-6.62E-04	-662.02	-0.5	-1.75E-03	-1754.39	-0.36	-1.28E-03	-1276.60	-1.23E-03	-1231.00
17	24	384	23.4	-0.18	-6.27E-04	-627.18	-0.48	-1.68E-03	-1684.21	-0.38	-1.35E-03	-1347.52	-1.22E-03	-1219.64
18	24	408	22.9	-0.175	-6.10E-04	-609.76	-0.485	-1.70E-03	-1701.75	-0.355	-1.26E-03	-1258.87	-1.19E-03	-1190.13
19	24	432	23.6	-0.175	-6.10E-04	-609.76	-0.485	-1.70E-03	-1701.75	-0.335	-1.19E-03	-1187.94	-1.17E-03	-1166.48
20	24	456	22.7	-0.185	-6.45E-04	-644.60	-0.49	-1.72E-03	-1719.30	-0.315	-1.12E-03	-1117.02	-1.16E-03	-1160.31

				SHRINKAGE TESTING RESULTS - G4 Hornfels											
				2.5% Cement; No Polymer (B)											
Specimen Name				B1			B2			B3			AVERAGE		
Specimen Height (mm)				287			285			282					
Weight (g)				Wet/Dry	5702	5507	Wet/Dry	5683.5	5494.5	Wet/Dry	5627.5	5446			
Day	Time Interval (hours)	Cumulative Time (hours)	Temperature (^{0}C)	Dimensional change (mm)	Axial shrinkage (mm/mm)	Axial shrinkage [X 10^{-6}] mm/mm	Dimensional change (mm)	Axial shrinkage (mm/mm)	Axial shrinkage [X 10^{-6}] mm/mm	Dimensional change (mm)	Axial shrinkage (mm/mm)	Axial shrinkage [X 10^{-6}] mm/mm	Axial shrinkage (mm/mm)	Axial shrinkage [X 10^{-6}] mm/mm
21	24	480	23.1	-0.19	-6.62E-04	-662.02	-0.44	-1.54E-03	-1543.86	-0.305	-1.08E-03	-1081.56	-1.10E-03	-1095.81
22	24	504	23.7	-0.17	-5.92E-04	-592.33	-0.435	-1.53E-03	-1526.32	-0.305	-1.08E-03	-1081.56	-1.07E-03	-1066.74
23	24	528	23.4	-0.16	-5.57E-04	-557.49	-0.435	-1.53E-03	-1526.32	-0.3	-1.06E-03	-1063.83	-1.05E-03	-1049.21
24	24	552	22.8	-0.165	-5.75E-04	-574.91	-0.41	-1.44E-03	-1438.60	-0.29	-1.03E-03	-1028.37	-1.01E-03	-1013.96
25	24	576	24.2	-0.16	-5.57E-04	-557.49	-0.39	-1.37E-03	-1368.42	-0.28	-9.93E-04	-992.91	-9.73E-04	-972.94
26	24	600	23.5	-0.15	-5.23E-04	-522.65	-0.39	-1.37E-03	-1368.42	-0.28	-9.93E-04	-992.91	-9.61E-04	-961.33
27	24	624	22.8	-0.15	-5.23E-04	-522.65	-0.375	-1.32E-03	-1315.79	-0.26	-9.22E-04	-921.99	-9.20E-04	-920.14
28 start	24	648	23.3	-0.15	-5.23E-04	-522.65	-0.365	-1.28E-03	-1280.70	-0.25	-8.87E-04	-886.52	-8.97E-04	-896.62
28 end	24	672	23.2	-0.14	-4.88E-04	-487.80	-0.33	-1.16E-03	-1157.89	-0.245	-8.69E-04	-868.79	-8.38E-04	-838.16

169

			SHRINKAGE TESTING RESULTS - G4 Hornfels											
			4% Cement; No Polymer (C)											
Specimen Number			C1 (01/04/2015)			C2 (01/04/2015)			C3 (01/04/2015)			AVERAGE	
Specimen Height (mm)			288.5			286			287				
Weight (g)			Wet/Dry	5780.5	5602	Wet/Dry	5743.5	5570.5	Wet/Dry	5763.5	5591.5		
Day	Time Interval (hours)	Cumulative Time (hours)	Temperature (°C)	Dimensional change (mm)	Axial shrinkage (mm/mm)	Axial shrinkage [X 10⁻⁶] mm/mm	Dimensional change (mm)	Axial shrinkage (mm/mm)	Axial shrinkage [X 10⁻⁶] mm/mm	Dimensional change (mm)	Axial shrinkage (mm/mm)	Axial shrinkage [X 10⁻⁶] mm/mm	Axial shrinkage (mm/mm)	Axial shrinkage [X 10⁻⁶] mm/mm
1	0	0	22.6	0	0.00E+00	0.00	0	0.00E+00	0.00	0	0.00E+00	0.00	0.00E+00	0.00
	1	1		-0.03	-1.04E-04	-103.99	-0.085	-2.97E-04	-297.20	-0.06	-2.09E-04	-209.06	-2.03E-04	-203.42
	1.5	2.5		-0.01	-3.47E-05	-34.66	-0.04	-1.40E-04	-139.86	-0.06	-2.09E-04	-209.06	-1.28E-04	-127.86
	1.5	4		-0.025	-8.67E-05	-86.66	-0.05	-1.75E-04	-174.83	-0.06	-2.09E-04	-209.06	-1.57E-04	-156.85
	1.5	5.5		-0.05	-1.73E-04	-173.31	-0.05	-1.75E-04	-174.83	-0.06	-2.09E-04	-209.06	-1.86E-04	-185.73
2	18.5	24	23.1	-0.07	-2.43E-04	-242.63	-0.06	-2.10E-04	-209.79	-0.07	-2.44E-04	-243.90	-2.32E-04	-232.11
	3	27		-0.09	-3.12E-04	-311.96	-0.075	-2.62E-04	-262.24	-0.075	-2.61E-04	-261.32	-2.79E-04	-278.51
	3	30		-0.1	-3.47E-04	-346.62	-0.11	-3.85E-04	-384.62	-0.08	-2.79E-04	-278.75	-3.37E-04	-336.66
3	18	48	23.6	-0.21	-7.28E-04	-727.90	-0.245	-8.57E-04	-856.64	-0.15	-5.23E-04	-522.65	-7.02E-04	-702.40
	6	54		-0.25	-8.67E-04	-866.55	-0.31	-1.08E-03	-1083.92	-0.175	-6.10E-04	-609.76	-8.53E-04	-853.41
4	18	72	23.2	-0.31	-1.07E-03	-1074.52	-0.375	-1.31E-03	-1311.19	-0.245	-8.54E-04	-853.66	-1.08E-03	-1079.79
	6	78		-0.34	-1.18E-03	-1178.51	-0.4	-1.40E-03	-1398.60	-0.27	-9.41E-04	-940.77	-1.17E-03	-1172.63
5	18	96	24.1	-0.37	-1.28E-03	-1282.50	-0.425	-1.49E-03	-1486.01	-0.3	-1.05E-03	-1045.30	-1.27E-03	-1271.27
	6	102		-0.4	-1.39E-03	-1386.48	-0.46	-1.61E-03	-1608.39	-0.325	-1.13E-03	-1132.40	-1.38E-03	-1375.76
6	18	120	23	-0.43	-1.49E-03	-1490.47	-0.51	-1.78E-03	-1783.22	-0.38	-1.32E-03	-1324.04	-1.53E-03	-1532.58
	6	126		-0.43	-1.49E-03	-1490.47	-0.52	-1.82E-03	-1818.18	-0.39	-1.36E-03	-1358.89	-1.56E-03	-1555.84

				SHRINKAGE TESTING RESULTS - G4 Hornfels											
				4% Cement; No Polymer (C)											
Specimen Number				C1 (01/04/2015)			C2 (01/04/2015)			C3 (01/04/2015)			AVERAGE	
Specimen Height (mm)				288.5			286			287				
Weight (g)				Wet/Dry	5780.5	5602	Wet/Dry	5743.5	5570.5	Wet/Dry	5763.5	5591.5		
Day	Time Interval (hours)	Cumulative Time (hours)	Temperature (^{0}C)	Dimensional change (mm)	Axial shrinkage (mm/mm)	Axial shrinkage [X 10^{-6}] mm/mm	Dimensional change (mm)	Axial shrinkage (mm/mm)	Axial shrinkage [X 10^{-6}] mm/mm	Dimensional change (mm)	Axial shrinkage (mm/mm)	Axial shrinkage [X 10^{-6}] mm/mm	Axial shrinkage (mm/mm)	Axial shrinkage [X 10^{-6}] mm/mm
7	18	144	23.5	-0.435	-1.51E-03	-1507.80	-0.53	-1.85E-03	-1853.15	-0.4	-1.39E-03	-1393.73	-1.58E-03	-1584.89
	6	150		-0.435	-1.51E-03	-1507.80	-0.53	-1.85E-03	-1853.15	-0.4	-1.39E-03	-1393.73	-1.58E-03	-1584.89
8	18	168	24.1	-0.405	-1.40E-03	-1403.81	-0.53	-1.85E-03	-1853.15	-0.4	-1.39E-03	-1393.73	-1.55E-03	-1550.23
	6	174		-0.405	-1.40E-03	-1403.81	-0.53	-1.85E-03	-1853.15	-0.405	-1.41E-03	-1411.15	-1.56E-03	-1556.04
9	18	192	24.2	-0.4	-1.39E-03	-1386.48	-0.54	-1.89E-03	-1888.11	-0.415	-1.45E-03	-1445.99	-1.57E-03	-1573.53
	6	198		-0.4	-1.39E-03	-1386.48	-0.54	-1.89E-03	-1888.11	-0.41	-1.43E-03	-1428.57	-1.57E-03	-1567.72
10	24	216	23.7	-0.405	-1.40E-03	-1403.81	-0.595	-2.08E-03	-2080.42	-0.435	-1.52E-03	-1515.68	-1.67E-03	-1666.64
11	24	240	23.4	-0.4	-1.39E-03	-1386.48	-0.585	-2.05E-03	-2045.45	-0.44	-1.53E-03	-1533.10	-1.66E-03	-1655.01
12	24	264	23.3	-0.375	-1.30E-03	-1299.83	-0.565	-1.98E-03	-1975.52	-0.425	-1.48E-03	-1480.84	-1.59E-03	-1585.40
13	24	288	24	-0.35	-1.21E-03	-1213.17	-0.55	-1.92E-03	-1923.08	-0.415	-1.45E-03	-1445.99	-1.53E-03	-1527.41
14	24	312	23.9	-0.32	-1.11E-03	-1109.19	-0.515	-1.80E-03	-1800.70	-0.33	-1.15E-03	-1149.83	-1.35E-03	-1353.24
15	24	336	23.7	-0.34	-1.18E-03	-1178.51	-0.545	-1.91E-03	-1905.59	-0.345	-1.20E-03	-1202.09	-1.43E-03	-1428.73
16	24	360	23.2	-0.37	-1.28E-03	-1282.50	-0.61	-2.13E-03	-2132.87	-0.37	-1.29E-03	-1289.20	-1.57E-03	-1568.19
17	24	384	23.4	-0.385	-1.33E-03	-1334.49	-0.625	-2.19E-03	-2185.31	-0.39	-1.36E-03	-1358.89	-1.63E-03	-1626.23
18	24	408	22.9	-0.39	-1.35E-03	-1351.82	-0.635	-2.22E-03	-2220.28	-0.395	-1.38E-03	-1376.31	-1.65E-03	-1649.47
19	24	432	23.6	-0.4	-1.39E-03	-1386.48	-0.66	-2.31E-03	-2307.69	-0.41	-1.43E-03	-1428.57	-1.71E-03	-1707.58

171

				SHRINKAGE TESTING RESULTS - G4 Hornfels												
				4% Cement; No Polymer (C)												
Specimen Number				C1 (01/04/2015)			C2 (01/04/2015)			C3 (01/04/2015)			AVERAGE			
Specimen Height (mm)				288.5			286			287						
Weight (g)				Wet/Dry	5780.5	5602	Wet/Dry	5743.5	5570.5	Wet/Dry	5763.5	5591.5				
Day	Time Interval (hours)	Cumulative Time (hours)	Temperature (^{0}C)	Dimensional change (mm)	Axial shrinkage (mm/mm)	Axial shrinkage [X 10^{-6}] mm/mm	Dimensional change (mm)	Axial shrinkage (mm/mm)	Axial shrinkage [X 10^{-6}] mm/mm	Dimensional change (mm)	Axial shrinkage (mm/mm)	Axial shrinkage [X 10^{-6}] mm/mm	Axial shrinkage (mm/mm)	Axial shrinkage [X 10^{-6}] mm/mm		
20	24	456	22.7	-0.4	-1.39E-03	-1386.48	-0.64	-2.24E-03	-2237.76	-0.395	-1.38E-03	-1376.31	-1.67E-03	-1666.85		
21	24	480	23.1	-0.38	-1.32E-03	-1317.16	-0.605	-2.12E-03	-2115.38	-0.38	-1.32E-03	-1324.04	-1.59E-03	-1585.53		
22	24	504	23.7	-0.37	-1.28E-03	-1282.50	-0.59	-2.06E-03	-2062.94	-0.365	-1.27E-03	-1271.78	-1.54E-03	-1539.07		
23	24	528	23.4	-0.37	-1.28E-03	-1282.50	-0.59	-2.06E-03	-2062.94	-0.37	-1.29E-03	-1289.20	-1.54E-03	-1544.88		
24	24	552	22.8	-0.37	-1.28E-03	-1282.50	-0.59	-2.06E-03	-2062.94	-0.37	-1.29E-03	-1289.20	-1.54E-03	-1544.88		
25	24	576	24.2	-0.37	-1.28E-03	-1282.50	-0.585	-2.05E-03	-2045.45	-0.355	-1.24E-03	-1236.93	-1.52E-03	-1521.63		
26	24	600	23.5	-0.33	-1.14E-03	-1143.85	-0.47	-1.64E-03	-1643.36	-0.315	-1.10E-03	-1097.56	-1.29E-03	-1294.92		
27	24	624	22.8	-0.335	-1.16E-03	-1161.18	-0.505	-1.77E-03	-1765.73	-0.325	-1.13E-03	-1132.40	-1.35E-03	-1353.11		
28 start	24	648	23.3	-0.34	-1.18E-03	-1178.51	-0.51	-1.78E-03	-1783.22	-0.325	-1.13E-03	-1132.40	-1.36E-03	-1364.71		
28 end	24	672	23.2	-0.32	-1.11E-03	-1109.19	-0.455	-1.59E-03	-1590.91	-0.3	-1.05E-03	-1045.30	-1.25E-03	-1248.46		

					SHRINKAGE TESTING RESULTS - G4 Hornfels								
					4% Cement + Polymer (D)								
	Specimen Name			D1			D2			D3		AVERAGE	
	Specimen Height (mm)			287.5			291			291			
	Weight (g)			Wet/Dry	5738	5552.5	Wet/Dry	5799.5	5607	Wet/Dry	5803	5604.5		
Day	Time Interval (hours)	Cumulative Time (hours)	Temperature (^{0}C)	Dimensional change (mm)	Axial shrinkage (mm/mm)	Axial shrinkage [X 10^{-6}] mm/mm	Dimensional change (mm)	Axial shrinkage (mm/mm)	Axial shrinkage [X 10^{-6}] mm/mm	Dimensional change (mm)	Axial shrinkage (mm/mm)	Axial shrinkage [X 10^{-6}] mm/mm	Axial shrinkage (mm/mm)	Axial shrinkage [X 10^{-6}] mm/mm
	0	0	22.7	0	0.00E+00	0.00	0	0.00E+00	0.00	0	0.00E+00	0.00	0.00E+00	0.00
1	1	1		-0.04	-1.39E-04	-139.13	-0.035	-1.20E-04	-120.27	-0.045	-1.55E-04	-154.64	-1.38E-04	-138.01
	1.5	2.5		-0.04	-1.39E-04	-139.13	-0.035	-1.20E-04	-120.27	-0.045	-1.55E-04	-154.64	-1.38E-04	-138.01
	1.5	4		-0.04	-1.39E-04	-139.13	-0.035	-1.20E-04	-120.27	-0.045	-1.55E-04	-154.64	-1.38E-04	-138.01
	1.5	5.5		-0.04	-1.39E-04	-139.13	-0.04	-1.37E-04	-137.46	-0.045	-1.55E-04	-154.64	-1.44E-04	-143.74
2	18.5	24	23.2	-0.135	-4.70E-04	-469.57	-0.19	-6.53E-04	-652.92	-0.07	-2.41E-04	-240.55	-4.54E-04	-454.35
	3	27		-0.155	-5.39E-04	-539.13	-0.24	-8.25E-04	-824.74	-0.08	-2.75E-04	-274.91	-5.46E-04	-546.26
	3	30		-0.2	-6.96E-04	-695.65	-0.27	-9.28E-04	-927.84	-0.09	-3.09E-04	-309.28	-6.44E-04	-644.26
3	18	48	23.4	-0.29	-1.01E-03	-1008.70	-0.355	-1.22E-03	-1219.93	-0.13	-4.47E-04	-446.74	-8.92E-04	-891.79
	6	54		-0.33	-1.15E-03	-1147.83	-0.43	-1.48E-03	-1477.66	-0.135	-4.64E-04	-463.92	-1.03E-03	-1029.80
4	18	72	23.2	-0.36	-1.25E-03	-1252.17	-0.525	-1.80E-03	-1804.12	-0.17	-5.84E-04	-584.19	-1.21E-03	-1213.50
	6	78		-0.39	-1.36E-03	-1356.52	-0.55	-1.89E-03	-1890.03	-0.18	-6.19E-04	-618.56	-1.29E-03	-1288.37
5	18	96	24.1	-0.435	-1.51E-03	-1513.04	-0.6	-2.06E-03	-2061.86	-0.215	-7.39E-04	-738.83	-1.44E-03	-1437.91
	6	102		-0.445	-1.55E-03	-1547.83	-0.61	-2.10E-03	-2096.22	-0.22	-7.56E-04	-756.01	-1.47E-03	-1466.69
6	18	120	23	-0.46	-1.60E-03	-1600.00	-0.645	-2.22E-03	-2216.49	-0.265	-9.11E-04	-910.65	-1.58E-03	-1575.72
	6	126		-0.46	-1.60E-03	-1600.00	-0.655	-2.25E-03	-2250.86	-0.265	-9.11E-04	-910.65	-1.59E-03	-1587.17

SHRINKAGE TESTING RESULTS - G4 Hornfels													
4% Cement + Polymer (D)													
Specimen Name				D1			D2			D3		AVERAGE	
Specimen Height (mm)				287.5			291			291			
Weight (g)			Wet/Dry	5738	5552.5	Wet/Dry	5799.5	5607	Wet/Dry	5803	5604.5		
Day	Time Interval (hours)	Cumulative Time (hours)	Temperature (°C)	Dimensional change (mm)	Axial shrinkage (mm/mm)	Axial shrinkage [X 10⁻⁶] mm/mm	Dimensional change (mm)	Axial shrinkage (mm/mm)	Axial shrinkage [X 10⁻⁶] mm/mm	Dimensional change (mm)	Axial shrinkage (mm/mm)	Axial shrinkage [X 10⁻⁶] mm/mm	Axial shrinkage (mm/mm)	Axial shrinkage [X 10⁻⁶] mm/mm

Day	Time Interval (hours)	Cumulative Time (hours)	Temperature (^{0}C)	Dimensional change (mm)	Axial shrinkage (mm/mm)	Axial shrinkage [X 10^{-6}] mm/mm	Dimensional change (mm)	Axial shrinkage (mm/mm)	Axial shrinkage [X 10^{-6}] mm/mm	Dimensional change (mm)	Axial shrinkage (mm/mm)	Axial shrinkage [X 10^{-6}] mm/mm	Axial shrinkage (mm/mm)	Axial shrinkage [X 10^{-6}] mm/mm
	18	144	23.5	-0.475	-1.65E-03	-1652.17	-0.68	-2.34E-03	-2336.77	-0.275	-9.45E-04	-945.02	-1.64E-03	-1644.65
	6	150		-0.475	-1.65E-03	-1652.17	-0.68	-2.34E-03	-2336.77	-0.275	-9.45E-04	-945.02	-1.64E-03	-1644.65
8	18	168	24.1	-0.475	-1.65E-03	-1652.17	-0.75	-2.58E-03	-2577.32	-0.285	-9.79E-04	-979.38	-1.74E-03	-1736.29
	6	174		-0.47	-1.63E-03	-1634.78	-0.75	-2.58E-03	-2577.32	-0.285	-9.79E-04	-979.38	-1.73E-03	-1730.49
9	18	192	24.2	-0.5	-1.74E-03	-1739.13	-0.76	-2.61E-03	-2611.68	-0.3	-1.03E-03	-1030.93	-1.79E-03	-1793.91
	6	198		-0.5	-1.74E-03	-1739.13	-0.76	-2.61E-03	-2611.68	-0.285	-9.79E-04	-979.38	-1.78E-03	-1776.73
10	24	216	23.7	-0.505	-1.76E-03	-1756.52	-0.745	-2.56E-03	-2560.14	-0.29	-9.97E-04	-996.56	-1.77E-03	-1771.07
11	24	240	23.4	-0.5	-1.74E-03	-1739.13	-0.73	-2.51E-03	-2508.59	-0.325	-1.12E-03	-1116.84	-1.79E-03	-1788.19
12	24	264	23.3	-0.5	-1.74E-03	-1739.13	-0.66	-2.27E-03	-2268.04	-0.36	-1.24E-03	-1237.11	-1.75E-03	-1748.10
13	24	288	24	-0.48	-1.67E-03	-1669.57	-0.7	-2.41E-03	-2405.50	-0.38	-1.31E-03	-1305.84	-1.79E-03	-1793.64
14	24	312	23.9	-0.495	-1.72E-03	-1721.74	-0.74	-2.54E-03	-2542.96	-0.39	-1.34E-03	-1340.21	-1.87E-03	-1868.30
15	24	336	23.7	-0.515	-1.79E-03	-1791.30	-0.77	-2.65E-03	-2646.05	-0.41	-1.41E-03	-1408.93	-1.95E-03	-1948.76
16	24	360	23.2	-0.515	-1.79E-03	-1791.30	-0.77	-2.65E-03	-2646.05	-0.405	-1.39E-03	-1391.75	-1.94E-03	-1943.04
17	24	384	23.4	-0.52	-1.81E-03	-1808.70	-0.78	-2.68E-03	-2680.41	-0.39	-1.34E-03	-1340.21	-1.94E-03	-1943.10
18	24	408	22.9	-0.53	-1.84E-03	-1843.48	-0.76	-2.61E-03	-2611.68	-0.39	-1.34E-03	-1340.21	-1.93E-03	-1931.79
19	24	432	23.6	-0.54	-1.88E-03	-1878.26	-0.71	-2.44E-03	-2439.86	-0.4	-1.37E-03	-1374.57	-1.90E-03	-1897.56

174

				SHRINKAGE TESTING RESULTS - G4 Hornfels												
				4% Cement + Polymer (D)												
Specimen Name				**D1**			**D2**			**D3**			**AVERAGE**			
Specimen Height (mm)				287.5			291			291						
Weight (g)				Wet/Dry	5738	5552.5	Wet/Dry	5799.5	5607	Wet/Dry	5803	5604.5				
Day	**Time Interval (hours)**	**Cumulative Time (hours)**	**Temperature (⁰C)**	**Dimensional change (mm)**	**Axial shrinkage (mm/mm)**	**Axial shrinkage [X 10⁻⁶] mm/mm**	**Dimensional change (mm)**	**Axial shrinkage (mm/mm)**	**Axial shrinkage [X 10⁻⁶] mm/mm**	**Dimensional change (mm)**	**Axial shrinkage (mm/mm)**	**Axial shrinkage [X 10⁻⁶] mm/mm**	**Axial shrinkage (mm/mm)**	**Axial shrinkage [X 10⁻⁶] mm/mm**		
20	24	456	22.7	-0.535	-1.86E-03	-1860.87	-0.69	-2.37E-03	-2371.13	-0.405	-1.39E-03	-1391.75	-1.87E-03	-1874.59		
21	24	480	23.1	-0.53	-1.84E-03	-1843.48	-0.67	-2.30E-03	-2302.41	-0.41	-1.41E-03	-1408.93	-1.85E-03	-1851.61		
22	24	504	23.7	-0.525	-1.83E-03	-1826.09	-0.67	-2.30E-03	-2302.41	-0.37	-1.27E-03	-1271.48	-1.80E-03	-1799.99		
23	24	528	23.4	-0.52	-1.81E-03	-1808.70	-0.66	-2.27E-03	-2268.04	-0.38	-1.31E-03	-1305.84	-1.79E-03	-1794.19		
24	24	552	22.8	-0.52	-1.81E-03	-1808.70	-0.565	-1.94E-03	-1941.58	-0.395	-1.36E-03	-1357.39	-1.70E-03	-1702.55		
25	24	576	24.2	-0.51	-1.77E-03	-1773.91	-0.57	-1.96E-03	-1958.76	-0.375	-1.29E-03	-1288.66	-1.67E-03	-1673.78		
26	24	600	23.5	-0.505	-1.76E-03	-1756.52	-0.58	-1.99E-03	-1993.13	-0.365	-1.25E-03	-1254.30	-1.67E-03	-1667.98		
27	24	624	22.8	-0.5	-1.74E-03	-1739.13	-0.545	-1.87E-03	-1872.85	-0.375	-1.29E-03	-1288.66	-1.63E-03	-1633.55		
28 start	24	648	23.3	-0.5	-1.74E-03	-1739.13	-0.53	-1.82E-03	-1821.31	-0.355	-1.22E-03	-1219.93	-1.59E-03	-1593.46		
28 end	24	672	23.2	-0.5	-1.74E-03	-1739.13	-0.53	-1.82E-03	-1821.31	-0.34	-1.17E-03	-1168.38	-1.58E-03	-1576.27		

175

B.2: RECYCLED CONCRETE AGGREGATES (RCA)

				SHRINKAGE TESTING RESULTS - RCA											
				0% Cement; No Polymer (E)											
Specimen Name				E1			E2			E3			AVERAGE		
Specimen Height (mm)				278			278			276					
Wet weight (g)				Wet/Dry	5057	4736.5	Wet/Dry	5060	4739.5	Wet/Dry	5020	4698.5			
Day	Time Interval (hours)	Cumulative Time (hours)	Temperature (⁰C)	Dimensional change (mm)	Axial shrinkage (mm/mm)	Axial shrinkage [X 10⁻⁶] mm/mm	Dimensional change (mm)	Axial shrinkage (mm/mm)	Axial shrinkage [X 10⁻⁶] mm/mm	Dimensional change (mm)	Axial shrinkage (mm/mm)	Axial shrinkage [X 10⁻⁶] mm/mm	Axial shrinkage (mm/mm)	Axial shrinkage [X 10⁻⁶] mm/mm
1	0	0	23.4	0	0.00E+00	0.00	0	0.00E+00	0.00	0	0.00E+00	0.00	0.00E+00	0.00
	1	1		-0.06	-2.16E-04	-215.83	-0.045	-1.62E-04	-161.87	-0.085	-3.08E-04	-307.97	-2.29E-04	-228.56
	1.5	2.5		-0.065	-2.34E-04	-233.81	-0.05	-1.80E-04	-179.86	-0.095	-3.44E-04	-344.20	-2.53E-04	-252.62
	1.5	4		-0.065	-2.34E-04	-233.81	-0.04	-1.44E-04	-143.88	-0.095	-3.44E-04	-344.20	-2.41E-04	-240.63
	1.5	5.5		-0.06	-2.16E-04	-215.83	-0.02	-7.19E-05	-71.94	-0.095	-3.44E-04	-344.20	-2.11E-04	-210.66
2	18.5	24	23.8	0.05	1.80E-04	179.86	0.11	3.96E-04	395.68	-0.06	-2.17E-04	-217.39	1.19E-04	119.38
	3	27		0.06	2.16E-04	215.83	0.125	4.50E-04	449.64	-0.05	-1.81E-04	-181.16	1.61E-04	161.44
	3	30		0.065	2.34E-04	233.81	0.145	5.22E-04	521.58	-0.04	-1.45E-04	-144.93	2.03E-04	203.49
3	18	48	24.2	0.075	2.70E-04	269.78	0.14	5.04E-04	503.60	-0.045	-1.63E-04	-163.04	2.03E-04	203.45
	6	54		0.08	2.88E-04	287.77	0.14	5.04E-04	503.60	-0.05	-1.81E-04	-181.16	2.03E-04	203.40
4	18	72	23.6	0.09	3.24E-04	323.74	0.135	4.86E-04	485.61	-0.06	-2.17E-04	-217.39	1.97E-04	197.32
	6	78		0.085	3.06E-04	305.76	0.13	4.68E-04	467.63	-0.065	-2.36E-04	-235.51	1.79E-04	179.29
5	18	96	23.5	0.08	2.88E-04	287.77	0.11	3.96E-04	395.68	-0.08	-2.90E-04	-289.86	1.31E-04	131.20
	6	102		0.07	2.52E-04	251.80	0.09	3.24E-04	323.74	-0.07	-2.54E-04	-253.62	1.07E-04	107.31

176

SHRINKAGE TESTING RESULTS - RCA													
0% Cement; No Polymer (E)													
Specimen Name				E1			E2			E3			AVERAGE
Specimen Height (mm)				278			278			276			
Wet weight (g)			Wet/Dry	5057	4736.5	Wet/Dry	5060	4739.5	Wet/Dry	5020	4698.5		
Day	Time Interval (hours)	Cumulative Time (hours)	Temperature (^{0}C)	Dimensional change (mm)	Axial shrinkage (mm/mm)	Axial shrinkage [X 10^{-6}] mm/mm	Dimensional change (mm)	Axial shrinkage (mm/mm)	Axial shrinkage [X 10^{-6}] mm/mm	Dimensional change (mm)	Axial shrinkage (mm/mm)	Axial shrinkage [X 10^{-6}] mm/mm	Axial shrinkage (mm/mm)	Axial shrinkage [X 10^{-6}] mm/mm
6	18	120	23.8	0.065	2.34E-04	233.81	0.085	3.06E-04	305.76	-0.08	-2.90E-04	-289.86	8.32E-05	83.24
	6	126		0.06	2.16E-04	215.83	0.075	2.70E-04	269.78	-0.09	-3.26E-04	-326.09	5.32E-05	53.17
7	18	144	23.2	0.05	1.80E-04	179.86	0.06	2.16E-04	215.83	-0.095	-3.44E-04	-344.20	1.72E-05	17.16
	6	150		0.05	1.80E-04	179.86	0.055	1.98E-04	197.84	-0.1	-3.62E-04	-362.32	5.13E-06	5.13
8	18	168	24.2	0.04	1.44E-04	143.88	0.03	1.08E-04	107.91	-0.11	-3.99E-04	-398.55	-4.89E-05	-48.92
	6	174		0.035	1.26E-04	125.90	0.02	7.19E-05	71.94	-0.11	-3.99E-04	-398.55	-6.69E-05	-66.90
9	18	192	23.4	0.02	7.19E-05	71.94	-0.01	-3.60E-05	-35.97	-0.125	-4.53E-04	-452.90	-1.39E-04	-138.98
	6	198		0.015	5.40E-05	53.96	-0.02	-7.19E-05	-71.94	-0.13	-4.71E-04	-471.01	-1.63E-04	-163.00
10	24	216	23.9	0	0.00E+00	0.00	-0.055	-1.98E-04	-197.84	-0.15	-5.43E-04	-543.48	-2.47E-04	-247.11
11	24	240	23.5	-0.015	-5.40E-05	-53.96	-0.075	-2.70E-04	-269.78	-0.16	-5.80E-04	-579.71	-3.01E-04	-301.15
12	24	264	22.9	-0.025	-8.99E-05	-89.93	-0.09	-3.24E-04	-323.74	-0.17	-6.16E-04	-615.94	-3.43E-04	-343.20
13	24	288	22.7	-0.04	-1.44E-04	-143.88	-0.11	-3.96E-04	-395.68	-0.18	-6.52E-04	-652.17	-3.97E-04	-397.25
14	24	312	23.2	-0.05	-1.80E-04	-179.86	-0.125	-4.50E-04	-449.64	-0.19	-6.88E-04	-688.41	-4.39E-04	-439.30
15	24	336	23.6	-0.055	-1.98E-04	-197.84	-0.14	-5.04E-04	-503.60	-0.2	-7.25E-04	-724.64	-4.75E-04	-475.36
16	24	360	23.8	-0.06	-2.16E-04	-215.83	-0.16	-5.76E-04	-575.54	-0.205	-7.43E-04	-742.75	-5.11E-04	-511.37
17	24	384	23.7	-0.065	-2.34E-04	-233.81	-0.17	-6.12E-04	-611.51	-0.21	-7.61E-04	-760.87	-5.35E-04	-535.40

					SHRINKAGE TESTING RESULTS - RCA									
					0% Cement; No Polymer (E)									
Specimen Name				E1			E2			E3			AVERAGE	
Specimen Height (mm)				278			278			276				
Wet weight (g)				Wet/Dry	5057	4736.5	Wet/Dry	5060	4739.5	Wet/Dry	5020	4698.5		
Day	Time Interval (hours)	Cumulative Time (hours)	Temperature (^{0}C)	Dimensional change (mm)	Axial shrinkage (mm/mm)	Axial shrinkage [X 10^{-6}] mm/mm	Dimensional change (mm)	Axial shrinkage (mm/mm)	Axial shrinkage [X 10^{-6}] mm/mm	Dimensional change (mm)	Axial shrinkage (mm/mm)	Axial shrinkage [X 10^{-6}] mm/mm	Axial shrinkage (mm/mm)	Axial shrinkage [X 10^{-6}] mm/mm
18	24	408	23.4	-0.09	-3.24E-04	-323.74	-0.205	-7.37E-04	-737.41	-0.23	-8.33E-04	-833.33	-6.31E-04	-631.49
19	24	432	23.7	-0.1	-3.60E-04	-359.71	-0.22	-7.91E-04	-791.37	-0.245	-8.88E-04	-887.68	-6.80E-04	-679.59
20	24	456	24.1	-0.095	-3.42E-04	-341.73	-0.205	-7.37E-04	-737.41	-0.24	-8.70E-04	-869.57	-6.50E-04	-649.57
21	24	480	23.9	-0.095	-3.42E-04	-341.73	-0.195	-7.01E-04	-701.44	-0.24	-8.70E-04	-869.57	-6.38E-04	-637.58
22	24	504	23.3	-0.1	-3.60E-04	-359.71	-0.2	-7.19E-04	-719.42	-0.24	-8.70E-04	-869.57	-6.50E-04	-649.57
23	24	528	23.1	-0.11	-3.96E-04	-395.68	-0.22	-7.91E-04	-791.37	-0.25	-9.06E-04	-905.80	-6.98E-04	-697.62
24	24	552	22.7	-0.115	-4.14E-04	-413.67	-0.245	-8.81E-04	-881.29	-0.26	-9.42E-04	-942.03	-7.46E-04	-745.66
25	24	576	22.8	-0.12	-4.32E-04	-431.65	-0.245	-8.81E-04	-881.29	-0.265	-9.60E-04	-960.14	-7.58E-04	-757.70
26	24	600	23.1	-0.12	-4.32E-04	-431.65	-0.245	-8.81E-04	-881.29	-0.265	-9.60E-04	-960.14	-7.58E-04	-757.70
27	24	624	23.4	-0.12	-4.32E-04	-431.65	-0.24	-8.63E-04	-863.31	-0.265	-9.60E-04	-960.14	-7.52E-04	-751.70
28 start	24	648	23.6	-0.13	-4.68E-04	-467.63	-0.27	-9.71E-04	-971.22	-0.28	-1.01E-03	-1014.49	-8.18E-04	-817.78
28 end	24	672	23.8	-0.14	-5.04E-04	-503.60	-0.28	-1.01E-03	-1007.19	-0.285	-1.03E-03	-1032.61	-8.48E-04	-847.80

				SHRINKAGE TESTING RESULTS - RCA										
				2.5% Cement; No Polymer (F)										
	Specimen Name			F1			F2			F3			AVERAGE	
	Specimen Height (mm)			281			283			286				
	Weight (g)			Wet/Dry	5110	4848	Wet/Dry	5161	4897.5	Wet/Dry	5208	4941		
Day	Time Interval (hours)	Cumulative Time (hours)	Temperature (^{0}C)	Dimensional change (mm)	Axial shrinkage (mm/mm)	Axial shrinkage [X 10^{-6}] mm/mm	Dimensional change (mm)	Axial shrinkage (mm/mm)	Axial shrinkage [X 10^{-6}] mm/mm	Dimensional change (mm)	Axial shrinkage (mm/mm)	Axial shrinkage [X 10^{-6}] mm/mm	Axial shrinkage (mm/mm)	Axial shrinkage [X 10^{-6}] mm/mm
1	0	0	23.7	0	0.00E+00	0.00	0	0.00E+00	0.00	0	0.00E+00	0.00	0.00E+00	0.00
	1	1		-0.115	-4.09E-04	-409.25	-0.1	-3.53E-04	-353.36	-0.085	-2.97E-04	-297.20	-3.53E-04	-353.27
	1.5	2.5		-0.14	-4.98E-04	-498.22	-0.1	-3.53E-04	-353.36	-0.095	-3.32E-04	-332.17	-3.95E-04	-394.58
	1.5	4		-0.15	-5.34E-04	-533.81	-0.1	-3.53E-04	-353.36	-0.1	-3.50E-04	-349.65	-4.12E-04	-412.27
	1.5	5.5		-0.15	-5.34E-04	-533.81	-0.105	-3.71E-04	-371.02	-0.1	-3.50E-04	-349.65	-4.18E-04	-418.16
2	18.5	24	23.9	-0.17	-6.05E-04	-604.98	-0.115	-4.06E-04	-406.36	-0.21	-7.34E-04	-734.27	-5.82E-04	-581.87
	3	27		-0.185	-6.58E-04	-658.36	-0.12	-4.24E-04	-424.03	-0.265	-9.27E-04	-926.57	-6.70E-04	-669.65
	3	30		-0.19	-6.76E-04	-676.16	-0.125	-4.42E-04	-441.70	-0.295	-1.03E-03	-1031.47	-7.16E-04	-716.44
3	18	48	23.8	-0.2	-7.12E-04	-711.74	-0.13	-4.59E-04	-459.36	-0.33	-1.15E-03	-1153.85	-7.75E-04	-774.98
	6	54		-0.195	-6.94E-04	-693.95	-0.13	-4.59E-04	-459.36	-0.35	-1.22E-03	-1223.78	-7.92E-04	-792.36
4	18	72	23.6	-0.2	-7.12E-04	-711.74	-0.15	-5.30E-04	-530.04	-0.38	-1.33E-03	-1328.67	-8.57E-04	-856.82
	6	78		-0.2	-7.12E-04	-711.74	-0.165	-5.83E-04	-583.04	-0.395	-1.38E-03	-1381.12	-8.92E-04	-891.97
5	18	96	23.5	-0.205	-7.30E-04	-729.54	-0.18	-6.36E-04	-636.04	-0.4	-1.40E-03	-1398.60	-9.21E-04	-921.39
	6	102		-0.21	-7.47E-04	-747.33	-0.18	-6.36E-04	-636.04	-0.405	-1.42E-03	-1416.08	-9.33E-04	-933.15
6	18	120	23.8	-0.21	-7.47E-04	-747.33	-0.2	-7.07E-04	-706.71	-0.42	-1.47E-03	-1468.53	-9.74E-04	-974.19
	6	126		-0.21	-7.47E-04	-747.33	-0.2	-7.07E-04	-706.71	-0.425	-1.49E-03	-1486.01	-9.80E-04	-980.02

179

		SHRINKAGE TESTING RESULTS - RCA												
		2.5% Cement; No Polymer (F)												
Specimen Name			F1			F2			F3			AVERAGE		
Specimen Height (mm)			281			283			286					
Weight (g)			Wet/Dry	5110	4848	Wet/Dry	5161	4897.5	Wet/Dry	5208	4941			
Day	Time Interval (hours)	Cumulative Time (hours)	Temperature (^{0}C)	Dimensional change (mm)	Axial shrinkage (mm/mm)	Axial shrinkage [X 10^{-6}] mm/mm	Dimensional change (mm)	Axial shrinkage (mm/mm)	Axial shrinkage [X 10^{-6}] mm/mm	Dimensional change (mm)	Axial shrinkage (mm/mm)	Axial shrinkage [X 10^{-6}] mm/mm	Axial shrinkage (mm/mm)	Axial shrinkage [X 10^{-6}] mm/mm
7	18	144	23.2	-0.215	-7.65E-04	-765.12	-0.21	-7.42E-04	-742.05	-0.43	-1.50E-03	-1503.50	-1.00E-03	-1003.56
	6	150		-0.215	-7.65E-04	-765.12	-0.215	-7.60E-04	-759.72	-0.435	-1.52E-03	-1520.98	-1.02E-03	-1015.27
8	18	168	24.2	-0.22	-7.83E-04	-782.92	-0.24	-8.48E-04	-848.06	-0.455	-1.59E-03	-1590.91	-1.07E-03	-1073.96
	6	174		-0.22	-7.83E-04	-782.92	-0.25	-8.83E-04	-883.39	-0.47	-1.64E-03	-1643.36	-1.10E-03	-1103.22
9	18	192	23.4	-0.235	-8.36E-04	-836.30	-0.28	-9.89E-04	-989.40	-0.485	-1.70E-03	-1695.80	-1.17E-03	-1173.83
	6	198		-0.245	-8.72E-04	-871.89	-0.295	-1.04E-03	-1042.40	-0.5	-1.75E-03	-1748.25	-1.22E-03	-1220.85
10	24	216	23.9	-0.26	-9.25E-04	-925.27	-0.32	-1.13E-03	-1130.74	-0.505	-1.77E-03	-1765.73	-1.27E-03	-1273.91
11	24	240	23.5	-0.27	-9.61E-04	-960.85	-0.33	-1.17E-03	-1166.08	-0.505	-1.77E-03	-1765.73	-1.30E-03	-1297.56
12	24	264	22.9	-0.285	-1.01E-03	-1014.23	-0.345	-1.22E-03	-1219.08	-0.51	-1.78E-03	-1783.22	-1.34E-03	-1338.84
13	24	288	22.7	-0.295	-1.05E-03	-1049.82	-0.355	-1.25E-03	-1254.42	-0.51	-1.78E-03	-1783.22	-1.36E-03	-1362.49
14	24	312	23.2	-0.305	-1.09E-03	-1085.41	-0.37	-1.31E-03	-1307.42	-0.505	-1.77E-03	-1765.73	-1.39E-03	-1386.19
15	24	336	23.6	-0.31	-1.10E-03	-1103.20	-0.38	-1.34E-03	-1342.76	-0.51	-1.78E-03	-1783.22	-1.41E-03	-1409.73
16	24	360	23.8	-0.315	-1.12E-03	-1121.00	-0.39	-1.38E-03	-1378.09	-0.51	-1.78E-03	-1783.22	-1.43E-03	-1427.44
17	24	384	23.7	-0.33	-1.17E-03	-1174.38	-0.425	-1.50E-03	-1501.77	-0.54	-1.89E-03	-1888.11	-1.52E-03	-1521.42
18	24	408	23.4	-0.345	-1.23E-03	-1227.76	-0.45	-1.59E-03	-1590.11	-0.55	-1.92E-03	-1923.08	-1.58E-03	-1580.31
19	24	432	23.7	-0.36	-1.28E-03	-1281.14	-0.45	-1.59E-03	-1590.11	-0.52	-1.82E-03	-1818.18	-1.56E-03	-1563.14

180

						SHRINKAGE TESTING RESULTS - RCA										
						2.5% Cement; No Polymer (F)										
Specimen Name				F1			F2			F3			AVERAGE		
Specimen Height (mm)				281			283			286					
Weight (g)				Wet/Dry	5110	4848	Wet/Dry	5161	4897.5	Wet/Dry	5208	4941			
Day	Time Interval (hours)	Cumulative Time (hours)	Temperature (°C)	Dimensional change (mm)	Axial shrinkage (mm/mm)	Axial shrinkage [X 10⁻⁶] mm/mm	Dimensional change (mm)	Axial shrinkage (mm/mm)	Axial shrinkage [X 10⁻⁶] mm/mm	Dimensional change (mm)	Axial shrinkage (mm/mm)	Axial shrinkage [X 10⁻⁶] mm/mm	Axial shrinkage (mm/mm)	Axial shrinkage [X 10⁻⁶] mm/mm
20	24	456	24.1	-0.36	-1.28E-03	-1281.14	-0.445	-1.57E-03	-1572.44	-0.51	-1.78E-03	-1783.22	-1.55E-03	-1545.60
21	24	480	23.9	-0.36	-1.28E-03	-1281.14	-0.445	-1.57E-03	-1572.44	-0.51	-1.78E-03	-1783.22	-1.55E-03	-1545.60
22	24	504	23.3	-0.365	-1.30E-03	-1298.93	-0.46	-1.63E-03	-1625.44	-0.525	-1.84E-03	-1835.66	-1.59E-03	-1586.68
23	24	528	23.1	-0.37	-1.32E-03	-1316.73	-0.47	-1.66E-03	-1660.78	-0.54	-1.89E-03	-1888.11	-1.62E-03	-1621.87
24	24	552	22.7	-0.38	-1.35E-03	-1352.31	-0.475	-1.68E-03	-1678.45	-0.54	-1.89E-03	-1888.11	-1.64E-03	-1639.62
25	24	576	22.8	-0.385	-1.37E-03	-1370.11	-0.485	-1.71E-03	-1713.78	-0.53	-1.85E-03	-1853.15	-1.65E-03	-1645.68
26	24	600	23.1	-0.39	-1.39E-03	-1387.90	-0.495	-1.75E-03	-1749.12	-0.52	-1.82E-03	-1818.18	-1.65E-03	-1651.73
27	24	624	23.4	-0.4	-1.42E-03	-1423.49	-0.5	-1.77E-03	-1766.78	-0.545	-1.91E-03	-1905.59	-1.70E-03	-1698.62
28 start	24	648	23.6	-0.405	-1.44E-03	-1441.28	-0.52	-1.84E-03	-1837.46	-0.55	-1.92E-03	-1923.08	-1.73E-03	-1733.94
28 end	24	672	23.8	-0.41	-1.46E-03	-1459.07	-0.5	-1.77E-03	-1766.78	-0.5	-1.75E-03	-1748.25	-1.66E-03	-1658.04

SHRINKAGE TESTING RESULTS -RCA														
4% Cement; No Polymer (G)														
Specimen Name			G1			G2			G3			AVERAGE		
Specimen Height (mm)			287			290			291					
Weight (g)			Wet/Dry	5268.5	5029	Wet/Dry	5298.5	5050	Wet/Dry	5335.5	5092			
Day	Time Interval (hours)	Cumulative Time (hours)	Temperature (⁰C)	Dimensional change (mm)	Axial shrinkage (mm/mm)	Axial shrinkage [X 10⁻⁶] mm/mm	Dimensional change (mm)	Axial shrinkage (mm/mm)	Axial shrinkage [X 10⁻⁶] mm/mm	Dimensional change (mm)	Axial shrinkage (mm/mm)	Axial shrinkage [X 10⁻⁶] mm/mm	Axial shrinkage (mm/mm)	Axial shrinkage [X 10⁻⁶] mm/mm
	0	0	23.9	0	0.00E+00	0.00	0	0.00E+00	0.00	0	0.00E+00	0.00	0.00E+00	0.00
1	1	1		-0.13	-4.53E-04	-452.96	-0.065	-2.24E-04	-224.14	-0.07	-2.41E-04	-240.55	-3.06E-04	-305.88
	1.5	2.5		-0.14	-4.88E-04	-487.80	-0.03	-1.03E-04	-103.45	-0.06	-2.06E-04	-206.19	-2.66E-04	-265.81
	1.5	4		-0.14	-4.88E-04	-487.80	-0.01	-3.45E-05	-34.48	-0.04	-1.37E-04	-137.46	-2.20E-04	-219.91
	1.5	5.5		-0.14	-4.88E-04	-487.80	-0.025	-8.62E-05	-86.21	-0.03	-1.03E-04	-103.09	-2.26E-04	-225.70
2	18.5	24	23.6	-0.245	-8.54E-04	-853.66	-0.05	-1.72E-04	-172.41	-0.045	-1.55E-04	-154.64	-3.94E-04	-393.57
	3	27		-0.26	-9.06E-04	-905.92	-0.07	-2.41E-04	-241.38	-0.06	-2.06E-04	-206.19	-4.51E-04	-451.16
	3	30		-0.27	-9.41E-04	-940.77	-0.06	-2.07E-04	-206.90	-0.065	-2.23E-04	-223.37	-4.57E-04	-457.01
3	18	48	24	-0.32	-1.11E-03	-1114.98	-0.115	-3.97E-04	-396.55	-0.11	-3.78E-04	-378.01	-6.30E-04	-629.85
	6	54		-0.32	-1.11E-03	-1114.98	-0.12	-4.14E-04	-413.79	-0.12	-4.12E-04	-412.37	-6.47E-04	-647.05
4	18	72	23.6	-0.34	-1.18E-03	-1184.67	-0.15	-5.17E-04	-517.24	-0.155	-5.33E-04	-532.65	-7.45E-04	-744.85
	6	78		-0.35	-1.22E-03	-1219.51	-0.16	-5.52E-04	-551.72	-0.175	-6.01E-04	-601.37	-7.91E-04	-790.87
5	18	96	23.5	-0.385	-1.34E-03	-1341.46	-0.2	-6.90E-04	-689.66	-0.23	-7.90E-04	-790.38	-9.40E-04	-940.50
	6	102		-0.4	-1.39E-03	-1393.73	-0.22	-7.59E-04	-758.62	-0.25	-8.59E-04	-859.11	-1.00E-03	-1003.82
6	18	120	23.8	-0.425	-1.48E-03	-1480.84	-0.24	-8.28E-04	-827.59	-0.29	-9.97E-04	-996.56	-1.10E-03	-1101.66
	6	126		-0.445	-1.55E-03	-1550.52	-0.265	-9.14E-04	-913.79	-0.315	-1.08E-03	-1082.47	-1.18E-03	-1182.26

182

						SHRINKAGE TESTING RESULTS -RCA									
						4% Cement; No Polymer (G)									
Specimen Name				G1			G2			G3			AVERAGE		
Specimen Height (mm)				287			290			291					
Weight (g)				Wet/Dry	5268.5	5029	Wet/Dry	5298.5	5050	Wet/Dry	5335.5	5092			
Day	Time Interval (hours)	Cumulative Time (hours)	Temperature (⁰C)	Dimensional change (mm)	Axial shrinkage (mm/mm)	Axial shrinkage [X 10⁻⁶] mm/mm	Dimensional change (mm)	Axial shrinkage (mm/mm)	Axial shrinkage [X 10⁻⁶] mm/mm	Dimensional change (mm)	Axial shrinkage (mm/mm)	Axial shrinkage [X 10⁻⁶] mm/mm	Axial shrinkage (mm/mm)	Axial shrinkage [X 10⁻⁶] mm/mm
7	18	144	23.2	-0.46	-1.60E-03	-1602.79	-0.29	-1.00E-03	-1000.00	-0.34	-1.17E-03	-1168.38	-1.26E-03	-1257.06
	6	150		-0.455	-1.59E-03	-1585.37	-0.29	-1.00E-03	-1000.00	-0.34	-1.17E-03	-1168.38	-1.25E-03	-1251.25
8	18	168	24.2	-0.455	-1.59E-03	-1585.37	-0.295	-1.02E-03	-1017.24	-0.345	-1.19E-03	-1185.57	-1.26E-03	-1262.72
	6	174		-0.45	-1.57E-03	-1567.94	-0.305	-1.05E-03	-1051.72	-0.355	-1.22E-03	-1219.93	-1.28E-03	-1279.87
9	18	192	23.4	-0.45	-1.57E-03	-1567.94	-0.315	-1.09E-03	-1086.21	-0.36	-1.24E-03	-1237.11	-1.30E-03	-1297.09
	6	198		-0.44	-1.53E-03	-1533.10	-0.32	-1.10E-03	-1103.45	-0.365	-1.25E-03	-1254.30	-1.30E-03	-1296.95
10	24	216	23.9	-0.435	-1.52E-03	-1515.68	-0.33	-1.14E-03	-1137.93	-0.375	-1.29E-03	-1288.66	-1.31E-03	-1314.09
11	24	240	23.5	-0.43	-1.50E-03	-1498.26	-0.34	-1.17E-03	-1172.41	-0.39	-1.34E-03	-1340.21	-1.34E-03	-1336.96
12	24	264	22.9	-0.415	-1.45E-03	-1445.99	-0.345	-1.19E-03	-1189.66	-0.395	-1.36E-03	-1357.39	-1.33E-03	-1331.01
13	24	288	22.7	-0.425	-1.48E-03	-1480.84	-0.37	-1.28E-03	-1275.86	-0.42	-1.44E-03	-1443.30	-1.40E-03	-1400.00
14	24	312	23.2	-0.46	-1.60E-03	-1602.79	-0.435	-1.50E-03	-1500.00	-0.47	-1.62E-03	-1615.12	-1.57E-03	-1572.64
15	24	336	23.6	-0.48	-1.67E-03	-1672.47	-0.465	-1.60E-03	-1603.45	-0.5	-1.72E-03	-1718.21	-1.66E-03	-1664.71
16	24	360	23.8	-0.44	-1.53E-03	-1533.10	-0.42	-1.45E-03	-1448.28	-0.46	-1.58E-03	-1580.76	-1.52E-03	-1520.71
17	24	384	23.7	-0.42	-1.46E-03	-1463.41	-0.395	-1.36E-03	-1362.07	-0.445	-1.53E-03	-1529.21	-1.45E-03	-1451.56
18	24	408	23.4	-0.42	-1.46E-03	-1463.41	-0.41	-1.41E-03	-1413.79	-0.455	-1.56E-03	-1563.57	-1.48E-03	-1480.26
19	24	432	23.7	-0.435	-1.52E-03	-1515.68	-0.44	-1.52E-03	-1517.24	-0.475	-1.63E-03	-1632.30	-1.56E-03	-1555.07
20	24	456	24.1	-0.455	-1.59E-03	-1585.37	-0.475	-1.64E-03	-1637.93	-0.515	-1.77E-03	-1769.76	-1.66E-03	-1664.35

183

SHRINKAGE TESTING RESULTS -RCA													
4% Cement; No Polymer (G)													
Specimen Name				G1 (13/06/2015)			G2 (13/06/2015)			G3 (13/06/2015)			AVERAGE	
Specimen Height (mm)				287			290			291				
Weight (g)				Wet/Dry	5268.5	5029	Wet/Dry	5298.5	5050	Wet/Dry	5335.5	5092		
Day	Time Interval (hours)	Cumulative Time (hours)	Temperature (⁰C)	Dimensional change (mm)	Axial shrinkage (mm/mm)	Axial shrinkage [X 10⁻⁶] mm/mm	Dimensional change (mm)	Axial shrinkage (mm/mm)	Axial shrinkage [X 10⁻⁶] mm/mm	Dimensional change (mm)	Axial shrinkage (mm/mm)	Axial shrinkage [X 10⁻⁶] mm/mm	Axial shrinkage (mm/mm)	Axial shrinkage [X 10⁻⁶] mm/mm
21	24	480	23.9	-0.45	-1.57E-03	-1567.94	-0.47	-1.62E-03	-1620.69	-0.515	-1.77E-03	-1769.76	-1.65E-03	-1652.80
22	24	504	23.3	-0.45	-1.57E-03	-1567.94	-0.47	-1.62E-03	-1620.69	-0.515	-1.77E-03	-1769.76	-1.65E-03	-1652.80
23	24	528	23.1	-0.45	-1.57E-03	-1567.94	-0.475	-1.64E-03	-1637.93	-0.515	-1.77E-03	-1769.76	-1.66E-03	-1658.54
24	24	552	22.7	-0.46	-1.60E-03	-1602.79	-0.495	-1.71E-03	-1706.90	-0.54	-1.86E-03	-1855.67	-1.72E-03	-1721.78
25	24	576	22.8	-0.485	-1.69E-03	-1689.90	-0.525	-1.81E-03	-1810.34	-0.555	-1.91E-03	-1907.22	-1.80E-03	-1802.49
26	24	600	23.1	-0.415	-1.45E-03	-1445.99	-0.44	-1.52E-03	-1517.24	-0.48	-1.65E-03	-1649.48	-1.54E-03	-1537.57
27	24	624	23.4	-0.38	-1.32E-03	-1324.04	-0.4	-1.38E-03	-1379.31	-0.465	-1.60E-03	-1597.94	-1.43E-03	-1433.76
28 start	24	648	23.6	-0.38	-1.32E-03	-1324.04	-0.405	-1.40E-03	-1396.55	-0.475	-1.63E-03	-1632.30	-1.45E-03	-1450.97
28 end	24	672	23.8	-0.39	-1.36E-03	-1358.89	-0.415	-1.43E-03	-1431.03	-0.47	-1.62E-03	-1615.12	-1.47E-03	-1468.35

B.3: NEW CONCRETE (NC)

					SHRINKAGE TESTING RESULTS - NC									

				0% Cement; No Polymer (H)										

Specimen Name				H1			H2			H3			AVERAGE	
Specimen Height (mm)				273			273			270				
Wet weight (g)				Wet/Dry	5015	4722	Wet/Dry	5006.5	4727	Wet/Dry	4947	4666		
Day	Time Interval (hours)	Cumulative Time (hours)	Temperature (^{0}C)	Dimensional change (mm)	Axial shrinkage (mm/mm)	Axial shrinkage [X 10^{-6}] mm/mm	Dimensional change (mm)	Axial shrinkage (mm/mm)	Axial shrinkage [X 10^{-6}] mm/mm	Dimensional change (mm)	Axial shrinkage (mm/mm)	Axial shrinkage [X 10^{-6}] mm/mm	Axial shrinkage (mm/mm)	Axial shrinkage [X 10^{-6}] mm/mm
	0	0	24.1	0	0.00E+00	0.00	0	0.00E+00	0.00	0	0.00E+00	0.00	0.00E+00	0.00
	1	1		-0.08	-2.93E-04	-293.04	-0.09	-3.30E-04	-329.67	-0.105	-3.89E-04	-388.89	-3.37E-04	-337.20
1	1.5	2.5		-0.095	-3.48E-04	-347.99	-0.11	-4.03E-04	-402.93	-0.12	-4.44E-04	-444.44	-3.98E-04	-398.45
	1.5	4		-0.1	-3.66E-04	-366.30	-0.115	-4.21E-04	-421.25	-0.125	-4.63E-04	-462.96	-4.17E-04	-416.84
	1.5	5.5		-0.115	-4.21E-04	-421.25	-0.125	-4.58E-04	-457.88	-0.125	-4.63E-04	-462.96	-4.47E-04	-447.36
	18.5	24	23.8	-0.115	-4.21E-04	-421.25	-0.125	-4.58E-04	-457.88	-0.1	-3.70E-04	-370.37	-4.16E-04	-416.50
2	3	27		-0.12	-4.40E-04	-439.56	-0.12	-4.40E-04	-439.56	-0.105	-3.89E-04	-388.89	-4.23E-04	-422.67
	3	30		-0.105	-3.85E-04	-384.62	-0.11	-4.03E-04	-402.93	-0.11	-4.07E-04	-407.41	-3.98E-04	-398.32
3	18	48	23.7	-0.1	-3.66E-04	-366.30	-0.145	-5.31E-04	-531.14	-0.15	-5.56E-04	-555.56	-4.84E-04	-484.33
	6	54		-0.105	-3.85E-04	-384.62	-0.16	-5.86E-04	-586.08	-0.17	-6.30E-04	-629.63	-5.33E-04	-533.44
4	18	72	23.2	-0.11	-4.03E-04	-402.93	-0.17	-6.23E-04	-622.71	-0.2	-7.41E-04	-740.74	-5.89E-04	-588.79
	6	78		-0.105	-3.85E-04	-384.62	-0.18	-6.59E-04	-659.34	-0.23	-8.52E-04	-851.85	-6.32E-04	-631.94
5	18	96	23.5	-0.13	-4.76E-04	-476.19	-0.22	-8.06E-04	-805.86	-0.26	-9.63E-04	-962.96	-7.48E-04	-748.34
	6	102		-0.15	-5.49E-04	-549.45	-0.24	-8.79E-04	-879.12	-0.28	-1.04E-03	-1037.04	-8.22E-04	-821.87
6	18	120	23.7	-0.18	-6.59E-04	-659.34	-0.27	-9.89E-04	-989.01	-0.305	-1.13E-03	-1129.63	-9.26E-04	-925.99
	6	126		-0.2	-7.33E-04	-732.60	-0.285	-1.04E-03	-1043.96	-0.32	-1.19E-03	-1185.19	-9.87E-04	-987.25

185

				SHRINKAGE TESTING RESULTS - NC										
				0% Cement; No Polymer (H)										
	Specimen Name			H1			H2			H3			AVERAGE	
	Specimen Height (mm)			273			273			270				
	Wet weight (g)			Wet/Dry	5015	4722	Wet/Dry	5006.5	4727	Wet/Dry	4947	4666		
Day	Time Interval (hours)	Cumulative Time (hours)	Temperature (^{0}C)	Dimensional change (mm)	Axial shrinkage (mm/mm)	Axial shrinkage [X 10^{-6}] mm/mm	Dimensional change (mm)	Axial shrinkage (mm/mm)	Axial shrinkage [X 10^{-6}] mm/mm	Dimensional change (mm)	Axial shrinkage (mm/mm)	Axial shrinkage [X 10^{-6}] mm/mm	Axial shrinkage (mm/mm)	Axial shrinkage [X 10^{-6}] mm/mm
7	18	144	24.1	-0.22	-8.06E-04	-805.86	-0.295	-1.08E-03	-1080.59	-0.325	-1.20E-03	-1203.70	-1.03E-03	-1030.05
	6	150		-0.24	-8.79E-04	-879.12	-0.305	-1.12E-03	-1117.22	-0.33	-1.22E-03	-1222.22	-1.07E-03	-1072.85
8	18	168	24.2	-0.255	-9.34E-04	-934.07	-0.315	-1.15E-03	-1153.85	-0.335	-1.24E-03	-1240.74	-1.11E-03	-1109.55
	6	174		-0.26	-9.52E-04	-952.38	-0.32	-1.17E-03	-1172.16	-0.335	-1.24E-03	-1240.74	-1.12E-03	-1121.76
9	18	192	23.5	-0.265	-9.71E-04	-970.70	-0.33	-1.21E-03	-1208.79	-0.34	-1.26E-03	-1259.26	-1.15E-03	-1146.25
	6	198		-0.27	-9.89E-04	-989.01	-0.34	-1.25E-03	-1245.42	-0.35	-1.30E-03	-1296.30	-1.18E-03	-1176.91
10	24	216	23.8	-0.28	-1.03E-03	-1025.64	-0.35	-1.28E-03	-1282.05	-0.36	-1.33E-03	-1333.33	-1.21E-03	-1213.68
11	24	240	23.7	-0.3	-1.10E-03	-1098.90	-0.385	-1.41E-03	-1410.26	-0.375	-1.39E-03	-1388.89	-1.30E-03	-1299.35
12	24	264	23.3	-0.32	-1.17E-03	-1172.16	-0.4	-1.47E-03	-1465.20	-0.4	-1.48E-03	-1481.48	-1.37E-03	-1372.95
13	24	288	22.8	-0.34	-1.25E-03	-1245.42	-0.42	-1.54E-03	-1538.46	-0.41	-1.52E-03	-1518.52	-1.43E-03	-1434.13
14	24	312	22.4	-0.36	-1.32E-03	-1318.68	-0.43	-1.58E-03	-1575.09	-0.42	-1.56E-03	-1555.56	-1.48E-03	-1483.11
15	24	336	22.7	-0.36	-1.32E-03	-1318.68	-0.44	-1.61E-03	-1611.72	-0.425	-1.57E-03	-1574.07	-1.50E-03	-1501.49
16	24	360	23.1	-0.37	-1.36E-03	-1355.31	-0.455	-1.67E-03	-1666.67	-0.44	-1.63E-03	-1629.63	-1.55E-03	-1550.54
17	24	384	23.5	-0.38	-1.39E-03	-1391.94	-0.465	-1.70E-03	-1703.30	-0.45	-1.67E-03	-1666.67	-1.59E-03	-1587.30
18	24	408	23.7	-0.39	-1.43E-03	-1428.57	-0.475	-1.74E-03	-1739.93	-0.455	-1.69E-03	-1685.19	-1.62E-03	-1617.89
19	24	432	23.4	-0.395	-1.45E-03	-1446.89	-0.48	-1.76E-03	-1758.24	-0.465	-1.72E-03	-1722.22	-1.64E-03	-1642.45
20	24	456	23.2	-0.395	-1.45E-03	-1446.89	-0.46	-1.68E-03	-1684.98	-0.46	-1.70E-03	-1703.70	-1.61E-03	-1611.86

186

colspan="16"	**SHRINKAGE TESTING RESULTS - NC**
colspan="16"	**0% Cement; No Polymer (H)**
colspan="4"	**Specimen Name**	colspan="3"	**H1**		**H2**	colspan="3"	**H3**	colspan="2"	**AVERAGE**
colspan="4"	**Specimen Height (mm)**	colspan="3"	273	colspan="3"	273	colspan="3"	270	colspan="2"	
colspan="4"	**Wet weight (g)**	**Wet/Dry**	5015	4722	**Wet/Dry**	5006.5	4727	**Wet/Dry**	4947	4666		
Day	**Time Interval (hours)**	**Cumulative Time (hours)**	**Temperature (^{0}C)**	**Dimensional change (mm)**	**Axial shrinkage (mm/mm)**	**Axial shrinkage [X 10^{-6}] mm/mm**	**Dimensional change (mm)**	**Axial shrinkage (mm/mm)**	**Axial shrinkage [X 10^{-6}] mm/mm**	**Dimensional change (mm)**	**Axial shrinkage (mm/mm)**	**Axial shrinkage [X 10^{-6}] mm/mm**	**Axial shrinkage (mm/mm)**	**Axial shrinkage [X 10^{-6}] mm/mm**
21	24	480	24.3	-0.41	-1.50E-03	-1501.83	-0.49	-1.79E-03	-1794.87	-0.47	-1.74E-03	-1740.74	-1.68E-03	-1679.15
22	24	504	24.1	-0.42	-1.54E-03	-1538.46	-0.51	-1.87E-03	-1868.13	-0.485	-1.80E-03	-1796.30	-1.73E-03	-1734.30
23	24	528	23.6	-0.435	-1.59E-03	-1593.41	-0.525	-1.92E-03	-1923.08	-0.5	-1.85E-03	-1851.85	-1.79E-03	-1789.45
24	24	552	23.1	-0.44	-1.61E-03	-1611.72	-0.53	-1.94E-03	-1941.39	-0.51	-1.89E-03	-1888.89	-1.81E-03	-1814.00
25	24	576	22.9	-0.43	-1.58E-03	-1575.09	-0.5	-1.83E-03	-1831.50	-0.505	-1.87E-03	-1870.37	-1.76E-03	-1758.99
26	24	600	23.3	-0.43	-1.58E-03	-1575.09	-0.48	-1.76E-03	-1758.24	-0.49	-1.81E-03	-1814.81	-1.72E-03	-1716.05
27	24	624	23.8	-0.43	-1.58E-03	-1575.09	-0.495	-1.81E-03	-1813.19	-0.49	-1.81E-03	-1814.81	-1.73E-03	-1734.36
28 start	24	648	23.5	-0.43	-1.58E-03	-1575.09	-0.495	-1.81E-03	-1813.19	-0.5	-1.85E-03	-1851.85	-1.75E-03	-1746.71
28 end	24	672	23.4	-0.435	-1.59E-03	-1593.41	-0.5	-1.83E-03	-1831.50	-0.5	-1.85E-03	-1851.85	-1.76E-03	-1758.92

SHRINKAGE TESTING RESULTS - NC													
2.5% Cement; No Polymer (I)													
Specimen Name			**I1**			**I2**			**I3**			**AVERAGE**	
Specimen Height (mm)			278			279			270				
Wet weight (g)			**Wet/Dry**	5127	4852	**Wet/Dry**	5139	4869	**Wet/Dry**	4963	4702		
Day	**Time Interval (hours)**	**Cumulative Time (hours)**	**Temperature (^{0}C)**	**Dimensional change (mm)**	**Axial shrinkage (mm/mm)**	**Axial shrinkage [X 10^{-6}] mm/mm**	**Dimensional change (mm)**	**Axial shrinkage (mm/mm)**	**Axial shrinkage [X 10^{-6}] mm/mm**	**Dimensional change (mm)**	**Axial shrinkage (mm/mm)**	**Axial shrinkage [X 10^{-6}] mm/mm**	**Axial shrinkage (mm/mm)**	**Axial shrinkage [X 10^{-6}] mm/mm**

Day	Time Interval (hours)	Cumulative Time (hours)	Temperature (°C)	Dim change (mm) I1	Axial shrinkage (mm/mm) I1	Axial shrinkage [X10⁻⁶] I1	Dim change (mm) I2	Axial shrinkage (mm/mm) I2	Axial shrinkage [X10⁻⁶] I2	Dim change (mm) I3	Axial shrinkage (mm/mm) I3	Axial shrinkage [X10⁻⁶] I3	Axial shrinkage (mm/mm) AVG	Axial shrinkage [X10⁻⁶] AVG
	0	0	24.3	0	0.00E+00	0.00	0	0.00E+00	0.00	0	0.00E+00	0.00	0.00E+00	0.00
1	1	1		-0.1	-3.60E-04	-359.71	-0.11	-3.94E-04	-394.27	-0.11	-4.07E-04	-407.41	-3.87E-04	-387.13
	1.5	2.5		-0.1	-3.60E-04	-359.71	-0.13	-4.66E-04	-465.95	-0.14	-5.19E-04	-518.52	-4.48E-04	-448.06
	1.5	4		-0.11	-3.96E-04	-395.68	-0.145	-5.20E-04	-519.71	-0.16	-5.93E-04	-592.59	-5.03E-04	-502.66
	1.5	5.5		-0.115	-4.14E-04	-413.67	-0.145	-5.20E-04	-519.71	-0.16	-5.93E-04	-592.59	-5.09E-04	-508.66
2	18.5	24	24.1	-0.14	-5.04E-04	-503.60	-0.17	-6.09E-04	-609.32	-0.26	-9.63E-04	-962.96	-6.92E-04	-691.96
	3	27		-0.155	-5.58E-04	-557.55	-0.175	-6.27E-04	-627.24	-0.285	-1.06E-03	-1055.56	-7.47E-04	-746.78
	3	30		-0.17	-6.12E-04	-611.51	-0.185	-6.63E-04	-663.08	-0.315	-1.17E-03	-1166.67	-8.14E-04	-813.75
3	18	48	23.9	-0.21	-7.55E-04	-755.40	-0.21	-7.53E-04	-752.69	-0.37	-1.37E-03	-1370.37	-9.59E-04	-959.48
	6	54		-0.24	-8.63E-04	-863.31	-0.225	-8.06E-04	-806.45	-0.4	-1.48E-03	-1481.48	-1.05E-03	-1050.41
4	18	72	23.2	-0.28	-1.01E-03	-1007.19	-0.24	-8.60E-04	-860.22	-0.455	-1.69E-03	-1685.19	-1.18E-03	-1184.20
	6	78		-0.3	-1.08E-03	-1079.14	-0.25	-8.96E-04	-896.06	-0.49	-1.81E-03	-1814.81	-1.26E-03	-1263.34
5	18	96	23.5	-0.32	-1.15E-03	-1151.08	-0.28	-1.00E-03	-1003.58	-0.515	-1.91E-03	-1907.41	-1.35E-03	-1354.02
	6	102		-0.33	-1.19E-03	-1187.05	-0.295	-1.06E-03	-1057.35	-0.52	-1.93E-03	-1925.93	-1.39E-03	-1390.11
6	18	120	23.7	-0.36	-1.29E-03	-1294.96	-0.33	-1.18E-03	-1182.80	-0.545	-2.02E-03	-2018.52	-1.50E-03	-1498.76
	6	126		-0.385	-1.38E-03	-1384.89	-0.35	-1.25E-03	-1254.48	-0.56	-2.07E-03	-2074.07	-1.57E-03	-1571.15

188

				SHRINKAGE TESTING RESULTS - NC										
				2.5% Cement; No Polymer (I)										
Specimen Name				I1			I2			I3			AVERAGE	
Specimen Height (mm)				278			279			270				
Wet weight (g)				Wet/Dry	5127	4852	Wet/Dry	5139	4869	Wet/Dry	4963	4702		
Day	Time Interval (hours)	Cumulative Time (hours)	Temperature (^{0}C)	Dimensional change (mm)	Axial shrinkage (mm/mm)	Axial shrinkage [X 10^{-6}] mm/mm	Dimensional change (mm)	Axial shrinkage (mm/mm)	Axial shrinkage [X 10^{-6}] mm/mm	Dimensional change (mm)	Axial shrinkage (mm/mm)	Axial shrinkage [X 10^{-6}] mm/mm	Axial shrinkage (mm/mm)	Axial shrinkage [X 10^{-6}] mm/mm
7	18	144	24.1	-0.4	-1.44E-03	-1438.85	-0.365	-1.31E-03	-1308.24	-0.565	-2.09E-03	-2092.59	-1.61E-03	-1613.23
	6	150		-0.42	-1.51E-03	-1510.79	-0.37	-1.33E-03	-1326.16	-0.57	-2.11E-03	-2111.11	-1.65E-03	-1649.36
8	18	168	24.2	-0.435	-1.56E-03	-1564.75	-0.38	-1.36E-03	-1362.01	-0.575	-2.13E-03	-2129.63	-1.69E-03	-1685.46
	6	174		-0.445	-1.60E-03	-1600.72	-0.385	-1.38E-03	-1379.93	-0.58	-2.15E-03	-2148.15	-1.71E-03	-1709.60
9	18	192	23.5	-0.455	-1.64E-03	-1636.69	-0.4	-1.43E-03	-1433.69	-0.59	-2.19E-03	-2185.19	-1.75E-03	-1751.86
	6	198		-0.46	-1.65E-03	-1654.68	-0.405	-1.45E-03	-1451.61	-0.595	-2.20E-03	-2203.70	-1.77E-03	-1770.00
10	24	216	23.8	-0.475	-1.71E-03	-1708.63	-0.415	-1.49E-03	-1487.46	-0.605	-2.24E-03	-2240.74	-1.81E-03	-1812.28
11	24	240	23.7	-0.495	-1.78E-03	-1780.58	-0.44	-1.58E-03	-1577.06	-0.63	-2.33E-03	-2333.33	-1.90E-03	-1896.99
12	24	264	23.3	-0.52	-1.87E-03	-1870.50	-0.465	-1.67E-03	-1666.67	-0.64	-2.37E-03	-2370.37	-1.97E-03	-1969.18
13	24	288	22.8	-0.545	-1.96E-03	-1960.43	-0.475	-1.70E-03	-1702.51	-0.65	-2.41E-03	-2407.41	-2.02E-03	-2023.45
14	24	312	22.4	-0.575	-2.07E-03	-2068.35	-0.49	-1.76E-03	-1756.27	-0.665	-2.46E-03	-2462.96	-2.10E-03	-2095.86
15	24	336	22.7	-0.59	-2.12E-03	-2122.30	-0.495	-1.77E-03	-1774.19	-0.675	-2.50E-03	-2500.00	-2.13E-03	-2132.17
16	24	360	23.1	-0.605	-2.18E-03	-2176.26	-0.505	-1.81E-03	-1810.04	-0.685	-2.54E-03	-2537.04	-2.17E-03	-2174.44
17	24	384	23.5	-0.62	-2.23E-03	-2230.22	-0.52	-1.86E-03	-1863.80	-0.695	-2.57E-03	-2574.07	-2.22E-03	-2222.70
18	24	408	23.7	-0.63	-2.27E-03	-2266.19	-0.53	-1.90E-03	-1899.64	-0.705	-2.61E-03	-2611.11	-2.26E-03	-2258.98
19	24	432	23.4	-0.65	-2.34E-03	-2338.13	-0.54	-1.94E-03	-1935.48	-0.715	-2.65E-03	-2648.15	-2.31E-03	-2307.25
20	24	456	23.2	-0.67	-2.41E-03	-2410.07	-0.545	-1.95E-03	-1953.41	-0.715	-2.65E-03	-2648.15	-2.34E-03	-2337.21

189

				SHRINKAGE TESTING RESULTS - NC										
				2.5% Cement; No Polymer (I)										
Specimen Name				I1			I2			I3			AVERAGE	
Specimen Height (mm)				278			279			270				
Wet weight (g)				Wet/Dry	5127	4852	Wet/Dry	5139	4869	Wet/Dry	4963	4702		
Day	Time Interval (hours)	Cumulative Time (hours)	Temperature (^{0}C)	Dimensional change (mm)	Axial shrinkage (mm/mm)	Axial shrinkage [X 10^{-6}] mm/mm	Dimensional change (mm)	Axial shrinkage (mm/mm)	Axial shrinkage [X 10^{-6}] mm/mm	Dimensional change (mm)	Axial shrinkage (mm/mm)	Axial shrinkage [X 10^{-6}] mm/mm	Axial shrinkage (mm/mm)	Axial shrinkage [X 10^{-6}] mm/mm
21	24	480	24.3	-0.675	-2.43E-03	-2428.06	-0.55	-1.97E-03	-1971.33	-0.72	-2.67E-03	-2666.67	-2.36E-03	-2355.35
22	24	504	24.1	-0.685	-2.46E-03	-2464.03	-0.565	-2.03E-03	-2025.09	-0.72	-2.67E-03	-2666.67	-2.39E-03	-2385.26
23	24	528	23.6	-0.7	-2.52E-03	-2517.99	-0.58	-2.08E-03	-2078.85	-0.725	-2.69E-03	-2685.19	-2.43E-03	-2427.34
24	24	552	23.1	-0.71	-2.55E-03	-2553.96	-0.59	-2.11E-03	-2114.70	-0.735	-2.72E-03	-2722.22	-2.46E-03	-2463.62
25	24	576	22.9	-0.73	-2.63E-03	-2625.90	-0.59	-2.11E-03	-2114.70	-0.745	-2.76E-03	-2759.26	-2.50E-03	-2499.95
26	24	600	23.3	-0.735	-2.64E-03	-2643.88	-0.575	-2.06E-03	-2060.93	-0.74	-2.74E-03	-2740.74	-2.48E-03	-2481.85
27	24	624	23.8	-0.73	-2.63E-03	-2625.90	-0.57	-2.04E-03	-2043.01	-0.745	-2.76E-03	-2759.26	-2.48E-03	-2476.06
28 start	24	648	23.5	-0.735	-2.64E-03	-2643.88	-0.58	-2.08E-03	-2078.85	-0.75	-2.78E-03	-2777.78	-2.50E-03	-2500.17
28 end	24	672	23.4	-0.735	-2.64E-03	-2643.88	-0.58	-2.08E-03	-2078.85	-0.75	-2.78E-03	-2777.78	-2.50E-03	-2500.17

			SHRINKAGE TESTING RESULTS - NC										
			4% Cement; No Polymer (J)										
Specimen Name			J1			J2			J3			AVERAGE	
Specimen Height (mm)			280			281			280				
Wet weight (g)			Wet/Dry	5196	4942	Wet/Dry	5224	4957	Wet/Dry	5207	4951		
Day	Time Interval (hours)	Cumulative Time (hours)	Temperature (^{0}C)	Dimensional change (mm)	Axial shrinkage (mm/mm)	Axial shrinkage [X 10^{-6}] mm/mm	Dimensional change (mm)	Axial shrinkage (mm/mm)	Axial shrinkage [X 10^{-6}] mm/mm	Dimensional change (mm)	Axial shrinkage (mm/mm)	Axial shrinkage [X 10^{-6}] mm/mm	Axial shrinkage (mm/mm)	Axial shrinkage [X 10^{-6}] mm/mm
	0	0	23.8	0	0.00E+00	0.00	0	0.00E+00	0.00	0	0.00E+00	0.00	0.00E+00	0.00
1	1	1		-0.11	-3.93E-04	-392.86	-0.13	-4.63E-04	-462.63	-0.15	-5.36E-04	-535.71	-4.64E-04	-463.73
	1.5	2.5		-0.11	-3.93E-04	-392.86	-0.14	-4.98E-04	-498.22	-0.165	-5.89E-04	-589.29	-4.93E-04	-493.45
	1.5	4		-0.115	-4.11E-04	-410.71	-0.145	-5.16E-04	-516.01	-0.17	-6.07E-04	-607.14	-5.11E-04	-511.29
	1.5	5.5		-0.12	-4.29E-04	-428.57	-0.155	-5.52E-04	-551.60	-0.18	-6.43E-04	-642.86	-5.41E-04	-541.01
2	18.5	24	23.7	-0.215	-7.68E-04	-767.86	-0.2	-7.12E-04	-711.74	-0.305	-1.09E-03	-1089.29	-8.56E-04	-856.30
	3	27		-0.24	-8.57E-04	-857.14	-0.205	-7.30E-04	-729.54	-0.33	-1.18E-03	-1178.57	-9.22E-04	-921.75
	3	30		-0.255	-9.11E-04	-910.71	-0.225	-8.01E-04	-800.71	-0.375	-1.34E-03	-1339.29	-1.02E-03	-1016.90
3	18	48	23.5	-0.32	-1.14E-03	-1142.86	-0.275	-9.79E-04	-978.65	-0.48	-1.71E-03	-1714.29	-1.28E-03	-1278.60
	6	54		-0.355	-1.27E-03	-1267.86	-0.305	-1.09E-03	-1085.41	-0.515	-1.84E-03	-1839.29	-1.40E-03	-1397.52
4	18	72	23.2	-0.425	-1.52E-03	-1517.86	-0.345	-1.23E-03	-1227.76	-0.58	-2.07E-03	-2071.43	-1.61E-03	-1605.68
	6	78		-0.45	-1.61E-03	-1607.14	-0.38	-1.35E-03	-1352.31	-0.62	-2.21E-03	-2214.29	-1.72E-03	-1724.58
5	18	96	23.5	-0.51	-1.82E-03	-1821.43	-0.415	-1.48E-03	-1476.87	-0.69	-2.46E-03	-2464.29	-1.92E-03	-1920.86
	6	102		-0.515	-1.84E-03	-1839.29	-0.44	-1.57E-03	-1565.84	-0.705	-2.52E-03	-2517.86	-1.97E-03	-1974.33
6	18	120	23.7	-0.53	-1.89E-03	-1892.86	-0.475	-1.69E-03	-1690.39	-0.735	-2.63E-03	-2625.00	-2.07E-03	-2069.42
	6	126		-0.535	-1.91E-03	-1910.71	-0.52	-1.85E-03	-1850.53	-0.74	-2.64E-03	-2642.86	-2.13E-03	-2134.70
7	18	144	24.1	-0.52	-1.86E-03	-1857.14	-0.53	-1.89E-03	-1886.12	-0.73	-2.61E-03	-2607.14	-2.12E-03	-2116.80
	6	150		-0.52	-1.86E-03	-1857.14	-0.545	-1.94E-03	-1939.50	-0.73	-2.61E-03	-2607.14	-2.13E-03	-2134.60

191

				SHRINKAGE TESTING RESULTS - NC										
				4% Cement; No Polymer (J)											
Specimen Name				J1			J2			J3			AVERAGE		
Specimen Height (mm)				280			281			280					
Wet weight (g)				Wet/Dry	5196	4942	Wet/Dry	5224	4957	Wet/Dry	5207	4951			
Day	Time Interval (hours)	Cumulative Time (hours)	Temperature (°C)	Dimensional change (mm)	Axial shrinkage (mm/mm)	Axial shrinkage [X 10⁻⁶] mm/mm	Dimensional change (mm)	Axial shrinkage (mm/mm)	Axial shrinkage [X 10⁻⁶] mm/mm	Dimensional change (mm)	Axial shrinkage (mm/mm)	Axial shrinkage [X 10⁻⁶] mm/mm	Axial shrinkage (mm/mm)	Axial shrinkage [X 10⁻⁶] mm/mm
8	18	168	24.2	-0.515	-1.84E-03	-1839.29	-0.565	-2.01E-03	-2010.68	-0.725	-2.59E-03	-2589.29	-2.15E-03	-2146.42
	6	174		-0.515	-1.84E-03	-1839.29	-0.575	-2.05E-03	-2046.26	-0.73	-2.61E-03	-2607.14	-2.16E-03	-2164.23
9	18	192	23.5	-0.52	-1.86E-03	-1857.14	-0.59	-2.10E-03	-2099.64	-0.73	-2.61E-03	-2607.14	-2.19E-03	-2187.98
	6	198		-0.52	-1.86E-03	-1857.14	-0.6	-2.14E-03	-2135.23	-0.735	-2.63E-03	-2625.00	-2.21E-03	-2205.79
10	24	216	23.8	-0.52	-1.86E-03	-1857.14	-0.605	-2.15E-03	-2153.02	-0.74	-2.64E-03	-2642.86	-2.22E-03	-2217.67
11	24	240	23.7	-0.56	-2.00E-03	-2000.00	-0.65	-2.31E-03	-2313.17	-0.795	-2.84E-03	-2839.29	-2.38E-03	-2384.15
12	24	264	23.3	-0.57	-2.04E-03	-2035.71	-0.67	-2.38E-03	-2384.34	-0.81	-2.89E-03	-2892.86	-2.44E-03	-2437.64
13	24	288	22.8	-0.57	-2.04E-03	-2035.71	-0.67	-2.38E-03	-2384.34	-0.805	-2.88E-03	-2875.00	-2.43E-03	-2431.69
14	24	312	22.4	-0.565	-2.02E-03	-2017.86	-0.675	-2.40E-03	-2402.14	-0.795	-2.84E-03	-2839.29	-2.42E-03	-2419.76
15	24	336	22.7	-0.565	-2.02E-03	-2017.86	-0.68	-2.42E-03	-2419.93	-0.795	-2.84E-03	-2839.29	-2.43E-03	-2425.69
16	24	360	23.1	-0.575	-2.05E-03	-2053.57	-0.69	-2.46E-03	-2455.52	-0.805	-2.88E-03	-2875.00	-2.46E-03	-2461.36
17	24	384	23.5	-0.585	-2.09E-03	-2089.29	-0.7	-2.49E-03	-2491.10	-0.815	-2.91E-03	-2910.71	-2.50E-03	-2497.03
18	24	408	23.7	-0.595	-2.13E-03	-2125.00	-0.71	-2.53E-03	-2526.69	-0.825	-2.95E-03	-2946.43	-2.53E-03	-2532.71
19	24	432	23.4	-0.595	-2.13E-03	-2125.00	-0.715	-2.54E-03	-2544.48	-0.825	-2.95E-03	-2946.43	-2.54E-03	-2538.64
20	24	456	23.2	-0.56	-2.00E-03	-2000.00	-0.69	-2.46E-03	-2455.52	-0.77	-2.75E-03	-2750.00	-2.40E-03	-2401.84
21	24	480	24.3	-0.595	-2.13E-03	-2125.00	-0.715	-2.54E-03	-2544.48	-0.81	-2.89E-03	-2892.86	-2.52E-03	-2520.78
22	24	504	24.1	-0.61	-2.18E-03	-2178.57	-0.735	-2.62E-03	-2615.66	-0.83	-2.96E-03	-2964.29	-2.59E-03	-2586.17

				SHRINKAGE TESTING RESULTS - NC											
				4% Cement; No Polymer (J)											
Specimen Name				J1			J2			J3			AVERAGE		
Specimen Height (mm)				280			281			280					
Wet weight (g)				Wet/Dry	5196	4942	Wet/Dry	5224	4957	Wet/Dry	5207	4951			
Day	Time Interval (hours)	Cumulative Time (hours)	Temperature (^{0}C)	Dimensional change (mm)	Axial shrinkage (mm/mm)	Axial shrinkage [X 10^{-6}] mm/mm	Dimensional change (mm)	Axial shrinkage (mm/mm)	Axial shrinkage [X 10^{-6}] mm/mm	Dimensional change (mm)	Axial shrinkage (mm/mm)	Axial shrinkage [X 10^{-6}] mm/mm	Axial shrinkage (mm/mm)	Axial shrinkage [X 10^{-6}] mm/mm
23	24	528	23.6	-0.625	-2.23E-03	-2232.14	-0.755	-2.69E-03	-2686.83	-0.85	-3.04E-03	-3035.71	-2.65E-03	-2651.56
24	24	552	23.1	-0.64	-2.29E-03	-2285.71	-0.77	-2.74E-03	-2740.21	-0.865	-3.09E-03	-3089.29	-2.71E-03	-2705.07
25	24	576	22.9	-0.575	-2.05E-03	-2053.57	-0.73	-2.60E-03	-2597.86	-0.78	-2.79E-03	-2785.71	-2.48E-03	-2479.05
26	24	600	23.3	-0.545	-1.95E-03	-1946.43	-0.69	-2.46E-03	-2455.52	-0.745	-2.66E-03	-2660.71	-2.35E-03	-2354.22
27	24	624	23.8	-0.57	-2.04E-03	-2035.71	-0.695	-2.47E-03	-2473.31	-0.775	-2.77E-03	-2767.86	-2.43E-03	-2425.63
28 start	24	648	23.5	-0.57	-2.04E-03	-2035.71	-0.715	-2.54E-03	-2544.48	-0.77	-2.75E-03	-2750.00	-2.44E-03	-2443.40
28 end	24	672	23.4	-0.57	-2.04E-03	-2035.71	-0.71	-2.53E-03	-2526.69	-0.77	-2.75E-03	-2750.00	-2.44E-03	-2437.47

APPENDIX C: SHRINKAGE RESULTS FOR ALL REPEATS OF SPECIMEN TYPES, ACCORDING TO THE CONSIDERED ASPECTS OF COMPARISON

C.1: G4 HORNFELS

C.2: RECYCLED CONCRETE AGGREGATES (RCA)

C.3: NEW CONCRETE (NC)

APPENDIX D: COEFFICIENTS OF VARIATION OF THE THREE REPEATS OF SPECIMEN TYPES

D.1: G4 HORNFELS

specimens	Final shrinkage	Time to pivot-point	Shrinkage magnitude at pivot-point	Highest shrinkage value
A1	-434.78	216	-507.25	-525.36
A2	-821.82	216	-763.64	-883.64
A3	-523.64	216	-407.27	-523.64
CV (A) [%]	-34.16	0	-32.86	-32.19
B1	-487.80	336	-644.60	-662.02
B2	-1157.89	312	-1964.91	-1157.89
B3	-868.79	264	-1365.25	-868.79
CV (B) [%]	-40.10	12.06	-49.90	-27.79
C1	-1109.19	120	-1490.47	-1507.80
C2	-1590.91	120	-1783.22	-2307.69
C3	-1045.30	120	-1324.04	-1533.10
CV (C) [%]	-23.89	0	-15.17	-25.50
D1	-1739.13	96	-1513.04	-1878.26
D2	-1821.31	78	-1890.03	-2680.41
D3	-1168.38	120	-910.65	-1408.93
CV (D) [%]	-22.56	21.50	-34.36	-32.32

197

D.2: RECYCLED CONCRETE AGGREGATES (RCA)

specimens	Final shrinkage	Time to pivot-point	Shrinkage magnitude at pivot-point	Highest shrinkage value
E1	-503.60	432.00	-359.71	-503.60
E2	-1007.19	432.00	-791.37	-1007.19
E3	-1032.61	432.00	-887.68	-1032.61
CV (E) [%]	-35.19	0.00	-41.37	-35.19
F1	-1459.07	408.00	-1227.76	-1459.07
F2	-1766.78	408.00	-1580.31	-1837.46
F3	-1748.25	408.00	-1923.08	-1923.08
CV (F) [%]	-10.41	0.00	-22.05	-14.19
G1	-1358.89	126.00	-1550.52	-1689.90
G2	-1431.03	126.00	-913.79	-1810.34
G3	-1615.12	126.00	-1182.26	-1907.22
CV (G) [%]	-9.00	0.00	-26.30	-6.04

D.3: NEW CONCRETE (NC)

specimens	Final shrinkage	Time to pivot-point	Shrinkage magnitude at pivot-point	Highest shrinkage value
H1	-1593.41	552.00	-1611.72	-1611.72
H2	-1758.92	552.00	-1941.39	-1941.39
H3	-1851.85	552.00	-1888.89	-1888.89
CV (H) [%]	-7.55	0.00	-9.76	-9.76
I1	-2643.88	576.00	-2625.90	-2643.88
I2	-2078.85	576.00	-2114.70	-2114.69
I3	-2777.78	576.00	-2759.26	-2814.81
CV (I) [%]	-14.84	0.00	-13.61	-14.46
J1	-2035.71	126.00	-1910.71	-2285.71
J2	-2437.47	126.00	-1850.53	-2740.21
J3	-2750.00	126.00	-2642.86	-3089.29
CV (J) [%]	-14.87	0.00	-20.66	-14.90

APPENDIX E: TEMPERATURE VARIATION VS SHRINKAGE RESULTS

E.1: RECYCLED CONCRETE AGGREGATES (RCA)

E.2: NEW CONCRETE (NC)

Temperature variation vs shrinkage results of specimens H

Temperature variation vs shrinkage results of specimens I

Temperature variation vs shrinkage results of specimens J

200

APPENDIX F: SUMMARY OUTPUTS FOR STATISTICAL ANALYSIS

F.1: ANALYSIS OF MATERIAL BY MATERIAL

G4 HORNFELS

FINAL SHRINKAGE

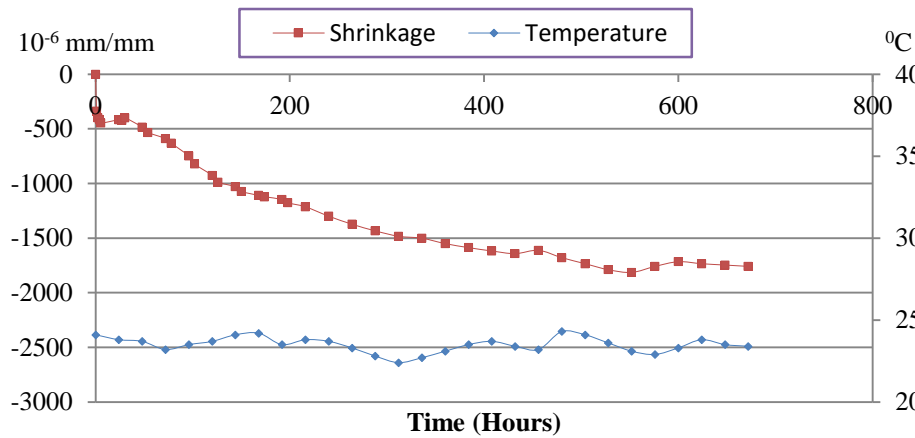| Regression Statistics	
Multiple R	0.858495143
R Square	0.737013911
Adjusted R Square	0.474027821
Standard Error	274.1820742
Observations	9

ANOVA

	df	SS	MS	F	Significance F
Regression	4	842715.563	210678.8907	2.802482491	0.171107928
Residual	4	300703.2392	75175.80981		
Total	8	1143418.802			

	Coefficients	Standard Error	t Stat	P-value	Lower 95%	Upper 95%
Intercept	-323676.2908	502240.3745	-0.644464896	0.554371338	-1718119.12	1070766.539
Cement content	-402.6461344	298.4464688	-1.349140219	0.248603354	-1231.266372	425.9741032
Moisture content	-2519312.13	3398670.464	-0.74126402	0.499691722	-11955534.1	6916909.843
Moisture loss	-121992.9563	165774.5768	-0.735896653	0.502615996	-582256.9687	338271.0561
Density	5194.105409	7034.24795	0.738402377	0.501249228	-14336.09788	24724.3087

SHRINKAGE MAGNITUDE AT PIVOT-POINT

Regression Statistics	
Multiple R	0.831732887
R Square	0.691779595
Adjusted R Square	0.383559189
Standard Error	449.8272438
Observations	9

ANOVA

	df	SS	MS	F	Significance F
Regression	4	1816593.942	454148.4855	2.244431526	0.22643769
Residual	4	809378.1971	202344.5493		
Total	8	2625972.139			

201

	Coefficients	Standard Error	t Stat	P-value	Lower 95%	Upper 95%
Intercept	-945776.834	823983.1289	-1.147810921	0.315026553	-3233520.759	1341967.091
Cement content	-690.3240847	489.6357754	-1.409872643	0.231384116	-2049.770937	669.1227672
Moisture content	-6495620.509	5575909.992	-1.164943573	0.308778364	-21976828.51	8985587.497
Moisture loss	-316779.3712	271972.2695	-1.164748788	0.30884875	-1071895.448	438336.7053
Density	13438.72831	11540.49322	1.164484746	0.308944187	-18602.8176	45480.27421

HIGHEST SHRINKAGE

Regression Statistics	
Multiple R	0.824546581
R Square	0.679877064
Adjusted R Square	0.359754128
Standard Error	515.6403652
Observations	9

ANOVA

	df	SS	MS	F	Significance F
Regression	4	2258746.046	564686.5115	2.123799916	0.241824521
Residual	4	1063539.945	265884.9862		
Total	8	3322285.991			

	Coefficients	Standard Error	t Stat	P-value	Lower 95%	Upper 95%
Intercept	-601108.8159	944538.0807	-0.636405062	0.55910723	-3223566.947	2021349.315
Cement content	-580.0661844	561.2731855	-1.033482802	0.359765507	-2138.410373	978.2780041
Moisture content	-4383777.245	6391707.715	-0.685853834	0.530491479	-22130002.84	13362448.36
Moisture loss	-213316.1683	311763.8656	-0.684223516	0.531418074	-1078911.427	652279.0904
Density	9054.088047	13228.95449	0.684414483	0.531309478	-27675.3779	45783.55399

RCA

FINAL SHRINKAGE

Regression Statistics	
Multiple R	0.893490228
R Square	0.798324787
Adjusted R Square	0.596649575
Standard Error	260.9019455
Observations	9

ANOVA

	df	SS	MS	F	Significance F
Regression	4	1077808.779	269452.1948	3.95846756	0.105613246
Residual	4	272279.3008	68069.82519		
Total	8	1350088.08			

	Coefficients	Standard Error	t Stat	P-value	Lower 95%	Upper 95%
Intercept	-298037.2541	238636.9833	-1.248914774	0.279796769	-960599.7383	364525.2302
Cement content	-177.856808	842.6720835	-0.211062893	0.843154968	-2517.489589	2161.775973
Moisture content	-702792.2465	661655.9682	-1.062171703	0.348031527	-2539843.721	1134259.228
Moisture loss	-72689.39144	66586.43318	-1.09165468	0.336330571	-257562.9679	112184.1851
Density	3521.671478	3291.932143	1.0697886	0.344974065	-5618.197407	12661.54036

SHRINKAGE MAGNITUDE AT PIVOT-POINT

Regression Statistics	
Multiple R	0.838870893
R Square	0.703704375
Adjusted R Square	0.407408751
Standard Error	367.9380461
Observations	9

ANOVA

	df	SS	MS	F	Significance F
Regression	4	1286098.997	321524.7492	2.375007649	0.211349056
Residual	4	541513.623	135378.4058		
Total	8	1827612.62			

	Coefficients	Standard Error	t Stat	P-value	Lower 95%	Upper 95%
Intercept	-213312.8787	336538.7912	-0.63384336	0.560618261	-1147694.358	721068.6007
Cement content	812.1817993	1188.381785	0.683435079	0.5318666	-2487.294992	4111.658591
Moisture content	-543909.9935	933103.0614	-0.58290452	0.591238269	-3134619.421	2046799.434
Moisture loss	-58001.82397	93903.79236	-0.61767286	0.570220719	-318720.5486	202716.9007
Density	2720.178965	4642.460898	0.585934707	0.589386575	-10169.35887	15609.7168

HIGHEST SHRINKAGE

Regression Statistics	
Multiple R	0.930928163
R Square	0.866627244
Adjusted R Square	0.733254488
Standard Error	260.4746548
Observations	9

ANOVA

	df	SS	MS	F	Significance F
Regression	4	1763421.556	440855.3891	6.497783125	0.048619929
Residual	4	271388.1831	67847.04578		
Total	8	2034809.74			

	Coefficients	Standard Error	t Stat	P-value	Lower 95%	Upper 95%
Intercept	-332535.976	238246.1569	-1.395766381	0.23527522	-994013.3521	328941.4
Cement content	-652.108702	841.2920017	-0.775127662	0.481536673	-2987.909762	1683.692358
Moisture content	-843326.7495	660572.3446	-1.276660696	0.270801921	-2677369.602	990716.1034
Moisture loss	-86102.62917	66477.38161	-1.295216916	0.264942073	-270673.4299	98468.1716
Density	4212.684255	3286.540798	1.281798862	0.269166952	-4912.215857	13337.58437

NC

FINAL SHRINKAGE

Regression Statistics	
Multiple R	0.818544694
R Square	0.670015417
Adjusted R Square	0.340030833
Standard Error	364.8223083
Observations	9

ANOVA

	df	SS	MS	F	Significance F
Regression	4	1080970.669	270242.6673	2.030444603	0.254805549
Residual	4	532381.2664	133095.3166		
Total	8	1613351.936			

	Coefficients	Standard Error	t Stat	P-value	Lower 95%	Upper 95%
Intercept	-49883.65414	55267.15701	-0.902591283	0.417781363	-203329.8817	103562.5734
Cement content	-507.2348833	313.3468617	-1.618764843	0.180809598	-1377.225244	362.755477
Moisture content	-19362.833	35430.90917	-0.546495516	0.613779481	-117734.8073	79009.14134
Moisture loss	-1300.92217	2932.996757	-0.443547088	0.680305313	-9444.226658	6842.382319
Density	117.1891877	166.473132	0.703952562	0.520282969	-345.0143248	579.3927002

SHRINKAGE MAGNITUDE AT PIVOT-POINT

Regression Statistics	
Multiple R	0.68209764
R Square	0.465257191
Adjusted R Square	-0.069485619
Standard Error	431.1058252
Observations	9

ANOVA

	df	SS	MS	F	Significance F
Regression	4	646808.7912	161702.1978	0.870057871	0.552030341
Residual	4	743408.9301	185852.2325		
Total	8	1390217.721			

	Coefficients	Standard Error	t Stat	P-value	Lower 95%	Upper 95%
Intercept	-88214.71384	65308.48797	-1.350738879	0.248134299	-269540.1456	93110.71792
Cement content	-332.4108162	370.2779526	-0.897733213	0.420078815	-1360.467225	695.6455929
Moisture content	-1639.299523	41868.24925	-0.039153763	0.970644052	-117884.1952	114605.5962
Moisture loss	-1030.702665	3465.88451	-0.297385173	0.780977324	-10653.54075	8592.135418
Density	49.13142081	196.719157	0.249754124	0.815079414	-497.0485198	595.3113614

HIGHEST SHRINKAGE

Regression Statistics	
Multiple R	0.842590073
R Square	0.709958031
Adjusted R Square	0.419916062
Standard Error	379.417128
Observations	9

ANOVA

	df	SS	MS	F	Significance F
Regression	4	1409501.973	352375.4931	2.4477769	0.20357385
Residual	4	575829.4281	143957.357		
Total	8	1985331.401			

	Coefficients	Standard Error	t Stat	P-value	Lower 95%	Upper 95%
Intercept	-15743.63811	57478.13528	-0.273906556	0.797718997	-175328.5255	143841.2492
Cement content	-343.6628954	325.8823916	-1.054561106	0.351110643	-1248.457466	561.1316756
Moisture content	-26473.32174	36848.33272	-0.718440151	0.512214769	-128780.6948	75834.05129
Moisture loss	-2143.274772	3050.332122	-0.702636528	0.52102044	-10612.35446	6325.804918
Density	137.4321338	173.1329368	0.793795429	0.471746631	-343.2619611	618.1262286

F.2: ANALYSIS OF THE THREE MATERIALS TOGETHER

FINAL SHRINKAGE

Regression Statistics	
Multiple R	0.890636979
R Square	0.793234229
Adjusted R Square	0.755640452
Standard Error	339.6261446
Observations	27

ANOVA

	df	SS	MS	F	Significance F
Regression	4	9735263.502	2433815.876	21.10014742	2.87197E-07
Residual	22	2537610.198	115345.9181		
Total	26	12272873.7			

	Coefficients	Standard Error	t Stat	P-value	Lower 95%	Upper 95%
Intercept	40306.85027	9863.862081	4.086315272	0.000488643	19850.45235	60763.24818
Cement content	-44.17197172	89.13786909	-0.49554664	0.625128132	-229.0325978	140.6886543
Moisture content	-925.831882	294.9290843	-3.13916779	0.004767248	-1537.477367	-314.1863972
Moisture loss	148.8486568	289.4992676	0.51415901	0.612267131	-451.5360774	749.2333909
Density	-14.95353444	3.583267228	-4.17315637	0.000395287	-22.38477584	-7.522293044

SHRINKAGE MAGNITUDE AT PIVOT-POINT

Regression Statistics	
Multiple R	0.758060494
R Square	0.574655712
Adjusted R Square	0.497320387
Standard Error	478.889829
Observations	27

ANOVA

	df	SS	MS	F	Significance F
Regression	4	6816493.597	1704123.399	7.430701461	0.000603573
Residual	22	5045380.303	229335.4683		
Total	26	11861873.9			

	Coefficients	Standard Error	t Stat	P-value	Lower 95%	Upper 95%
Intercept	39061.65007	13908.53826	2.808465516	0.010236786	10217.10717	67906.19298
Cement content	14.07828414	125.6888481	0.112009016	0.911831962	-246.5844328	274.7410011
Moisture content	-742.8074041	415.8647412	-1.78617548	0.087862296	-1605.258091	119.6432826
Moisture loss	-35.51815677	408.2084284	-0.08700986	0.931450781	-882.0906226	811.054309
Density	-14.86008846	5.052585784	-2.94108583	0.007556524	-25.33851004	-4.381666876

HIGHEST SHRINKAGE

Regression Statistics	
Multiple R	0.876560936
R Square	0.768359074
Adjusted R Square	0.726242542
Standard Error	375.9167915
Observations	27

ANOVA

	df	SS	MS	F	Significance F
Regression	4	10312288.69	2578072.174	18.24364534	9.73845E-07
Residual	22	3108895.551	141313.4341		
Total	26	13421184.24			

	Coefficients	Standard Error	t Stat	P-value	Lower 95%	Upper 95%
Intercept	40770.74527	10917.86202	3.734315857	0.00115044	18128.48526	63413.00527
Cement content	-118.8921093	98.66266859	-1.205036424	0.24099212	-323.505961	85.72174187
Moisture content	-888.4011934	326.4436406	-2.721453516	0.012463084	-1565.40387	-211.398519
Moisture loss	129.8192166	320.4336225	0.405136064	0.689290104	-534.719443	794.3578763
Density	-15.28636871	3.966156142	-3.854202449	0.000860087	-23.5116731	-7.061064308

F.3: ANALYSIS OF THE UCS AND THE ITS

INDEPENDENT VARIABLES AND UCS RESULTS

Regression Statistics	
Multiple R	0.991833066
R Square	0.983732832
Adjusted R Square	0.980775165
Standard Error	0.575609776
Observations	27

ANOVA

	df	SS	MS	F	Significance F
Regression	4	440.8026663	110.2006666	332.6043296	2.4951E-19
Residual	22	7.289185524	0.331326615		
Total	26	448.0918519			

	Coefficients	Standard Error	t Stat	P-value	Lower 95%	Upper 95%
Intercept	36.05275967	16.71760416	2.15657455	0.042232703	1.382570647	70.7229487
Cement content	2.391847238	0.151073849	15.83230488	1.64918E-13	2.078539251	2.705155225
Moisture content	-1.02699181	0.4998557	-2.054576574	0.051987375	-2.06362909	0.009645462
Moisture loss	0.582855629	0.490653065	1.187918044	0.247532748	-0.43469655	1.600407806
Density	-0.01210802	0.006073041	-1.993732975	0.058723722	-0.02470274	0.000486694

INDEPENDENT VARIABLES AND ITS RESULTS

Regression Statistics	
Multiple R	0.977679094
R Square	0.955856411
Adjusted R Square	0.947830304
Standard Error	99.88329382
Observations	27

ANOVA

	df	SS	MS	F	Significance F
Regression	4	4752623.524	1188155.881	119.0934046	1.42819E-14
Residual	22	219486.7925	9976.672385		
Total	26	4972110.316			

	Coefficients	Standard Error	t Stat	P-value	Lower 95%	Upper 95%
Intercept	8397.776928	2900.939902	2.894846916	0.008404186	2381.595794	14413.95806
Cement content	248.2937591	26.21524906	9.471348469	3.21272E-09	193.9266601	302.6608581
Moisture content	-221.7509099	86.73798779	-2.55656046	0.017991356	-401.6344868	-41.8673331
Moisture loss	114.4040234	85.14109077	1.343699293	0.192741462	-62.16779167	290.9758386
Density	-2.974125935	1.053830923	-2.82220408	0.009921833	-5.159637504	-0.788614366

UCS/ITS AND FINAL SHRINKAGE

Regression Statistics	
Multiple R	0.591875406
R Square	0.350316496
Adjusted R Square	0.296176204
Standard Error	576.3926466
Observations	27

ANOVA

	df	SS	MS	F	Significance F
Regression	2	4299390.107	2149695.054	6.470532069	0.005654863
Residual	24	7973483.593	332228.483		
Total	26	12272873.7			

	Coefficients	Standard Error	t Stat	P-value	Lower 95%	Upper 95%
Intercept	-830.9043983	232.9395569	-3.567038631	0.001560331	-1311.66801	-350.1407818
UCS	-438.8138923	133.2878585	-3.292227044	0.003069561	-713.906512	-163.7212729
ITS	3.703103255	1.265329798	2.92659136	0.007383264	1.091590904	6.314615605

UCS/ITS AND SHRINKAGE MAGNITUDE AT PIVOT-POINT

Regression Statistics	
Multiple R	0.614126337
R Square	0.377151158
Adjusted R Square	0.325247088
Standard Error	554.8330987
Observations	27

ANOVA

	df	SS	MS	F	Significance F
Regression	2	4473719.481	2236859.741	7.266311819	0.003408725
Residual	24	7388154.419	307839.7674		
Total	26	11861873.9			

	Coefficients	Standard Error	t Stat	P-value	Lower 95%	Upper 95%
Intercept	-803.8066821	224.2266222	-3.584795928	0.001492993	-1266.58769	-341.025679
UCS	-436.2254377	128.302323	-3.399980822	0.002357705	-701.028418	-171.422458
ITS	3.624831579	1.218001057	2.976049616	0.006568652	1.111000949	6.138662209

UCS/ITS AND HIGHEST SHRINKAGE

Regression Statistics	
Multiple R	0.674955006
R Square	0.45556426
Adjusted R Square	0.410194615
Standard Error	551.7763881
Observations	27

ANOVA

	df	SS	MS	F	Significance F
Regression	2	6114211.866	3057105.933	10.0411687	0.000678203
Residual	24	7306972.378	304457.1824		
Total	26	13421184.24			

	Coefficients	Standard Error	t Stat	P-value	Lower 95%	Upper 95%
Intercept	-824.4134991	222.9913031	-3.697065704	0.00112855	-1284.644929	-364.182069
UCS	-426.4685123	127.5954743	-3.342348266	0.00271573	-689.8126281	-163.124396
ITS	3.22449319	1.211290793	2.662030629	0.01364113	0.724511865	5.724474515